2012

Applications of Capillary Electrophoresis for Studying Serum Albumin Enantioselection of D,L-Tryptophan Analogs

Jelynn A. Stinson
Wright State University

APPLICATIONS OF CAPILLARY ELECTROPHORESIS FOR STUDYING SERUM ALBUMIN ENANTIOSELECTION OF D, L-TRYPTOPHAN ANALOGS

A dissertation in partial fulfillment of the
requirements for the degree of
Doctor of Philosophy

By

JELYNN ANNEULA STINSON
M.S., Wright State University, 2007

2012

WRIGHT STATE UNIVERSITY

SCHOOL OF GRADUATE STUDIES

August 6, 2012

I HEREBY RECOMMEND THAT THE DISSERTATION PREPARED UNDER MY SUPERVISION BY Jelynn Anneula Stinson ENTITLED Applications Of Capillary Electrophoresis For Studying Serum Albumin Enantioselection Of D, L-Tryptophan Analogs BE ACCEPTED IN PARTIAL FULFILLMENT OF THE REQUIREMENTS FOR THE DEGREE OF Doctor Of Philosophy.

_____
Roger K. Gilpin, Ph.D.
Dissertation Director

_____
Gerald M. Alter, Ph.D.
Director, Biomedical Sciences Ph.D. Program

_____
Andrew T. Hsu, Ph.D.
Dean, Graduate School

Signature of Committee
On Final Examination

_____
Roger K. Gilpin, Ph.D.

_____
Gerald M. Alter, Ph.D.

_____
Kenneth Turnbull, Ph.D.

_____
Daniel Ketcha, Ph.D.

_____
Richard J. Sherwood, Ph.D.

ABSTRACT

Stinson, Jelynn A., Biomedical Sciences Ph.D. Program, Wright State University, 2012. Applications of Capillary Electrophoresis for Studying Serum Albumin Enantioselection of D,L-Tryptophan Analogs.

The pharmacokinetic difference between drug enantiomers is the impetus for developing analytical techniques to assess enantiomeric purity. Capillary electrophoresis (CE) is an analytical technique that is used for characterizing drug-protein binding. The pitfall to using CE for drug-protein binding studies is protein chiral selectors tend to adsorb onto capillary walls and cause changes in electroosmotic flow that lead to decreased enantioselection and migration time irreproducibility between consecutive injections. The experimental parameters for minimizing the adverse effects of protein adsorption are not clear from the literature.

Rinsing protocols to improve enantioselection and migration time repeatability were developed using the tryptophan-bovine serum albumin system as a model. The enantioselection of bovine serum albumin (BSA) could be improved by: 1) increasing separation voltage; 2) using sample buffer ionic strength at least 3 orders of magnitude less than the separation buffer; 3) limiting the equilibration time with separation buffer; and 4) allowing for protein diffusion. Rinsing the capillary with sodium hydroxide, followed by water improved migration time repeatability RSD from 24.7% to 1.8% (n = 4).

Drug-protein binding is contingent upon the three dimensional structure of the binding site, and the presence of other competing drug molecules. Drug-drug displacement is difficult to predict and the effects of protein glycation on binding of drugs is not well defined. To highlight the use of CE for addressing questions of biochemical interest, CE was applied to characterize drug-drug displacement and the effects of protein glycation on the enantioselection of drugs by BSA. The tryptophan-bovine serum albumin, 5-fluoro-tryptophan-bovine serum albumin, and 5-hydroxy-tryptophan-bovine serum albumin systems were used as models.

A CE method for studying competitive binding was established using ibuprofen as the displacer molecule. Accurate calculation of selectivity was found to depend on the precomplexation of ibuprofen and BSA. A CE method for studying the effects of protein glycation was developed using BSA containing different degrees of glycation as chiral selectors. The enantioselection of tryptophan analogs by BSA was altered by glycation as reported in other analytical methods. These studies can serve as guidelines for optimizing serum albumin enantioselection and extending its use in other biopharmaceutical applications.

TABLE OF CONTENTS

Chapter 1: General Introduction

PAGE

Chapter 2: Materials and Methods

TABLE OF CONTENTS (CONTINUED)

PAGE

TABLE OF CONTENTS (CONTINUED)

PAGE

LIST OF FIGURES

PAGE

LIST OF FIGURES (CONTINUED)

PAGE

LIST OF FIGURES (CONTINUED)

PAGE

LIST OF FIGURES (CONTINUED)

PAGE

LIST OF TABLES

PAGE

ACKNOWLEDGEMENTS

I wish to thank my faculty advisor, Dr. Roger Gilpin for his insights and guidance throughout my time in the Biomedical Sciences Ph.D. program. His willingness in allowing autonomy and supporting my ideas towards the completion of this project was key in my development as a scientist. I wish to thank the members of my dissertation committee for challenging me to make connections across scientific disciplines. Your guidance has helped me to critically think about scientific approaches. I wish to thank Dr. Nicholas Reo for the nuclear magnetic resonance (NMR) analysis. He was instrumental in teaching me the basics of NMR and learning how to accurately interpret data.

I would like to thank members of the Gilpin lab past and present for making my stay in the laboratory enjoyable and conducive to scientific development. I have had the opportunity to work with Joseph Solch and Garrett VanNess of the WSU Chemistry Department. I appreciate their willingness in providing materials and advice in addressing research problems. I will definitely miss our days filled with lots of laughter.

Special thanks to my family for your love and support. I appreciate your encouragement to pursue with all diligence the task set before me. I appreciate your prayers and constantly reminding me that all things work together for good to those who love The Lord. You are my motivation.

Chapter 1

General Introduction

1.1. Background

Although the majority of active pharmaceutical ingredients (API) are marketed as racemates, typically only one isomer is pharmacologically active resulting in decreased therapeutic efficacy of the formulated product. Likewise, dissimilar properties of enantiomers can result in side effects that range from mild to deadly. Because of these problems, there has been increasing demand for the production of enantiomerically pure drugs by government agencies like the US Food and Drug Administration (FDA). In order to assure the quality of these products there has been increasing demand for reliable analytical methodology to assess enantiomeric purity (Núñez, et al., 2009). It is this latter need that is the basis of the current work, which is concerned with the characterization and optimization of serum albumin as a chiral selector for carrying out enantiomeric separation by capillary electrophoresis. Unlike other standard methods, capillary electrophoresis (CE) does not require the use of pure enantiomers, which makes it easy to carry out experiments under various conditions.

One of the major challenges to using a protein as a chiral selector is it has a tendency to adsorb onto the inner walls of the bare-fused capillaries used in this

technique. In this case, drug molecules will interact not only with the protein in the background electrolyte (BGE), but also with that adsorbed to the capillary wall. Adsorbed protein has been reported to cause fluctuations of electroosmotic flow (EOF). This leads to peak shape distortion like tailing and band broadening that adversely affects resolution and efficiency (Ventura, et al., 2012). There is limited information available in the literature pertaining to the experimental conditions that are most relevant for improving chiral recognition of drugs by proteins. Capillary rinsing strategies and adjustment of separation voltage have been reported to improve separation (Sokoliess & Koller, 2005; Ribeiro, et al., 2011). The presence of protein in the BGE presents a background absorbance that suppresses the sample signal if the protein concentration is too high and detection is at a wavelength where the protein absorbs strongly.

Tryptophan, one of the compounds used to carry out the CE chiral recognition studies, is an amino acid that exists as both D- and L-stereoisomers. The D-and L-structures, and two other tryptophan analogs used in the current study are shown in Figure 1. Since tryptophan is a chemical precursor to the biosynthesis of serotonin, it along with its analogs, are administered for treatment of diseases where there is impaired synthesis of serotonin (Muck-Seler & Pivac, 2011). Tryptophan is used as an additive in over the counter antidepressants, appetite suppressors, and in sleep aid products (Doghramiji, P., 2006; Robinson et. al, 2012). Tryptophan and its analogs also are administered in the treatment and diagnosis in more serious diseases such as carcinoid tumor metastases, migraines, and attention-deficit/hyperactivity disorder (Nikolaou, et.al., 2010; Johansson, et. al, 2011; Niederhofer, 2011).

Figure 1: Tryptophan and analogs : 5-fluoro-tryptophan; 5-hydroxy-tryptophan.

Figure 1.

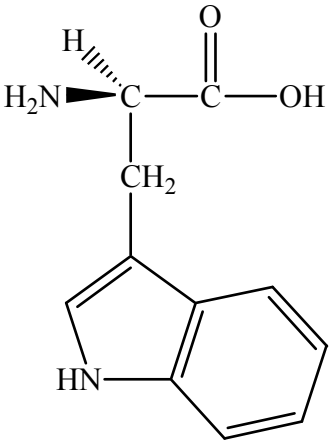

D,L-tryptophan

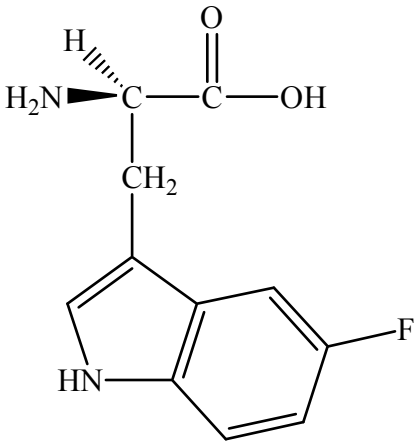

5-fluoro-D,L-tryptophan

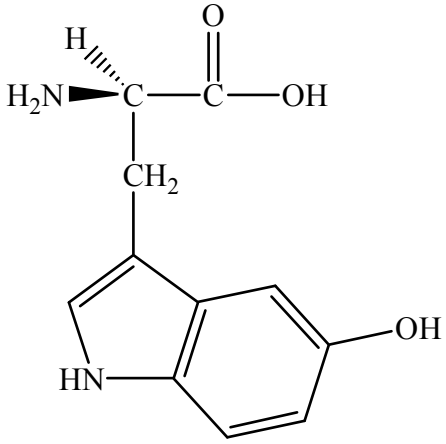

5-hydroxy-D,L-tryptophan

Despite the advances made in stereoselective synthesis, the direct enantiomeric synthesis of drugs may be expensive and not always achievable (Ye, 2011). For the analogs investigated in this work, a single step synthesis has been reported for 5-fluorotryptophan (Winn et al., 2008). There are a number of established techniques in the pharmaceutical field used for stereoselective analysis (Christodoulou, 2010). Of these, chiral separations performed using high pressure liquid chromatography (HPLC) continues to be the preferred approach (Wong et al., 2008; McConnell et al., 2007; Núñez, et al., 2009). Enantiomers are separated in HPLC either indirectly with chiral derivatization reagents or directly with chiral stationary phases (CSPs). The most important protein-based CSPs used in HPLC are based on human serum albumin (HSA), α_1-acid glycoprotein (AGP), crude ovumocoid (OVM) and cellobiohydrolase I (Lammerhofer, 2010). The AGP CSPs have been used in the enantioseparation of D,L-penicillamine, D,L-cysteine, and β_2 agonist, formoterol (Bhushan & Kumar, 2009; Akapo et al., 2009). Work has been carried out in our lab to develop methods using immobilized human serum albumin, bovine serum albumin (BSA), sheep albumin, and pig albumin in the enantioseparation of D,L-tryptophan (Tittelbach & Gilpin, 1995). Bovine serum albumin-gold conjugates as stationary phase have been described for use in chip-based enantioselective capillary electrochromatography (Li et al., 2009). Recently, HPLC has been combined with nuclear magnetic resonance (NMR) to screen the chromatographic enantiorecognition process on CSPs as well as to determine the absolute configuration of enantiomers (Uccello-Barretta et al., 2010; Cirilli et al., 2010; Thompson et al., 2009).

Other methods used for chiral separations include super-critical fluid chromatography, and preparative and simulated moving bed chromatography (Speybrouck et al., 2012; Zhang et al., 2012; Guiochon & Tarafder, 2011; Hsu et al., 2011). Spectroscopic techniques such as NMR provide a clear view of the binding mechanisms; however they have a high sample consumption rate (Oravcova et al., 1996; Liu et al., 2008; Mathur et al., 2007). Chromatographic assays also require the immobilization of the protein on a support, which alter the binding properties of the protein (Ascoli et al., 2006; Hage et al., 2009). The cost efficiency and environmental aspects of CE, such as the use of very small volumes of sample and buffer solutions, along with short analysis time, and ease of automation make it advantageous over other methods. Capillary electrophoresis has become a powerful tool for the separation of chiral drugs and biomolecules as reviewed by a number of publications on this topic (Altria & Elder, 2004; Natishan, 2005; Smith & Evans, 1994; Lu & Guonan, 2010; Liu et al., 2008). The first use of CE for chiral separation was demonstrated in 1985 by Zare and co-workers, who resolved racemic mixtures of dansylated amino acids (Gassmann et al., 1985).

Figure 2: Schematic of a Capillary Electrophoresis Instrument.

Figure 2.

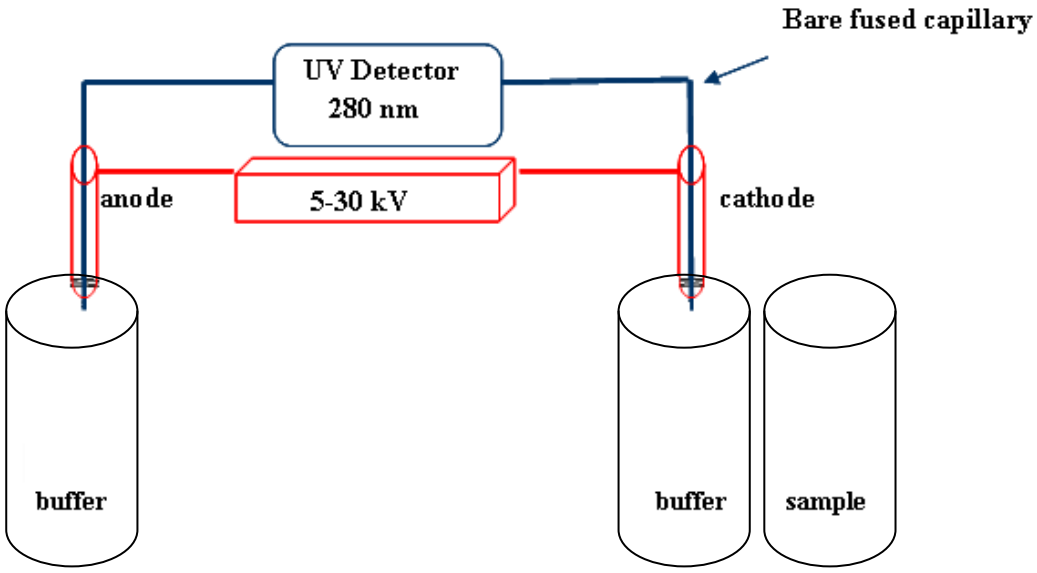
Bare fused capillary
UV Detector
280 nm
anode
5-30 kV
cathode
buffer
buffer
sample

1.2. Principles of separation in capillary electrophoresis

Capillary electrophoresis is a highly sensitive and selective method that separates components based on solute velocity in an electric field. The direction of movement is determined by the charge on the species, and the velocity is determined by the electrosmotic flow (EOF), electric field strength, shape of the solute, and ionic mobility. A general schematic of a capillary electrophoresis instrument is presented in Figure 2. Present commercially available systems also have a thermostatting system for temperature control.

Capillary electrophoretic separations are performed by first filling the capillary with an appropriate background electrolyte (BGE). A sample plug is then drawn into the capillary inlet by hydrodynamic or electrokinetic means. Both the cathode and the anode are submerged in vials containing the BGE, and a voltage is applied to the system. Solutes in the sample plug migrate along the capillary separating into zones according to their electrophoretic mobilites that are determined by their mass to charge ratio differences.

1.2.1. Electrophoretic Mobility

When a separation voltage is applied, an electric field E (V/L) (where V is the voltage and L is the length of the capillary), develops along the length of the capillary. Under the influence of this electric field, ionic species with charge *q* experience an electrostatic force (F_e),

$$F_e = qE \quad (1)$$

and a counteracting frictional force (F_{fr}) described mathematically by Stokes Law as:

$$F_{fr} = 6\pi\eta r\nu \quad (2)$$

where η is the viscosity of the background electrolyte, ν is the migration velocity, and *r* is the Stokes' radius of the solute. During electrophoretic separation these forces are equal in magnitude setting up a steady state in which ionic species travel at a constant velocity.

The velocity is a product of the electrophoretic mobility μ_{an} and the applied electric field

$$\nu = \mu_{an} \times E \quad (3)$$

The electrophoretic mobility for a charged species is approximated as

$$\mu_{an} = q/6\pi\eta r \quad (4)$$

The mobility can be experimentally determined from the migration time (t) of the solute using the following equation:

$$\mu = l/Et \quad (5)$$

From equation 4, larger solutes with smaller charges will have a lower mobility than smaller solutes with greater charge. Adjustments to the BGE's pH can affect the overall charge of the ionic species causing their mobility to increase or decrease accordingly. Along with this, the addition of buffer additives or change in separation temperature will affect the viscosity of the BGE resulting in changes to electrophoretic mobility.

1.2.2. Electroosmotic flow

Movement of solutes within the capillary is not limited to charged molecules. Neutral solutes migrate within the capillary as the result of the electroosmotic flow. When the capillary is filled with BGE, a charge develops on the inside wall of the capillary. By electrostatic attraction, counterions in the BGE absorb on the wall setting up a double electric layer at the capillary wall-BGE interface. According to a model proposed by Stern, the double layer is composed of a compact layer of tightly held ions and a diffuse layer (Giddings, 1969).

Figure 3: Simplistic model of a double electric layer.

Figure 3.

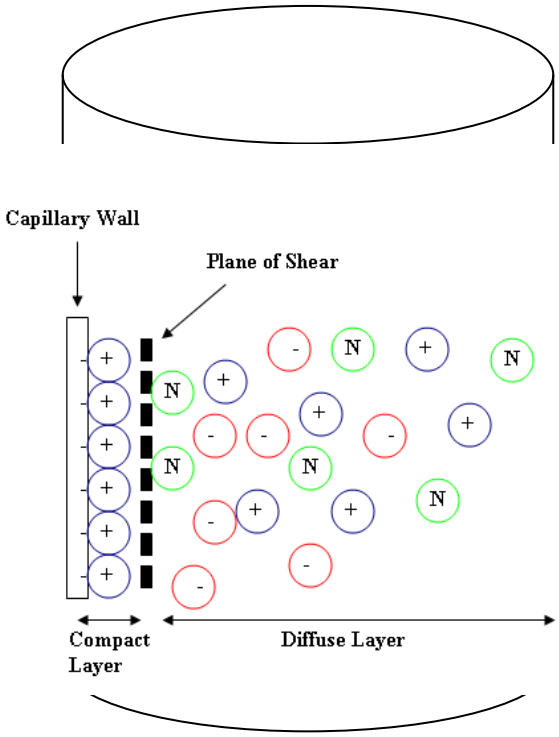

The electrical potential decreases with increasing distance from the capillary wall. The potential in the diffuse layer is referred to as the zeta potential (ζ). An imaginary boundary is present between these layers called the plane of shear Figure 3. As a result of viscous drag, when an electric field is applied, ions in the diffuse layer break away at the plane of shear, dragging with them the bulk liquid producing an electroosmotic flow. It is by EOF that neutral molecules are able to migrate. The mobility of the EOF is described by:

$$\mu_{EOF} = \frac{\varepsilon E \zeta}{4\pi\eta} \qquad (6)$$

where EOF mobility is directly proportional to the dielectric constant of the solution (ε), the applied electrical field (E), and the zeta potential (ζ) and inversely proportional to the viscosity of the BGE (η). If this parameter is not controlled it can lead to a decrease in separation (Bullock & Yuan, 1991). The apparent mobility of a charged solute is the sum of the EOF mobility (Eq. 6) and its ionic mobility (Eq. 4). The EOF mobility is measured experimentally using an uncharged solute.

1.2.3. Selectivity and efficiency

Since the EOF affects the amount of time a solute spends in the capillary, separation efficiency, selectivity, and resolution are related to the direction and velocity of the EOF. Unlike laminar flow in liquid chromatography, the electroosmotic flow has minimal effect on resistance to mass transfer. Therefore, the theoretical plate count in a capillary is much larger than that of a chromatography column of the same length.

Diffusion occurs during the time t, it takes for a sample zone to travel from the point of injection to the point of detection. The spatial variance $(\sigma^2 L)$ of the zone is given by:

$$\sigma^2 L = 2DL^2 / \mu V \tag{7}$$

where D is the diffusion coefficient of the solute, L is the total length of the capillary, V is the applied voltage, and μ is the apparent electrophoretic mobility of the solute. The efficiency is expressed by the theoretical plate number (N),

$$N = L^2 / \sigma^2 L \tag{8}$$

By substituting Eq. (7) into Eq. (8)

$$N = \mu V / 2D \tag{9}$$

It can be observed from Eq. (9), that: a) The efficiency can be improved by applying high voltages; b) Solutes with higher mobilities and low diffusion coefficients will produce higher plate counts.

The efficiency may be experimentally determined by:

$$N = 5.54(t / w_{1/2})^2 \tag{10}$$

where t is the migration time and $w_{1/2}$ the peak at half height. Equation (10) is correct only for Gaussian peaks. Selectivity is the thermodynamic measure of the differences in affinity of two ligands for binding to a substrate. The selectivity is given by:

$$\alpha = \Delta\mu / \mu_{average} = 2(\mu_1 - \mu_2) / (\mu_1 + \mu_2) \tag{11}$$

where μ_1 and μ_2 are the observed electrophoretic mobilities of each ligand. Differences in physiochemical properties between solutes determine differences in

selectivity. The most important parameter for optimizing the selectivity of charged solutes is pH (Guan et al., 2012).

1.2.4. Resolution

Resolution is a function of the selectivity (α), migration time (t), and the separation efficiency (N) (Jones et al., 1990). Resolution is defined according to selectivity and efficiency by:

$$R_s = \left(\frac{1}{4}\right)\left(\frac{\Delta\mu}{\mu_{average}}\right)N^{1/2} = \left(\frac{1}{4}\right)(\alpha)N^{1/2} \quad (12)$$

In CE there are many sources that can have adverse effects on resolution. Electrodispersion occurs when the electric field strength is non-linear along the length of the capillary. When the voltage drop along the capillary is not linear, samples travel along the capillary at different velocities causing peak dispersion to occur. A measurement for the extent of this dispersion is given by the baseline peak width (w_{base}),

$$w_{base} = 4\sigma \quad (13)$$

where σ is the standard deviation. The resolution can be determined from the migration time (t) by:

$$R_s = \frac{2(t_2 - t_1)}{w_1 + w_2} = \frac{t_2 - t_1}{4 \cdot \sigma} \quad (14)$$

where w is the baseline width in time. Conductivity differences between the sample zone and surrounding buffer zones, lead to peak shape distortion. The effects of electrodispersion are addressed by adjusting the BGE's ionic strength, sample plug injection length, and sample concentration.

1.3. Capillary Electrophoresis for enantioselective analysis

In the experimental set-up chiral separation is induced by the addition of chiral selectors to the background electrolyte. Upon the application of voltage, enantiomers, D and L migrate within the capillary interacting with a chiral selector P, forming drug- selector complexes with equilibrium constants K_D and K_L :

$$D + P \xleftrightarrow{K_D} DP \qquad \text{and} \qquad L + P \xleftrightarrow{K_L} LP \tag{15}$$

Two enantiomers of a given chiral compound have identical electrophoretic mobilities in free solution. The resolution of enantiomers is based upon interaction with the chiral selector. The "three-point interaction model" states that three points of interaction between the chiral selector and one of the enantiomers is required before discrimination by the selector is achieved as illustrated in Figure 4 (Davankov, 1998; Kitawaga & Otsuka, 2011). The molecular interaction between the selector and enantiomer involves coulomb forces, hydrogen bonding, steric hindrance, π-π interaction, ion-dipole, dipole-dipole, London dispersion, and dipole-induced dipole forces. The strongest interaction occurs with the Coulomb force (Kitawaga & Otsuka, 2011). For separation to be achieved, there are conditions that must be satisfied: (1) The equilibrium constants for selector-solute binding must be different for the two enantiomers; (2) There must be significant amounts of both chiral selector and solute; (3) Equilibration of the enantiomer in and out of the selector, must be faster than the time scale of separation; (4) Mobilities of complexed and free drug must be different. The enantiomer in complex with the selector will migrate at a velocity different from the free enantiomer. This results in measurable differences in electrophoretic mobility between free and complexed drugs.

Figure 4: The three point interaction model. Enantiomer (a) can interact only with two sites on the chiral selector, while its mirror image enantiomer (b) presents three groups that match three sites of the selector.

Figure 4.

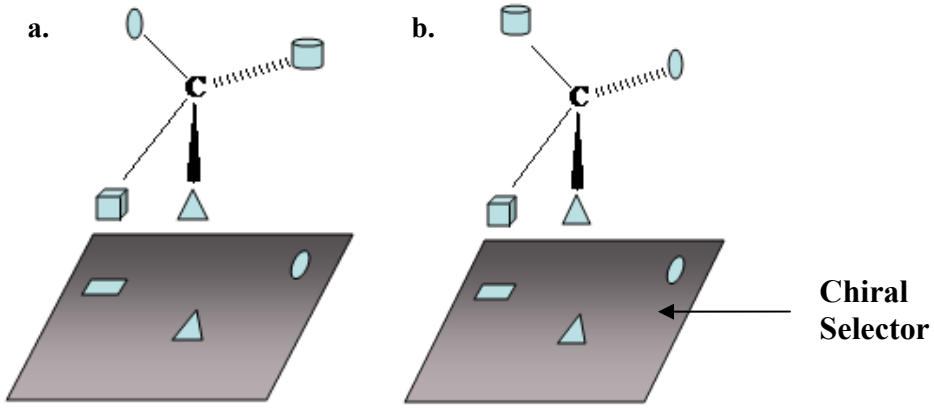

1.3.1. Common chiral selectors

The further development and use of novel chiral selectors are based upon cost, availability, solvent compatibility, and performance compared to established selectors. Selectors commonly used in CE chiral separations include cyclodextrins, micelles, macrocylic antibiotics, and proteins.

1.3.1.1. Cyclodextrins

The majority of chiral CE separations make use of cyclodextrins. Cyclodextrins are nonreducing oligosaccharides obtained from enzymatic digestion of starch. They are commonly found in the α-, β-, and γ-conformations, composed of 6, 7, and 8 α-(1-4)- linked glucopyranose units, respectively. The α- structure is represented schematically in Figure 5. Cyclodextrins have hydrophobic internal cavities and polar groups are on the outside. Drug molecules fit into these cavities forming inclusion complexes (Schmitt et al., 2002). Formation of inclusion complexes is influenced by the geometry and size of the drug molecules.

While hydrophobic interactions predominate in the formation of inclusion complexes, polar interactions also can occur along with hydrogen bonding and Van der Waals forces. The advantages associated with the use of cyclodextrins are their water solubility, ionizability, UV transparency, and stability in solution (Ilisz et al., 2009; Zhang et al., 2012). UV transparency of cyclodextrins is advantageous for development of CE methods.

1.3.1.2. Micelles

Micelles are formed when amphiphilic molecules containing both strongly polar and strongly nonpolar groups, aggregate in aqueous solutions above their critical micellar concentration. Amphiphilic molecules are frequently composed of a long nonpolar alkyl chain as the hydrophobic group and a polar head group (charged or neutral) as schematically represented in Figure 6 for sodium dodecyl sulfate (SDS). The ionic function of the surfactant hydrates readily, whereas the hydrophobic tail is intrinsically insoluble. In polar solvents, it is assumed that micelles are spherical in shape and oriented such that the polar groups are located on the outer zone and the alkyl groups constitute a hydrophobic core (Masci et al., 2012). The separation principle in micellar CE represents a hybrid technique based upon both a partitioning mechanism and electrokinetic migration. It is analogous to chromatography in that enantiomers are separated based upon residence time differences in the mobile (aqueous) phase and more stationary (micellar) phase.

Mostly anionic surface-active compounds like SDS have been used for the analysis of ionic and nonionic compounds (Lin et al., 2004). Cationic surfactants have been employed for anionic and neutral compounds (Wu et al., 2001). One important aspect to consider when using a cationic surfactant at high concentration is the direction of the electroosmotic flow is reversed. Since resolution is improved when chiral selector and EOF move in opposite directions, separation efficiency may be adversely affected if experimental methods are not modified to address changes in EOF.

Figure 5: Structure of α- cyclodextrin.

Figure 5.

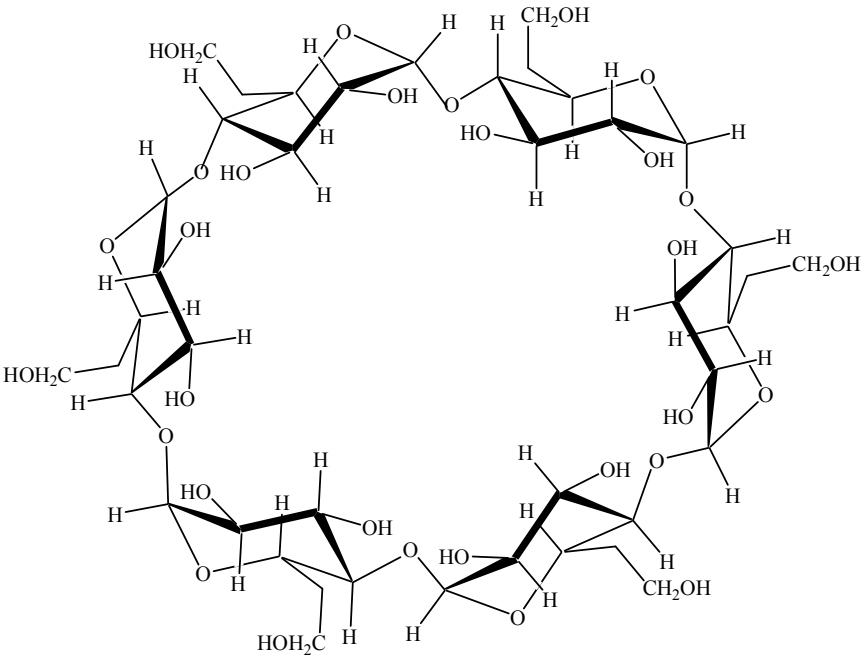

Figure 6: Schematic representation of the amphipathic molecule sodium dodecyl sulfate (SDS).

Figure 6.

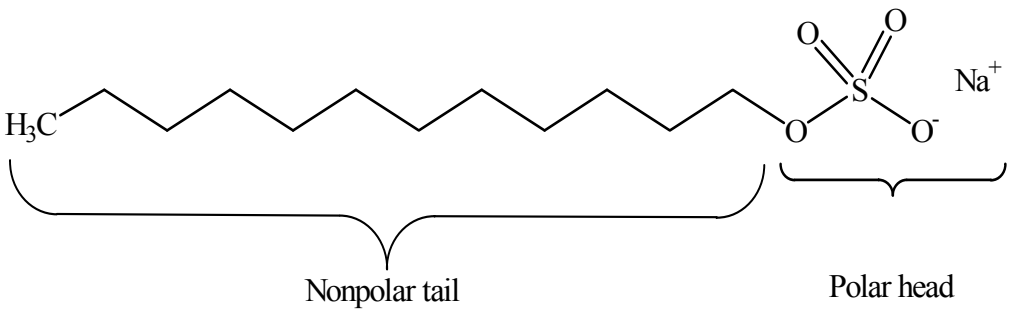

1.3.1.3. Macrocylic antibiotics

Macrocyclic antibiotics are a class of antibiotics used in therapy against infections caused by gram-negative and gram-positive bacteria. Natural and semisynthetic macrocyclic antibiotics comprise a variety of structural types, which include peptides, glycopeptides, ansa compounds, and peptide-heterocycle conjugates. A schematic of an ansa compound is represented in Figure 7. There are acidic, basic, and neutral types of antibiotics that differ in a number of physicochemical properties that determine their usefulness for chiral selection. Macrocyclic antibiotics contain functionalities such as ester, hydroxyl, amide, primary amine and aromatic groups which are involved in intermolecular interactions with chiral molecules (Armstrong et al., 1994). The chiral recognition in intermolecular interactions is maintained by stereogenic centers. The numbers of stereogenic centers in the antibiotics vary, allowing them to have multiple interactions with chiral molecules.

Macrocyclic antibodies interact with chiral molecules by hydrogen bonding, π-π interactions, hydrophobic interaction, dipole-dipole, and ionic interactions (Armstrong& Nair, 1997; Ward & Oswald, 1997). The selectivity of macrocyclic antibiotics is specific to the charge of the analyte and especially useful for the separation of acidic chiral analytes. Macrocyclic antibiotics use for the determination of trace levels of chiral compounds can be hindered by their high UV absorbance.

Figure. 7: Schematic of an ansa compound. $(n \geq 5)^{*}$ Where n denotes the number of atoms bridging the para positions on the molecule.

Figure 7.

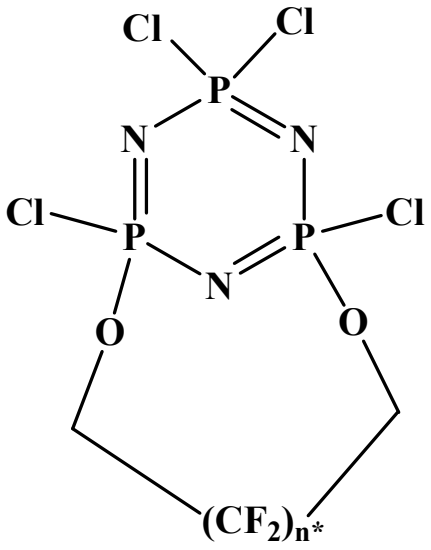

1.3.1.4. Proteins

Proteins are high molecular weight biopolymers which consist of L-amino acids. Many uniquely bind a single enantiomer of chiral molecules. Protein chiral recognition is affected by both charge and hydrophobic interactions. This mode of CE, utilizing protein as the chiral selector is referred to as affinity capillary electrophoresis (ACE). There are a number of proteins that have been used to carry out chiral CE separations. Examples include glycoproteins, enzymes such as lysozyme, fungal cellulase, as well as cytochrome *c* (Tanaka & Terabe, 2001). Alpha (1) acid glycoprotein is one of many glycoproteins found in plasma that is responsible for the binding of cationic drugs (Li & Lloyd, 1993; Tanaka & Terabe, 1997; Amini et al., 1997). The enantioselective binding of drugs is influenced by sugar moities and sialic acid residues. In the case of enzymes, the enzymatically active core is the dominating site for drug binding (Marle et al., 1993). Although a number of proteins have been employed, the most extensively studied in chiral CE are bovine serum albumin and human serum albumin.

1.3.1.4.1. Drug-serum albumin binding

The first study aimed at examining the suitability of CE applications for measuring drug-plasma protein binding was reported in 1992 (Kraak et al., 1992). Serum albumin is the most abundant protein in plasma (Fanali, et al., 2012). Bovine serum albumin (BSA) consists of a single polypeptide chain of 581 amino acid residues that are folded in a series of α-helices, and further organized into three domains. The tertiary structure of BSA is stabilized by 17 disulfide bridges. The warafin-azapropazone site (site I) and the indol-benzodiazepine site (site II) are the

two major sites in serum albumin for binding drugs (Sudlow, et al., 1976). Figure 8 shows the structure of albumin with different binding sites based upon Protein Data Bank file, 2BXG. Although both site I and II have been reported to bind aromatic and heterocyclic ligands site I tends to bind bulky heterocyclic anions (Peters, 1996; Carter & Ho, 1994). As a result of its ability to accommodate more than one ligand at a time, site I is described as a large and flexible region (Peters, 1996). By contrast site II, is smaller, less flexible and more stereospecific binding occurs at this location.

Figure 8: Albumin binding sites. The structure of albumin is shown with the major drug binding sites labeled (PDB ID: 2BXG).

Figure 8.

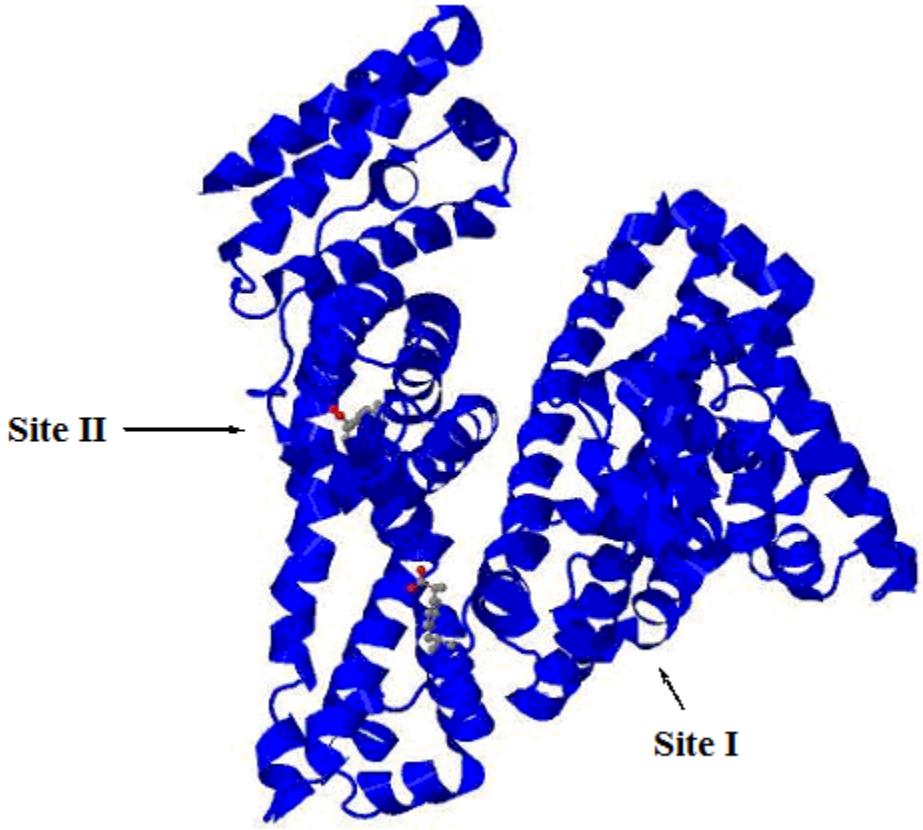

1.4. Factors that reduce tryptophan-serum albumin binding

It is accepted that the pharmacokinetic properties of drugs are influenced by reversible interactions with serum proteins (McMenamy & Oncley, 1958: Sudlow et al., 1975). Thus, the enantioselective binding of drugs by serum proteins is of great importance in the drug development process. Drug enantiomers tend to have different binding affinities for proteins. Drug binding constants provide quantitative measures by which drug binding and drug-drug displacement are determined and possible side effects are checked during preclinical trials (Betts et al., 2010, Rudnev et al., 2006).

In the presence of competing molecules, the extent of drug binding to serum proteins is reduced. Site II in serum albumin, is the high affinity binding site for both L-tryptophan and the non-steroidal anti-inflammatory drug ibuprofen (Sun & Wang, 2012). Ibuprofen and tryptophan are administered in the treatment of migraines. As a result of limited binding sites for these drugs, if administered concurrently, competition will exist between ibuprofen and L-tryptophan for binding (Berezhkovskiy, 2006). Inhibition of binding by one drug to another is a function of the relative concentrations of each drug, and specificity of binding (Langlois et al., 2012). There are a number of secondary drug binding sites on serum proteins that make drug-drug displacement difficult to predict. Strategies to investigate the effects of ibuprofen on interactions of tryptophan with serum albumin prove vital for providing insight into the usefulness of certain drug combinations. The displacement of L-tryptophan from serum albumin by ibuprofen has been studied by ultrafiltration and other in vitro assays (Basken et al., 2009).

The ability of proteins to select between optical isomers is attributed to their three dimensional structure. When protein modification induced by physiological changes occurs, an alteration of the protein's native binding efficiency is expected (Oettl & Stauber, 2007). Non-enzymatic glycation is a major in vivo mechanism that contributes to structural alteration of albumin. Glycation occurs most often at the N-terminal amino group and the side chains of the lysine residues. It also has been reported to occur at arginine, cysteine, histidine, and tryptophan residues (Munch et al., 1999). Glycation of a lysine side chain occurs through the Maillard reaction as shown in Figure 9. In the initial step of glycation, glucose attaches to free amine groups of albumin, forming a reversible Schiff base. Through an Amadori rearrangement a stable fructosamine product is formed. Schiff base and fructosamine products are the early glycation adducts which can be further modified by rearrangement, oxidation, polymerization, and cleavage to form irreversible conjugates called advanced glycation end products (Thornalley, 1999).

The extent of glycation is a function of glucose concentration and protein reaction time. Associated with the extent of glycation is a change in protein mass and charge. Knowledge about how glycation effects drug binding may lead to advancement in both treatment and diagnosis of diseases such as diabetes. Clinical implications of albumin glycation include drug binding may be altered for example at various stages of diabetes. In one study the binding of tryptophan by albumin, was found not to be affected by glycation, while in a different study low levels of glucose were reported to lower the affinity of albumin to bind (Bohney et al., 1992; Barzegar et al., 2007).

Figure 9: Formation of glycated albumin.

Figure 9.

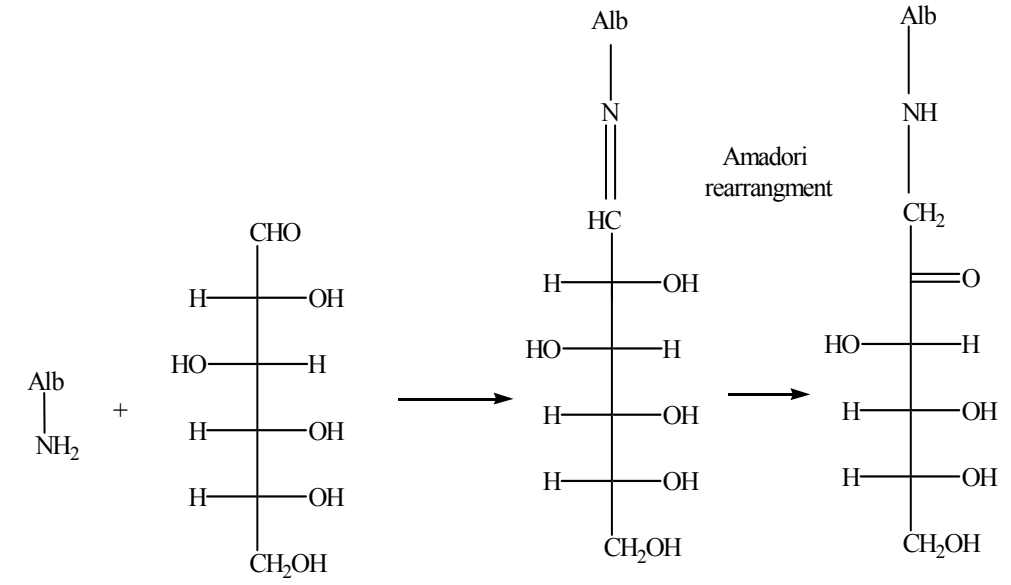

Albumin + D- glucose Schiff base Fructosamine

Studies to investigate the binding capacity of glycated albumin have been done using equilibrium dialysis, ultrafiltration, and high-performance liquid chromatography (Bohney & Feldhoff, 1991; Koizumi et al., 1998; Mikulikova et al., 2005). Disadvantages to using equilibrium dialysis are volume shifts, nonspecific adsorption to the dialysis apparatus, and Donan effects (Oravcova et al., 1996). A pitfall to ultrafiltration is the necessity for a large number of data points. The problematic aspect of high pressure liquid chromatography is the high sample consumption rate. Contradictory reports have given impetus to further develop simplistic methods that can provide accurate information for characterizing the effects of serum albumin glycation on drug binding.

The use of CE as an analytical tool for addressing biochemical questions of interest is demonstrated in this dissertation by developing methods to characterize the effects of ibuprofen and glycation of BSA on the enantioselection of chiral drugs.

1.5. HYPOTHESIS

I hypothesize that capillary electrophoresis can be systematically optimized to develop experimental protocols and associated fundamental models for examining protein-drug binding and modulation of those interactions through drug-drug displacement and subtle changes in protein structure.

Chapter 2

Materials and Methods

2.1. Chemicals

Bovine serum albumin (cat. No. BP671-1), sodium phosphate dibasic (cat. No. 5374-500), phosphoric acid (85%) (cat. No. 7664-38-2), methanol (cat. No. A452SK-4), and sodium hydroxide (NaOH) (cat. No. 1310-73-2) were purchased from Fisher Scientific (Fair Lawn, NJ, USA); D,L-tryptophan (CAS: 54-12-6) was purchased from ACRŌS Organics (Fair Lawn, NJ, USA); Ibuprofen (cat. No. I-1892), 5-fluoro-D,L-tryptophan (cat. No. 154-08-5), deuterium oxide (D_2O) (cat. No. 7789-20-0), and 5-hydroxy-D,L-tryptophan (cat. No. 114-03-4) were purchased from Sigma Aldrich (St. Louis, MO, USA). Sodium phosphate monobasic (cat. No. 4011-1) was purchased from J.T. Baker, Inc. (Phillipsburg, NJ, USA). D- (+)-glucose (cat. No.194672) was purchased from MP Biomedicals, LLC (Solon, OH, USA). Solutions were prepared in deionized water treated using a Water PRO Plus system by LABCONCO (LABCONCO Corp, Kansas City, MO, USA).

2.2. Instrumentation

2.2.1. Capillary electrophoresis (CE)

An Agilent G1600 HP^{3D} Core CE system (Santa Clara, CA, USA) was employed for separations. Data acquisition and instrument control were by ChemStation

software (Agilent, Waldbronn, Germany). Data were exported to Excel (Microsoft, Redmond, WA, USA) and then further mathematically processed using SigmaPlot 12 (Systat Software, Inc., San Jose, CA, USA) and BOMEM GRAMS/386 software (ABB Bomem Inc., Québec, Canada) for curve fitting. The separations were performed in bare fused-silica capillaries (cat. No. G1600-60311) purchased from Agilent with 48.5 cm total lengths, effective lengths of 40 cm, and internal diameters of 75μm. New capillaries were rinsed with NaOH (0.3 M) for 30 min, and deionized water for 30 min, then background electrolyte for 60 min at 920 mbar. When not in use, capillaries were rinsed with 0.1 M NaOH for 10 minutes, water for 10 minutes, air for 20 minutes, and stored dry. The capillary temperature was maintained at 25°C throughout separations. Samples were injected hydrodynamically using 20 mbar pressure for 5 seconds.

2.2.2. Mass Spectrometer

Mass spectra were acquired on a Bio-TOF III high resolution mass spectrometer (Bruker Daltonics, Billerica, MA, USA). Data was acquired by DataAnalysis 3.2 software (Bruker Daltonics, Billerica, MA, USA). Samples were injected into the mass spectrometer using a Cole Palmer syringe pump (cat. No.74900-05, Vernon Hill, IL, USA).

2.2.3. Proton Nuclear magnetic resonance

A Varian INOVA 600 NMR spectrometer (Palo Alto, CA, USA) equipped with : (1) a triple resonance inverse probe (1H/13C/X), (2) a broadband observe probe with a 13C/1Hdecouple channel (X/13C/1H), (3) an inverse nanoprobe for 1H MAS spectroscopy in small volumes (40 μl), (4) a variable temperature unit (FTS Systems,

XR401 air-jet crystal cooler, $-40°C$ to $+100°C$, and (5) a Zymark XP robotics sample changer.

2.3. Determine relevant parameters for improving enantioselection and migration time reproducibility

Consecutive runs were made of D,L tryptophan (0.5 mg/ml), chosen arbitrarily for simplicity, in the presence of 30 μM BSA. Previous studies aimed at assessing enantioselection of tryptophan enantiomers reported optimized resolution occurs when there is a concentration of 30 μM BSA in the background electrolyte (Hödl et al., 2006). Buffer concentration and temperature listed as optimal for BSA binding employed in HPLC separations were 25 mM sodium phosphate, pH 7.4 at 25°C (Gilpin et al., 1991). As a result of these findings, initial experiments were carried out under these conditions. The tryptophan-BSA model was used in this study. Four separate preconditioning experiments were carried out to investigate the effects of protein adsorption on enantioselection.

2.3.1. Ohm's Law plot

To assure joule heating would be minimized, an Ohm's Law plot was constructed to determine the buffering capacities of 25 mM, 50 mM, 75mM, and 100 mM sodium phosphate buffer systems before serum protein addition.

Solution preparation

A concentrated 0.1 M sodium phosphate buffer was prepared by placing 2.62 g of sodium phosphate monobasic, and 14.42 g sodium phosphate dibasic into a 1L volumetric flask. To the flask 800 ml of water was added, pH of solution was

adjusted to 7.4 using phosphoric acid (85%), then additional water was added to bring final volume to 1 L. The 25 mM, 50 mM, and 75 mM sodium phosphate buffers were prepared by pipeting 3.75 ml, 7.5 ml, and 11.25 ml of the 0.1 M buffer into separate volumetric flask, respectively. Each solution was brought to a final volume of 15 ml with deionized water. Prior to use, buffers were degassed by mixing with a magnetic stir bar while under vacuum. They were also filtered through a Fisherbrand 0.20 μm pore size, PTFE filter (Fisher Scientific, Fair Lawn, NJ, USA). Sodium hydroxide (0.1M) was prepared in deionized water. It was also degassed by stirring and vacuum suction.

CE instrumental set-up

The instrument settings were as follows: CE MODE, CE; INJECTION BY, No Injection; Lift Offset: 4 mm, Cassette Temperature, 25°C; CE Conditioning: Replenish (none), Postconditioning (none), Preconditioning (Use Table); Diode Array Detector (DAD) Signals: A- 200, B-240, C-260, D- 270, E- 280, and spectrum store- All in peak, with a threshold of 2.00 mAu; Time Table tab checked voltage, current, and temperature with a stoptime of 0.20 min; Switch Electric was set to on with a positive polarity and a voltage ramp of 0 to 30 kV was applied. At the capillary inlet were vials containing 1 ml of NaOH (0.1M), deionized water, and sodium phosphate buffer (25 mM - 100 mM). At the capillary outlet were vials containing 1 ml of sodium phosphate buffers (25 mM -100 mM), deionized water, and an empty vial for waste.

Separation method and data acquisition

The following steps were used for constructing the Ohm's plot for each buffer system tested: 1) Rinsed capillary 1 minute with NaOH (0.1M) with an applied pressure of 50.0 mbar; 2) Waited 4 minutes; 3) Rinsed capillary 1 minute with water with an applied pressure of 50.0 mbar; 4) Rinsed the capillary 1 minute with sodium phosphate buffer with an applied pressure of 50.0 mbar; 5) Switched on voltage for 2.5 minutes with a ramping time of 1 minute; 6) Recorded the current and voltage.

Data processing

Current and voltage signals were exported as CSV files to Excel (Microsoft, Redmond, WA, USA). The buffering capacity was evaluated by plotting the current as a function of applied voltage.

2.3.2. Applied voltage effects on peak shape

Solution preparation

The background electrolyte, 25 mM sodium phosphate containing 30 μM BSA, pH 7.4, was prepared from a 0.1 M concentrated solution. The 0.1 M concentrated sodium phosphate solution and 0.1M NaOH were prepared as described in section 2.3.1. The BGE was prepared as follows: 1) Added 0.1188 g of BSA to 15 ml of 0.1 M sodium phosphate buffer, pH 7.4; 2) Removed 3.75 ml of the BSA solution and placed it into a volumetric flask. 3) Diluted the solution to a final volume of 15 ml with deionized water. Samples were prepared by dissolving D,L-tryptophan in deionized water (0.5 mg/ml). The sample plug volume in the capillary was 17.97 nl. The total capillary volume was 2143 nl. The mole ratio of drug:BSA in the capillary interacting was 1:2. Prior to use, buffers and samples were degassed by mixing with a

magnetic stir bar while under vacuum. Buffers and samples were filtered through a Fisherbrand 0.20 μm pore size, PTFE filter (Fisher Scientific, Fair Lawn, NJ, USA).

CE instrumental set-up

The instrument settings were as follows: CE MODE, CE; INJECTION BY, Pressure 20 mbar for 5 seconds; Lift Offset: 4 mm, Cassette Temperature, 25°C; CE Conditioning: Replenish (none), Postconditioning (none), Preconditioning (Use Table) table set-up is described in the next section below ; DAD Signals: A- 191, B-200, C-254, D- 270, E- 280, and spectrum store- All in peak, with a threshold of 2.00 mAu; Time Table tab checked voltage, current, and temperature with a stop time of 30.0 min; Switch Electric was set to on with a positive polarity, constant voltages of 10 kV to 30 kV were applied.

Separation method and data acquisition

To test applied voltage, the CE preconditioning table was configured as follows: 1. FLUSH 3.00 min with NaOH (0.1 M); 2. FLUSH 3.00 min with water; 3. FLUSH 8 min with BGE. The outlet vials for all flushing steps were empty waste vials. Following preconditioning of the capillaries surface, a constant separation voltage of 10 kV to 30 kV was applied over a 30 minute separation. The migration time of enantiomers was recorded at each voltage.

Data processing

The 280 nm signal was exported as a CSV file to Excel (Microsoft, Redmond, WA, USA). The mobility determined from enantiomer migration time and applied voltage, as described in equation 5. The mobility of analyte was determined first in BGE void of BSA. The viscosity of the BGE changed upon the addition of BSA. To

account for changes in BGE viscosity associated with the addition of protein, a corrected migration time, $t_{drug} - t_{EOF}$, where t_{drug} and t_{EOF} is the migration time of the enantiomer and EOF, respectively, was used to create the plot.

To redraw electropharograms, corrected data were saved as text delimited files and exported to BOMEM GRAMS/386 program for curve fitting. The selectivity was measured for both enantiomers at each applied voltage. The difference in selectivity as a function of voltage was plotted.

2.3.3. Sodium hydroxide and water rinse effects on migration time

Solution preparations

The BGE was prepared as described in 2.3.2. The sodium hydroxide was prepared as described in 2.3.1.

CE instrumental set-up

The CE instrumental set-up was as described in 2.3.2. with the following modifications: 1) Switch electric was set to on with a positive polarity voltage of 15 kV; 2) preconditioning table set-up is described in the next section below.

Separation method and data acquisition

To test sodium hydroxide -water rinse times, the CE preconditioning table was initially configured as follows: 1) FLUSH 3.00 min with NaOH (0.1 M); 2) FLUSH 3.00 min with deionized water; 3) FLUSH 8 min with BGE. Flush times with NaOH (0.1 M) and water were increased by an increment of 3 min every fourth injection, to a final rinse time of 15 min. The outlet vials for all flushing steps were empty waste vials. Following preconditioning of the capillaries surface, a separation voltage of

15 kV was applied for 30 minutes. The migration times of enantiomers and acetone (n = 4) were recorded.

Data processing

The 280 nm signal was exported as a CSV file to Excel (Microsoft, Redmond, WA, USA). Fluctuation in migration time associated with change in BGE viscosity was corrected by subtracting the migration time of acetone. The difference in migration time of acetone as a function of NaOH/water rinse time between consecutive injections (n =4) was measured.

2.3.4. Evaluating the selectivity as a function of BGE rinse time

Solution preparations

The BGE and samples were prepared as described in 2.3.2. The sodium hydroxide was prepared as described in 2.3.1.

CE instrumental set-up

The CE instrumental set-up was as described in 2.3.2. with the following modifications: 1)Switch electric was set to on with a positive polarity voltage of 15 kV; 2)preconditioning table set-up is described in the next section below.

Separation method and data acquisition

To test BGE rinse times, the CE Preconditioning table was initially configured as follows: 1) FLUSH 3.00 min with NaOH (0.1 M); 2) FLUSH 3.00 min with deionized water; 3) FLUSH 8 min with BGE. Flush times with BGE were increased by an increment of 8 min every fourth injection, to a final rinse time of 32 min. The outlet vials for all flushing steps were empty waste vials. Following preconditioning

of the capillaries surface, a separation voltage of 15 kV was applied for 30 minutes. The migration times of enantiomers and acetone (n = 4) were recorded.

Data processing

Data was processed as described in 2.3.2. with the following modification: The change in the selectivity as a function of BGE rinse time was measured.

2.3.5. Evaluating the selectivity as a function of wait time

Solution preparations

The BGE and samples were prepared as described in 2.3.2. The sodium hydroxide was prepared as described in 2.3.1.

CE instrumental set-up

As described in 2.3.2. With the following modifications: Switch electric was set to on with a positive polarity voltage of 15 kV; preconditioning table set-up is described in the next section below.

Separation method and data acquisition

To test wait times, the CE Preconditioning table was initially configured as follows: 1) FLUSH 3.00 min with NaOH (0.1 M); 2) FLUSH 3.00 min with water; 3) FLUSH 8 min with BGE; 4) WAIT 10 min. Wait times prior to separation voltage application were increased by an increment of 10 min every fourth injection, to a final wait time of 60 min. The outlet vials for all flushing steps were empty waste vials. Following preconditioning of the capillaries surface, a separation voltage of 15 kV was applied for 30 minutes. The migration times of enantiomers and acetone (n = 4) were recorded.

Data processing

Data was processed as described in 2.3.2. with the following modification: The change in selectivity as a function of wait time was measured.

2.3.6. Evaluating the selectivity as a function of sample buffer ionic strength

Solution preparations

The BGE was prepared as described in 2.3.2. The sodium hydroxide was prepared as described in 2.3.1. Samples were prepared by dissolving tryptophan (0.5 mg/ml) in sodium phosphate buffer, pH 7.4, of ionic strengths 5 mM to 25 mM. All buffers were prepared from 0.1 M concentrated buffer. Prior to use, buffers and samples were degassed by mixing with a magnetic stir bar while under vacuum. Buffers and samples were filtered through a Fisherbrand 0.20 μm pore size, PTFE filter (Fisher Scientific, Fair Lawn, NJ, USA).

CE instrumental set-up

The CE instrumental set-up was as described in 2.3.2. with the following modifications: 1) Switch electric was set to on with a positive polarity voltage of 15 kV; 2) preconditioning table set-up is described in the next section below.

Separation method and data acquisition

The CE Preconditioning table was configured as follows: 1. FLUSH 3.00 min to with NaOH (0.1 M); 2. FLUSH 3.00 min with water; 3. FLUSH 8 min with BGE; 4. WAIT 10 min. The outlet vials for all flushing steps were empty waste vials. Following preconditioning of the capillaries surface, a separation voltage of 15 kV was applied for 30 minutes. The migration times of enantiomers and acetone (n = 4) were recorded.

Data processing

Data were processed as described in 2.3.2. With the following modification: The difference in selectivity as a function of sample buffer ionic strength was measured.

2.4. Capillary electrophoresis applications for studying competitive binding.

The displacement of L-tryptophan by ibuprofen can be determined by using ibuprofen as an additive to the BGE (Berezhkovskiy, 2006). The influence of ibuprofen on the enantioselection of 5-fluoro-D,L-tryptophan and D,L-tryptophan by BSA was studied. The tryptophan-BSA model was employed.

Solution preparations

For binding constant measurements BGEs containing 0, 10 μM, 15 μM , 20 μM, 30 μM, and 35 μM BSA were employed. The sodium phosphate 0.1M buffer was prepared as described in 2.3.1. To obtain the desired BSA molar concentrations, protein was added to 15 ml of 0.1M sodium phosphate, pH 7.4 as following: 10 μM, 0.0396 g; 15 μM, 0.0594 g; 20 μM, 0.0792 g; 30 μM, 0.1188 g; and 35 μM, 0.1386 g. For competitive binding studies, ibuprofen solution was added to BGE (35 μM) at a concentration ranging from 0 to 55.3 μM. Samples of D,L-tryptophan and 5-fluoro-D,L-tryptophan (0.0225 to 0.54 (mg/ml)) in 8 mM sodium phosphate, pH 7.4. Prior to use, samples and buffers were degassed and filtered through a Fisherbrand 0.20 μm pore size, PTFE filter (cat. No. 09-720-7) (Fisher Scientific, Fair Lawn, NJ, USA).

CE instrumental set-up

The CE instrumental set-up was as described in 2.3.2. with the following modifications: 1) Switch electric was set to on with a positive polarity voltage of 15 kV; 2) preconditioning table set-up is described in the next section below.

Separation method and data acquisition

The CE Preconditioning table was configured as follows: 1) FLUSH 3.00 min with NaOH (0.1 M); 2) FLUSH 3.00 min with deionized water; 3) FLUSH 8 min with BGE; 4) WAIT 10 min. The outlet vials for all flushing steps were empty waste vials. Following preconditioning of the capillaries surface, a separation voltage of 15 kV was applied for 30 minutes. The migration times of enantiomers and acetone (n = 4) were recorded.

Data processing

Data were processed as described in 2.3.2. with the following modification: The difference in selectivity as a function of ibuprofen concentration was measured.

2.5. Capillary electrophoresis applications for studying binding of glycated serum proteins.

Solution preparations

The BGE for control and test experiments were prepared in both deionized water (H_2O) and deuterium oxide (D_2O) as described in 2.3.2. D-glucose (14.5 mM) was added to the test BGE. Samples were prepared as described in 2.3.2. The sodium hydroxide was prepared as described in 2.3.1. A 50 ml methanol/water (80/20) solution containing 0.1% trifluoroacetic acid (TFA) was prepared by placing 39.96 ml methanol, 9.99 ml deionized water, and 50 µl TFA in a 50 ml volumetric flask.

The BGE employed for mass spectral analysis, was prepared as follows: 0.25 ml of BGE (H_2O) was placed into a microcentrifuge tube and diluted with methanol/water solution to a final volume of 1.0 ml.

Instrumental set-up

Capillary Electrophoresis

The CE instrumental set-up was as described in 2.4.2.

NMR

The instrument was set at the following: ^{1}H resonance frequency = 600 MHz; CPMG spin echo pulse sequence (Echo Time, TE = 30 msec). Measurements were taken at 25°C.

Mass Spectrometry

The instrument settings were as follows: ESI Ionization; Positive Polarity; Drying Gas Temperature 250°C; sample rate 2 GS/ s; delay time, 25 μs; Capillary, 4 kV; End Plate, 3.5 kV; Cylinder, 2 kV; Digitizer Summing, 500 spectra.

Separation method and data acquisition

Capillary Electrophoresis

Data were acquired as described in 2.4.3.

NMR

Data were acquired over 8 hours using: 1.0 s Relax. Delay; pulse of 34.6 degrees; Acq. Time 4.0 sec; Width 8,000 Hz.

Mass spectrometry

Mass spectra were recorded using 0.5 ml of BGE (H_2O) injected from a 0.5 ml Gastight syringe (cat. No. 1750, Hamilton Co., Reno, NV, USA) using a flow rate of

100 µl/hr. Mass spectrum was acquired by setting the Deconvoluted parameters tab in the DataAnalysis 3.2 software (Bruker Daltonics, Billerica, MA, USA) to the following: Proteins/Large Molecules; Adduct ions (+H, -H); low mass, 1000 (m/z) and high mass, 100,000 (m/z); abundance cutoff, 10%; maximum charge, +75.

Data processing

Capillary Electrophoresis

Data were processed as described in 2.3.2. with the following modifications: The difference in selectivity as a function of glycation extent was measured.

NMR

Data were processed by the following parameters: Line broadening 0.3 Hz; FT size 65536.

Mass Spectrometry

The number of glucose molecules was determined by the following steps: 1) A detailed deconvoluted mass was measured for unmodified BSA. Results were exported to Excel (Microsoft, Redmond, WA, USA) and externally calibrated by dividing the calculated mass by the literature reported mass for BSA (66.4 kD). The quotient was used as the calibration constant. 2) The corrected deconvoluted masses for weeks 1 -3 were determined by dividing the experimentally determined masses for each by the calibration constant. 3) The mass difference between control BSA and that for weeks 1-3 was measured. An observed change in BSA mass was used as a marker for extent of glycation.

Chapter 3

Results and Discussion

3.1. Determine relevant parameters for improving enantioselection and migration time reproducibility

Early work focused on elucidating the enantiomeric selectivity of serum albumins for D- and L- tryptophan, found that the L-enantiomer of tryptophan binds to site II with an affinity approximately 100 times higher than that of the D-enantiomer (McMenamy & Oncley, 1958). Investigations by Yang and Hage found that the D-enantiomer interacts with site I indirectly, but has no interaction with site II (Yang & Hage, 1993). The pH and ionic strength of the BGE used in this study is similar to that approximated under physiological conditions. The native state of the protein and its molecular function are preserved (Yang & Hage, 1993). Under these conditions optimum binding of D- and L-tryptophan to bovine serum albumin was found to occur (Gilpin et al., 1991). Therefore it is of importance to determine the relevant experimental parameters that are required for optimum enantioselectivity prior to carrying out further protein-drug binding investigations.

There is little information regarding the exact experimental conditions that are most relevant for improving chiral recognition by serum proteins in CE applications. Several factors affect the precision of measurement such as buffer viscosity, sample

plug length, and applied voltage. The major challenge is the change in EOF over time caused by protein interactions with the inner surface of the capillary. A protein's tendency to adsorb is determined by its primary structure, structural stability, charge, and size (Nakanishi et al., 2001). Protein adsorption to the capillary inner surface can be reduced by developing rinsing strategies. Adverse effects from conductivity can be minimized by using multivalent ions to prepare BGE. Phosphate buffers, similar to that employed in this study, have been reported to decelerate adsorption by stabilizing the native structure of the protein (Kurrat et al., 1997). The aim of this section was to determine the relevant parameters that improve enantioselection of D- and L-tryptophan by BSA.

3.1.1. Ohm's Law Plot

Band broadening at higher voltages is caused by Joule heating. This heat is generated by collisions that occur between solute ions and electrolyte ions. The extent of heating is based on the conductivity of the BGE and the voltage applied. Higher ionic strength buffers usually are employed to minimize ion-exchange effects between charged solute and ionized silanol groups on the capillary wall. High ionic strength buffers can yield increased heating at constant voltage. The amount of heat generated using high currents may be beyond the thermostat capabilities of the CE instrument employed.

Figure 10: Ohm's law plots showing the optimum voltage for sodium phosphate buffers, pH 7.4 (25- 100 mM). ACE conditions: capillary temperature 25°C.

Figure 10.

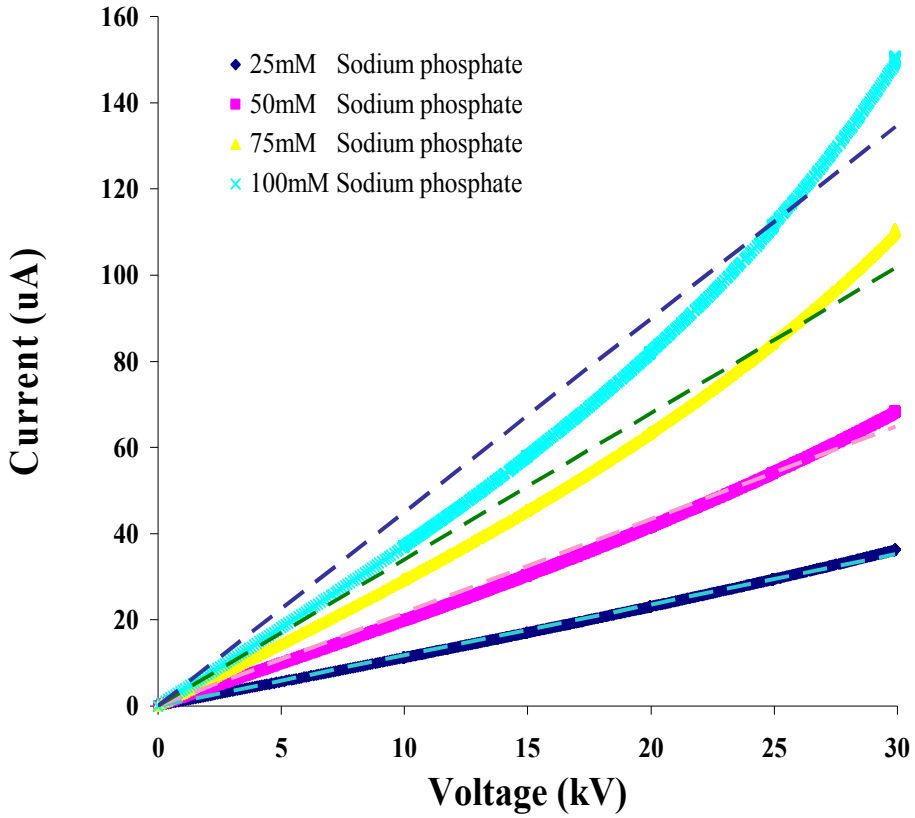
160
140
120
100
80
60
40
20
0
Current (uA)
25mM Sodium phosphate
50mM Sodium phosphate
75mM Sodium phosphate
100mM Sodium phosphate
0
5
10
15
20
25
30
Voltage (kV)

Although capillaries are cooled on the outer surface, a significant temperature difference between the BGE in the center and the inner capillary wall can occur leading to nonuniform temperature gradients within the capillary as well as localized changes in BGE viscosity. The generation of heat can evaporate BGE solution. Therefore heat dissipation should be efficient to avoid these adverse effects. Thermal effects can be circumvented by adjusting the ionic strength of the BGE.

In order to determine the maximum voltage that could be applied without exceeding the heat removal capacity of sodium phosphate buffers ranging in concentration from 25 – 100 mM, an Ohm's law plot was constructed, as illustrated in Figure 10. Each set of data was fitted by linear regression as represented by the dashed lines. The regression coefficients for the 25 mM, 50 mM, 75 mM, and 100 mM buffers were 0.996, 0.987, 0.970, and 0.951, respectively. Linearity in the plot was an indication that the generated heat was being adequately dissipated and capillary temperature was maintained. Deviation from linearity was an indication that the thermostatting capability of the system had been exceeded. Linearity was lost for both the 75 mM and 100 mM buffers at lower applied voltages, in comparison to those observed for the 25 mM and 50 mM concentrations. In contrast, the 25 mM buffer exhibited a linear relationship between current and the applied voltage across the entire range of voltages studied (0- 30 kV), indicating its ability to maintain capillary temperature at the maximum applied voltage allowed by the instrument. Subsequently, the 25 mM buffer system was employed for the remaining studies.

3.1.2. Applied voltage effects on peak shape

Human serum albumin adsorption to capillary walls decreases in the presence of an electric field (Yang & Hage, 1994). Mechanisms involved in separating D- and L- tryptophan depend upon the concentration of protein that is free floating in BGE. Therefore application of a separation voltage, which minimizes adsorption of protein to the inner walls of the capillary, will result in improved enantioselection, while those that do not will cause a loss in enantioselection.

This idea was studied by initially applying separation voltages of 10- 30 kV. Enantiomer peaks were not observed at applied voltages below 10 kV. Applied voltages >15 kV produced currents that were above 100 μA. To avoid diffusion caused by joule heating associated with high currents, voltages above 15 kV were not used in all later experiments. Electropharograms for D,L-tryptophan at separation voltages of 10 kV and 15 kV are illustrated in Figure 11 and Figure 12, respectively. Peak shape distortion was evident at voltages below 15 kV. By using a separation voltage of 15 kV, peak shape distortion was no longer observed and enantioselectivity was improved. These results indicated that the stability of absorbed BSA was highest in the presence of lower applied voltage. This is the same type of behavior seen in earlier studies (Yang & Hage, 1994).

Figure 11: Effect of applied voltage on D- and L- tryptophan separation as represented by peak distortion. BSA concentration in BGE was kept at 30 μM and D,L-tryptophan amount used was 0.54 mg/ml. ACE conditions: 25°C, 20 mbar injection for 5s, detection at 280 nm,10 kV separation voltage.

Figure 11.

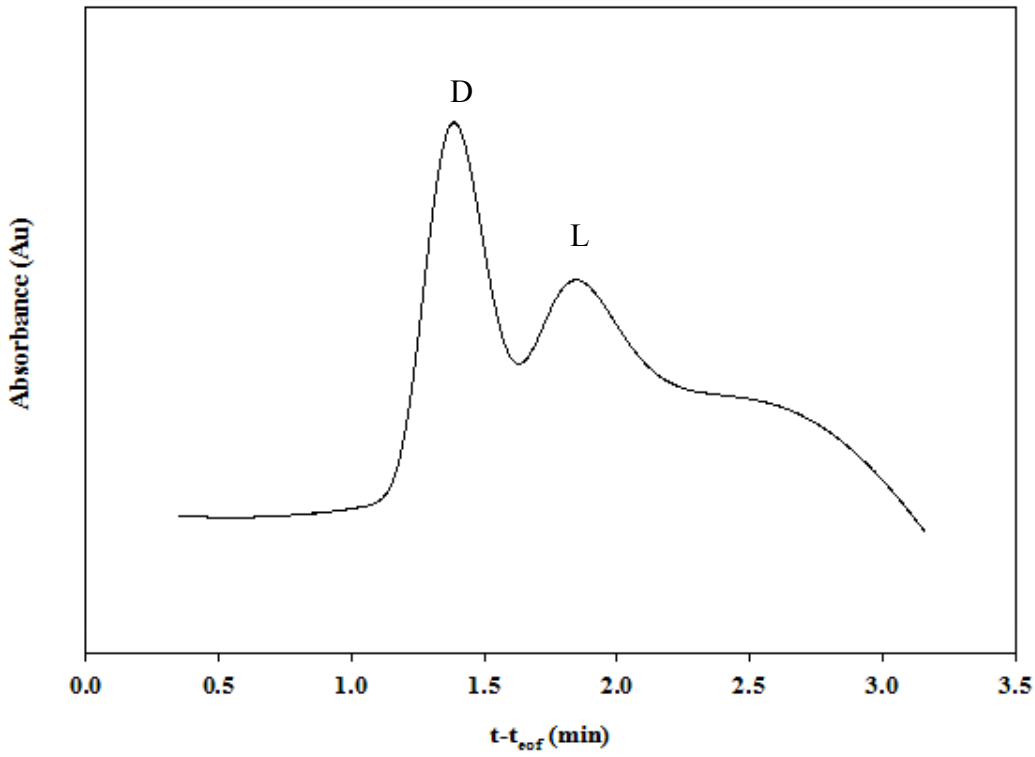

Figure 12: Effect of applied voltage on D- and L-tryptophan separation as represented by peak distortion. BSA concentration in BGE was kept at 30 μM and D,L-tryptophan amount used was 0.54 mg/ml. ACE conditions: 25°C, 20 mbar injection for 5s, detection at 280 nm, 15 kV separation voltage.

Figure 12.

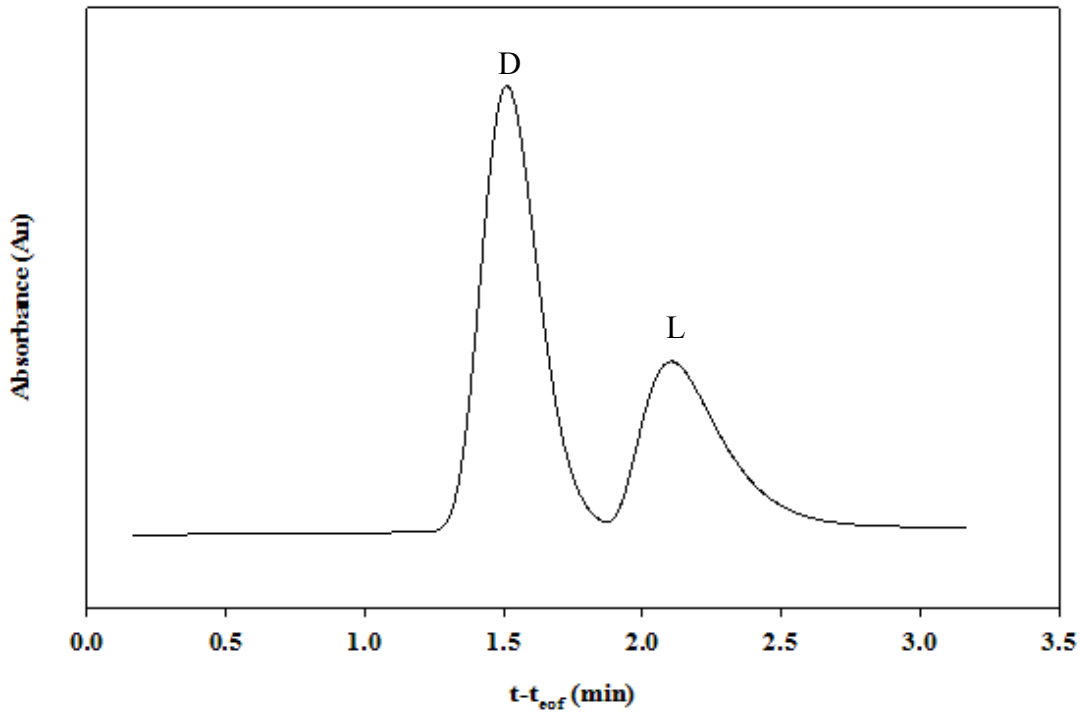

3.1.3. Sodium hydroxide and water rinse effects on migration time

At physiological pH, both the inner capillary wall and BSA are negatively charged. Protein-wall interactions primarily are due to H-bonding that occurs between the carbonyl and amino groups on the protein and the silanol groups on the capillary wall (van der Veen et al., 2004; Gray, 2004). In albumin the average density of amino groups that possess H-binding capability is $0.25/nm^2$ (Kurrat et.al, 1997). Protein adsorption modifies the surface charge of the capillary, contributing to changes in the mobility of the EOF. This allows for the EOF migration time to serve as a marker for protein adsorption (Graf et al., 2005). Rinsing the capillary with additives that cleave H-bonds promotes protein desorption (Docoslis et al., 2001).

Capillary surface regeneration was investigated by rinsing the capillary with 0.1 M NaOH and deionized water at variable times, followed by BGE.
It was found that NaOH rinsing for 3 min at 920 mbar, followed by deionized water for 3 min at 920 mbar was most effective at controlling shifts in EOF mobility, RSD 0.19%, (n = 4) (Figure 13). The repeatability drastically diminished as the rinse time increased.

Rinsing the capillary with excessive amounts of sodium hydroxide has been reported to permit successive saturation of available adsorption sites with protein residues (Ermakov et al., 1995), permitting protein clusters to pile up within consecutive runs. Decrease in the EOF migration time repeatability was substantial for the 9 min rinsing protocol, RSD 12.4%, (n = 4). There was a 3 minute difference in the EOF migration time between the first and second injections. The rinse time was increased to 12 minutes and there was an improvement in repeatability,

RSD 2.4% (n=4), but repeatability remained lower than that for the 3 min rinsing protocol. A 3 min rinsing protocol was used in subsequent studies.

The NaOH and water regime was further investigated by rinsing for 3 min with and without 0.1M NaOH and deionized water between consecutive injections. Each run included a rinse with BGE only. It was found that the RSD improved from 24.7% without NaOH- water rinse to 1.84% (n = 4) with NaOH-water rinse, indicating an improvement in precision due to the removal of protein from the capillary wall. Omission of NaOH-water rinsing, led to inverted peaks in the electropharogram indicating the protein had a higher absorbance at the detection window than D, L-tryptophan (Figure 14). These results indicated that the implementation of a 3 min rinsing protocol was best for stabilizing the EOF of successive separations.

Figure 13: The effect of sodium hydroxide/water rinse time on the repeatability of acetone (neutral marker) migration time in the presence of 30 μM BSA. ACE conditions: 25°C, 20 mbar injection for 5s, detection at 280 nm, 15 kV separation voltage.

Figure 13.

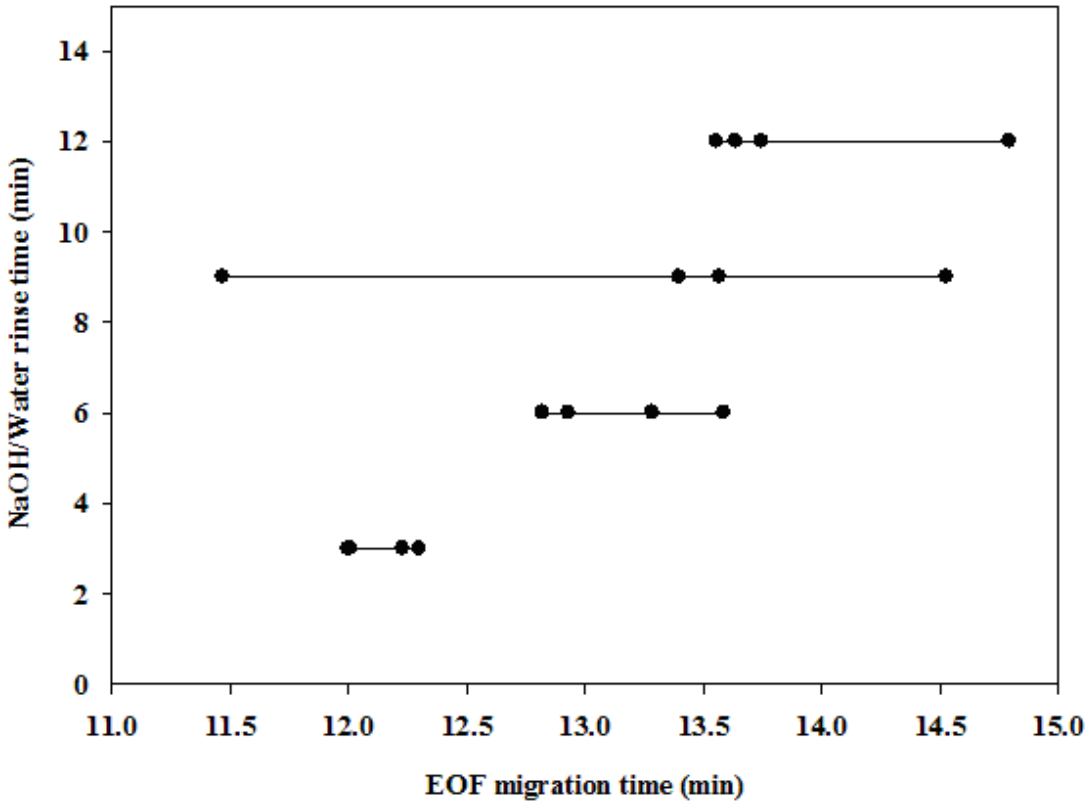
NaOH/Water rinse time (min)
EOF migration time (min)
0
2
4
6
8
10
12
14
11.0
11.5
12.0
12.5
13.0
13.5
14.0
14.5
15.0

Figure 14: D,L-tryptophan (0.54 mg/ml). ACE conditions: 25 mM sodium phosphate, pH 7.4, 30 µM BSA, 25°C, 20 mbar injection for 5s, 15 kV, detection at 280 nm. 0 min NaOH-water rinse between injections. Electropharogram obtained directly from ChemStation software (Agilent, Waldbronn, Germany) without further data processing.

Figure 14.

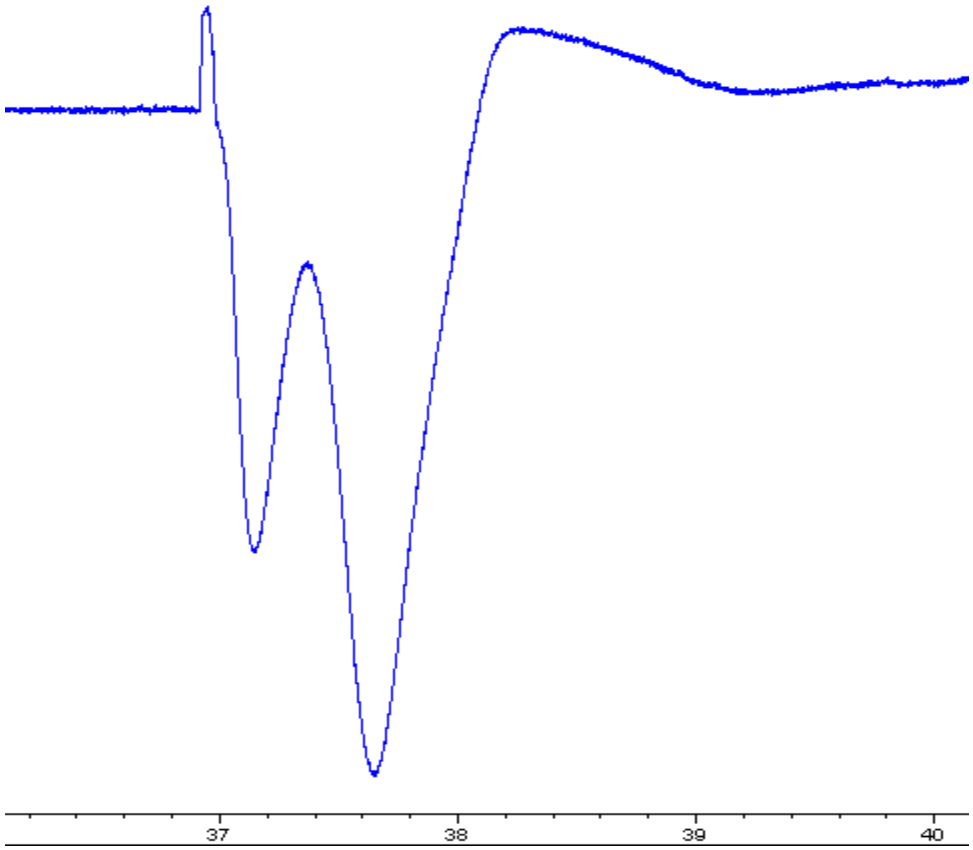

3.1.4. Evaluating selectivity as a function of BGE rinse time

To examine how the inherent tendency of proteins to absorb onto the capillary wall affects enantioselectivity of tryptophan by BSA, the capillary was rinsed with BGE for 6 – 32 minutes using 920 mbar pressure. Representative electropharograms are shown in Figures 15 – 18, for 8, 16, 24, and 32 minute rinse protocols, respectively. Selectivity, α, was calculated as a function of BGE rinse time for four separate injections. Subsequently, a plot of the average selectivity versus BGE rinse time was made (Figure 19) and fitted using a fourth-order polynomial, which yielded a regression coefficient of 1. The first-derivative curve of the selectivity with respect to BGE rinse time was plotted and appears in Figure 20.

The average selectivity (n = 4) for the 6 min, 8 min, 16 min, 24 min, and 32 min rinse times were 1.0×10^{-2}, 1.2×10^{-2}, 8.3×10^{-3}, 1.4×10^{-3}, and 0, respectively. Based upon the amount of protein adsorbed, a non-uniform distribution of the ζ-potential along the capillary occurred (Ren & Li, 2001). Differences in the ζ-potential led to changes in the EOF mobility thereby diminishing selectivity. To determine if the EOF mobility increased between rinsing protocols, the mobility of acetone (neutral marker) was measured at each rinse time. Increase in the EOF mobility was observed (Figure 21). These results were consistent with changes in the charge density on the surface of the capillary. Dissolved ions in the diffuse layer moved at a different velocity between each rinsing protocol (refer to Figure 3).

Figure 15: Electropharogram of D, L- tryptophan (0.54 mg/ml) separation after rinsing the capillary for 8 min with BGE prior to applying the voltage. ACE conditions: 25 mM sodium phosphate, pH 7.4, 30 μM BSA, 25°C, 20 mbar injection for 5s, 15 kV, detection at 280 nm.

Figure 15.

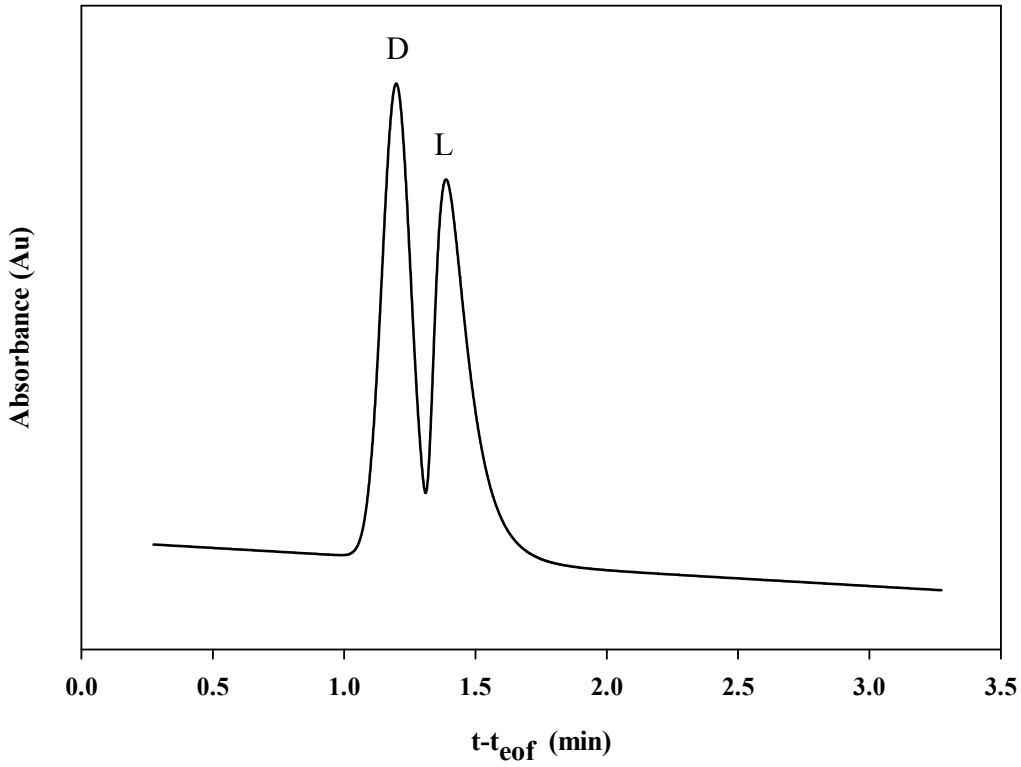

Figure 16: Electropharogram of D, L- tryptophan (0.54 mg/ml) separation after rinsing the capillary for 16 min with BGE prior to applying the voltage. ACE conditions: 25 mM sodium phosphate, pH 7.4, 30 μM BSA, 25°C, 20 mbar injection for 5s, 15 kV, detection at 280 nm.

Figure 16.

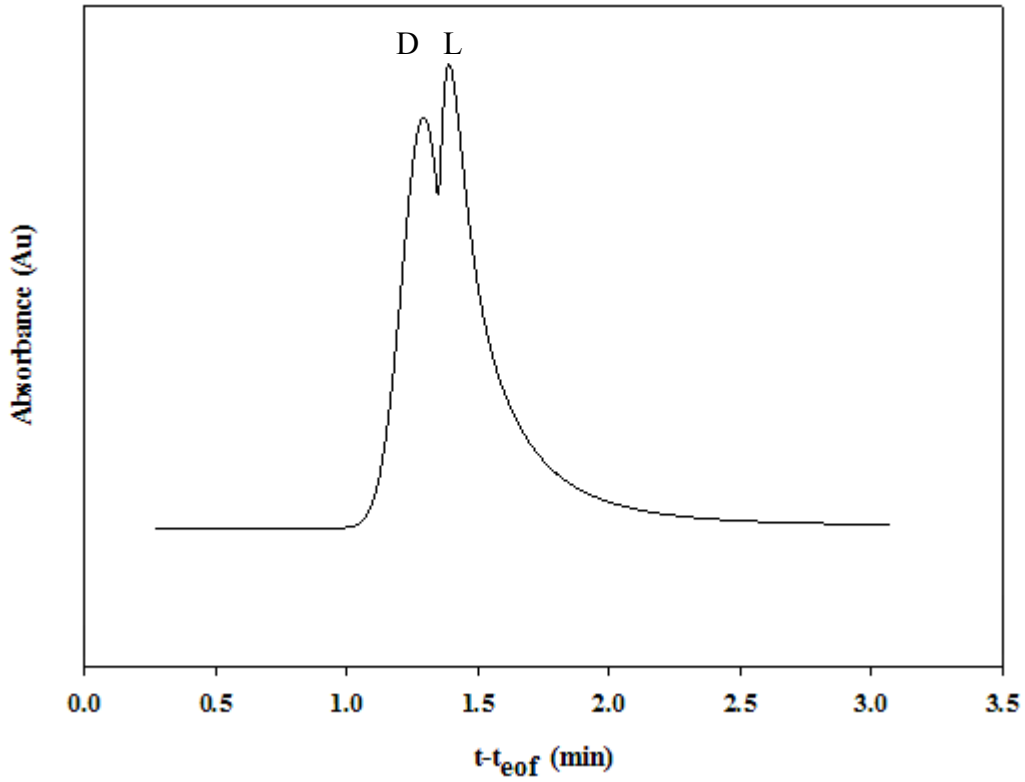

Figure 17: Electropharogram of D, L- tryptophan (0.54mg/ml) after rinsing the capillary for 24 min with BGE prior to applying the voltage. ACE conditions: 25 mM sodium phosphate, pH 7.4, 30 μM BSA, 25°C, 20 mbar injection for 5s, 15 kV, detection at 280 nm.

Figure 17.

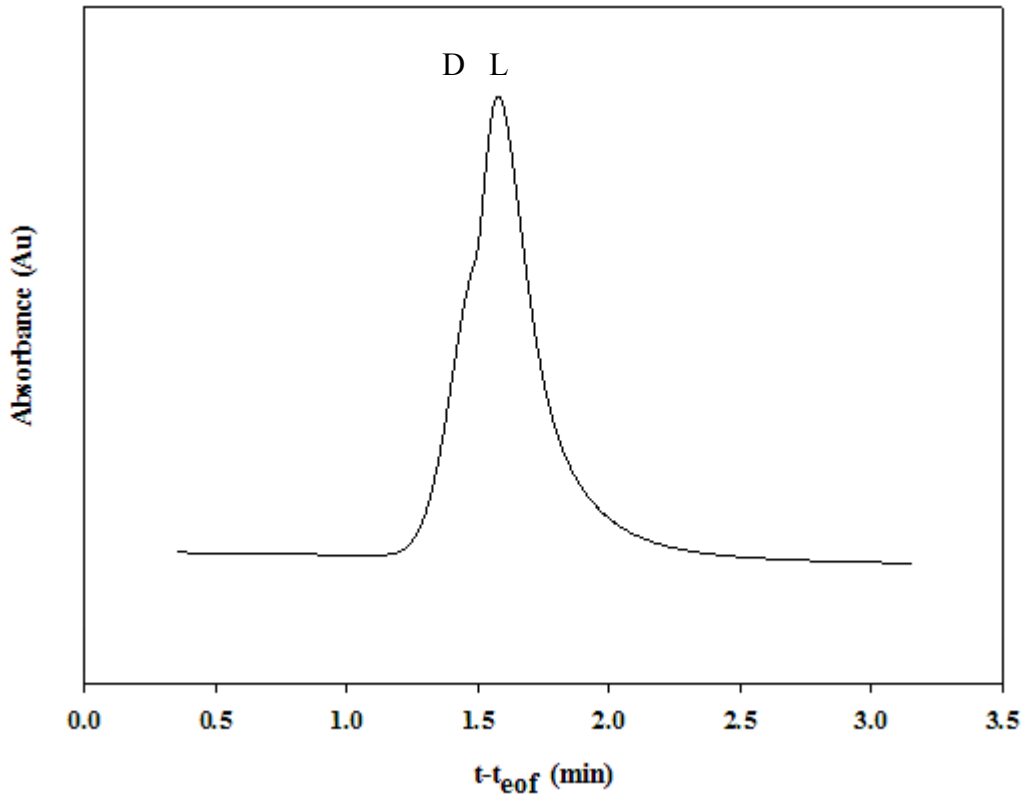

Figure 18: Electropharogram of D, L- tryptophan (0.54mg/ml) after rinsing the capillary for 32 min with BGE prior to applying the voltage. ACE conditions: 25 mM sodium phosphate, pH 7.4, 30 μM BSA, 25°C, 20 mbar injection for 5s, 15 kV, detection at 280 nm.

Figure 18.

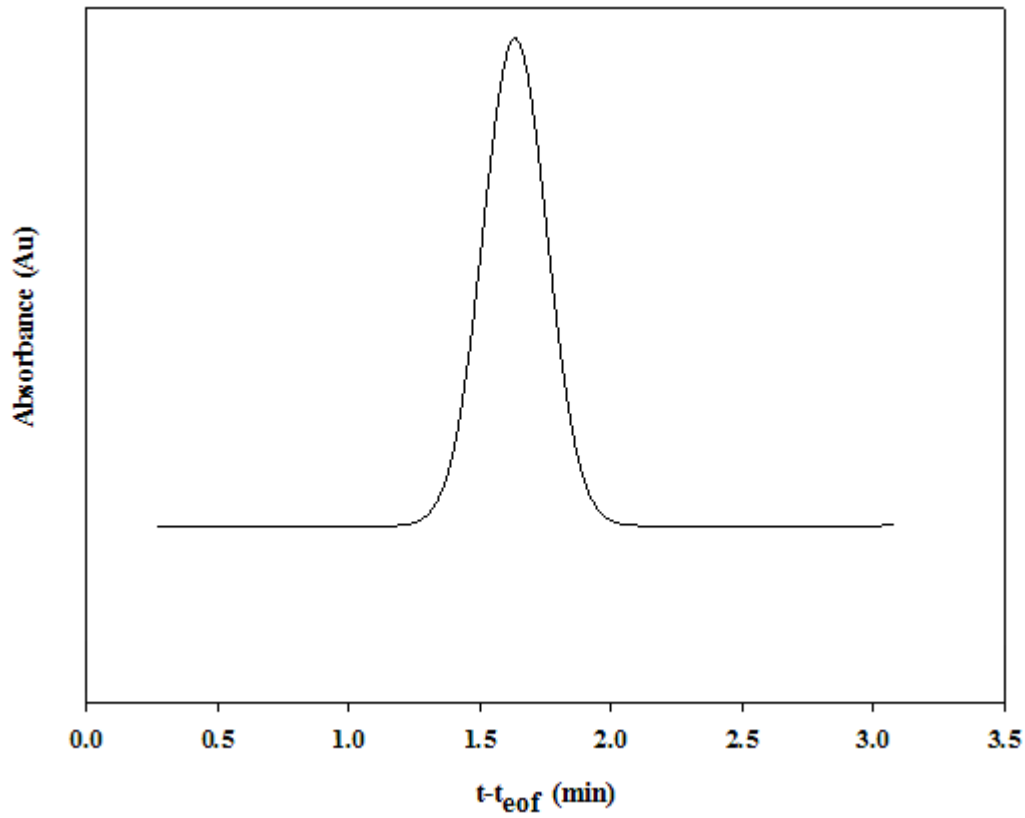

Figure 19: Selectivity versus BGE rinse time. ACE conditions: 25 mM sodium phosphate, pH 7.4, 30 μM BSA, 25°C, 20 mbar injection for 5s, 15 kV, detection at 280 nm. Equation of the 4th order polynomial fitting (solid line): $y = -1.6044E\text{-}07x^4 + 1.5587E\text{-}05x^3 - 5.1466E\text{-}04x^2 + 6.1121E\text{-}03x - 1.1095E\text{-}02$, $R^2 = 1$.

Figure 19.

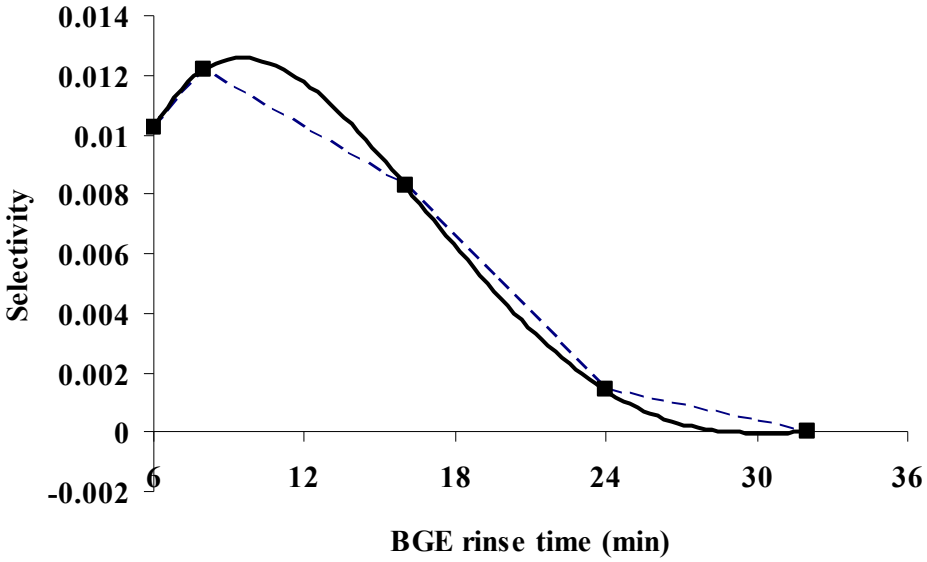
0.014
0.012
0.01
0.008
0.006
0.004
0.002
0
-0.002
Selectivity
6
12
18
24
30
36
BGE rinse time (min)

Figure 20: First derivative of selectivity as a function of BGE rinse time.

Figure 20.

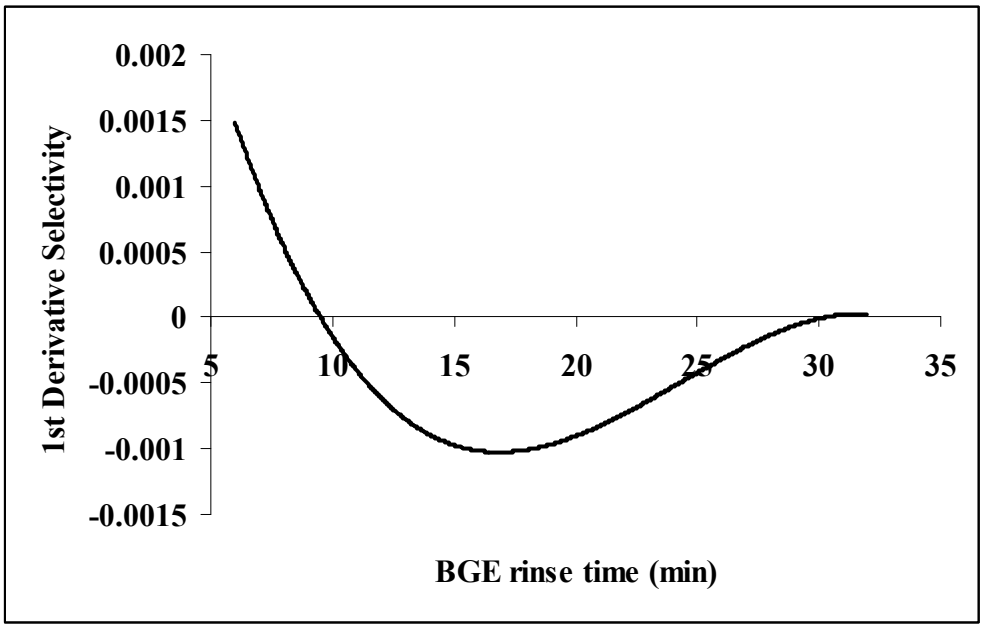
0.002
0.0015
0.001
0.0005
0
-0.0005
-0.001
-0.0015
1st Derivative Selectivity
5
10
15
20
25
30
35
BGE rinse time (min)

Figure 21: Electroosmotic flow rate as a function of BGE rinse time, measured by the mobility of acetone.

Figure 21.

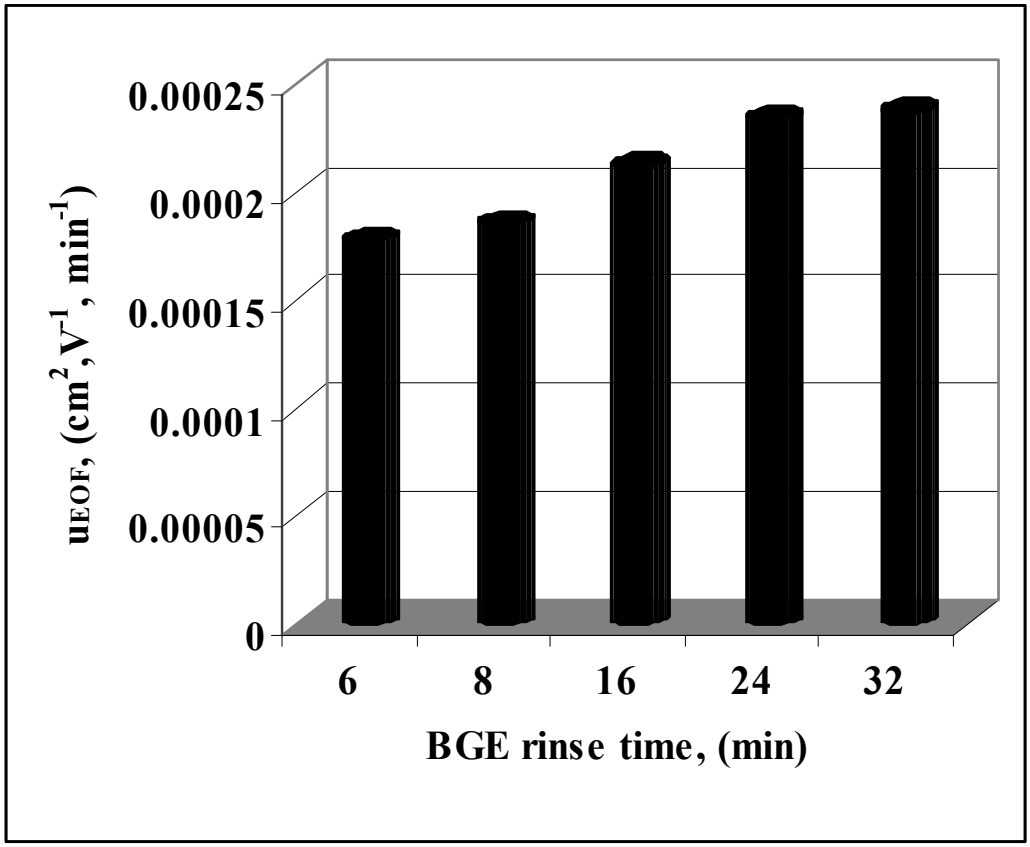
0.00025
0.0002
0.00015
0.0001
0.00005
0
u_{EOF}, (cm^2,V^{-1}, min^{-1})
6
8
16
24
32
BGE rinse time, (min)

Resolution diminished in cases where the EOF was too fast, due to the solute's inability to stack into uniformed zones within the capillary (Towns & Regnier, 1992; Tran et al., 2005). Increased concentrations of protein in the capillary promote environments for protein aggregation, thus leading to dispersion within the sample plug (Malmsten, 1998; Ding et al., 2005; Herr et al., 2000). The effects of rinsing the capillary with the BGE for a duration less than or equal to 8 minutes were negligible on selectivity. Subsequently, remaining experiments were carried out rinsing the capillary for 8 minutes.

3.1.5. Evaluating selectivity as a function of wait time

Prior to adsorption, proteins approach solvent regions directly adjacent to the inner surface of the capillary (Towns & Regnier, 1992). Based upon theory, the selectivity is expected to diminish with increased BGE rinsing time. However, the 8 min rinsing protocol gave the maximum selectivity not the 6 min rinsing protocol. To gather an understanding of this process and determine the effects of protein diffusion on selectivity, following the 8 minute capillary flush with BGE, a wait step was inserted into the rinsing protocol. During this wait step, the BGE was left at a standstill in the capillary for 10- 60 minutes prior to the application of voltage. Representative electropharograms are shown in Figures 22– 24, for 10, 40, and 60 minute wait periods, respectively.

Selectivity was calculated as a function of wait time for four separate injections. Subsequently, a plot of the average selectivity versus wait time was made (Figure 25) and fitted using a fourth-order polynomial, which yielded a regression coefficient of 1. The first-derivative curve of the selectivity with respect to wait time was plotted

and appears in Figure 26. The average selectivity (n = 4) for the 10 min, 20 min, 30 min, 40 min, and 60 min wait times were 2.8×10^{-2}, 2.4×10^{-2}, 1.9×10^{-2}, 1.1×10^{-2}, and 1.0×10^{-2}, respectively.

It is assumed that upon initial filling of the capillary, the concentration of charged ions in the BGE (i.e. protein) is much higher in the center of the capillary, than near the wall. During the wait step, charged ions in the BGE diffuse from the region of high concentration in the center of the capillary, to regions of lower concentration towards the wall. Since the chiral recognition of tryptophan decreases as the concentration of serum protein at the wall increases, enantioselection changes can serve as a marker for protein diffusion (Yang & Hage, 1994).

A pronounced decrease in selectivity was observed as a function of wait time. The effects of protein diffusing away from the central portion of the capillary further supported that observed with BGE rinse time. Differences in the ζ-potential along the capillary that occurred as the concentration of protein at the wall increased led to changes in the EOF mobility that diminished selectivity.

The fore mentioned results indicated that protein diffusion should be limited in the capillary prior to separation. It was expected that wait times below 10 minutes would result in higher selectivity. The 2.3×10^{-2} (n = 4) average selectivity measured without a wait step was 16% lower than the 10 min wait step selectivity. This suggested that controlled protein diffusion could improve chiral recognition. A 10 minute wait step was incorporated into subsequent rinsing protocols.

Figure 22: 10 minute wait. D,L-tryptophan (0.54 mg/ml). ACE conditions: 25 mM sodium phosphate, pH 7.4, 30 μM BSA, 25°C, 20 mbar injection for 5s, 15 kV, detection at 280 nm. The capillary was rinsed for 8 minutes with background electrolyte solution prior to wait period.

Figure 22.

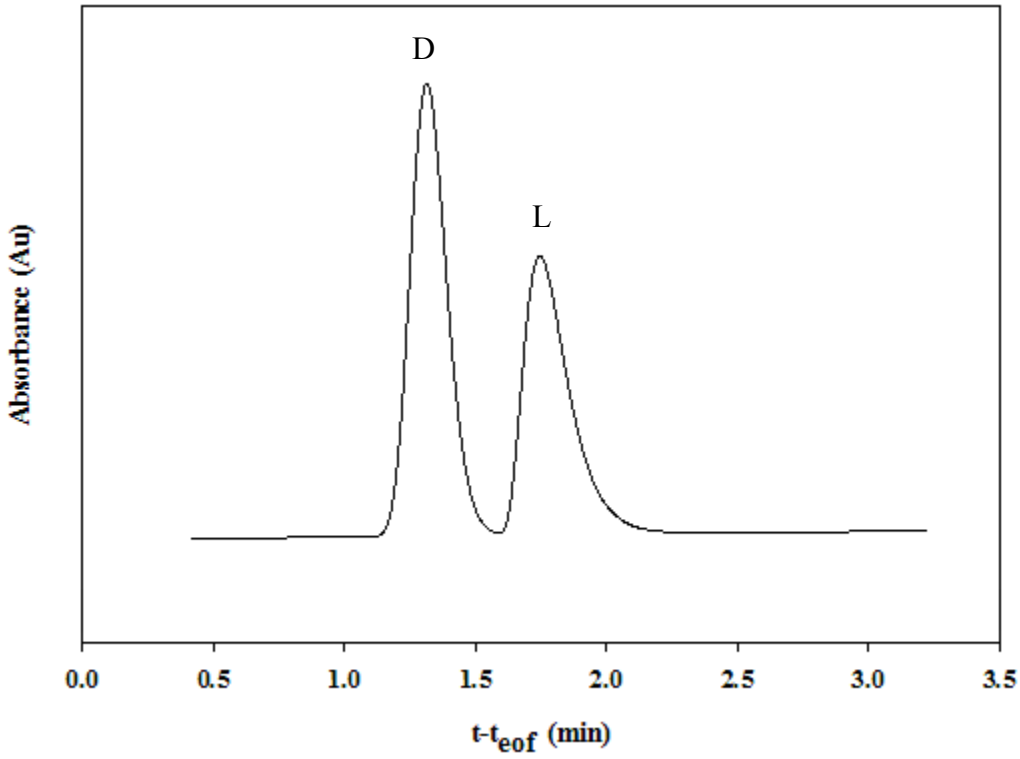

Figure 23: 40 minute wait. D,L-tryptophan (0.54 mg/ml). ACE conditions: 25 mM sodium phosphate, pH 7.4, 30 μM BSA, 25°C, 20 mbar injection for 5s, 15 kV, detection at 280 nm. The capillary was rinsed for 8 minutes with background electrolyte solution prior to wait period.

Figure 23.

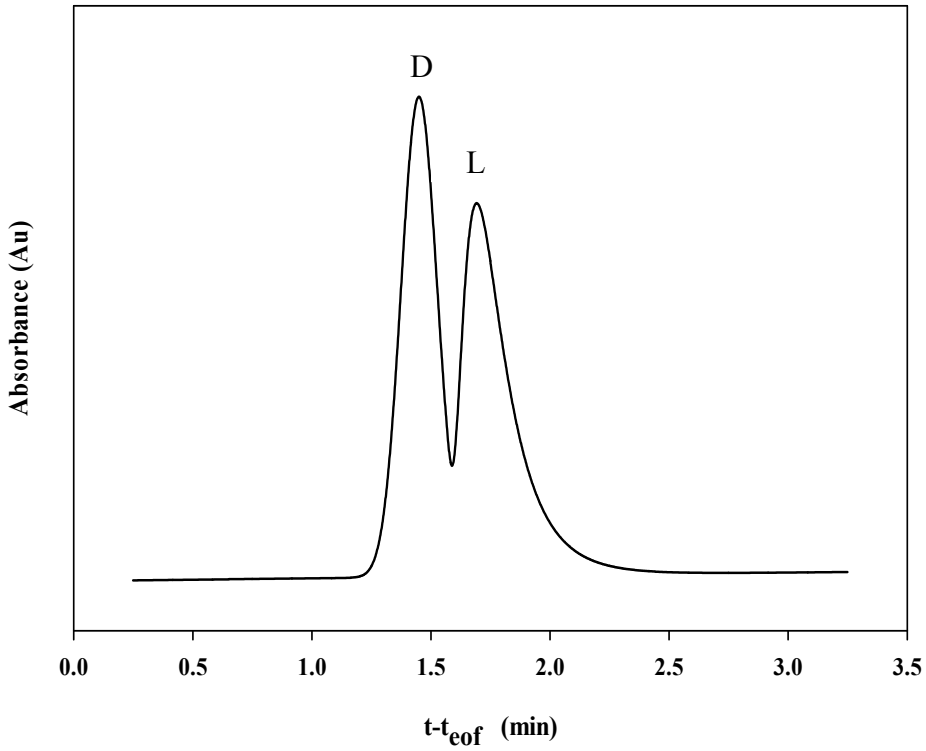

Figure 24: 60 minute wait. D,L- tryptophan (0.54 mg/ml). ACE conditions: 25 mM sodium phosphate, pH 7.4, 30 μM BSA, 25°C, 20 mbar injection for 5s, 15 kV, detection at 280 nm. The capillary was rinsed for 8 minutes with background electrolyte solution prior to wait period.

Figure 24.

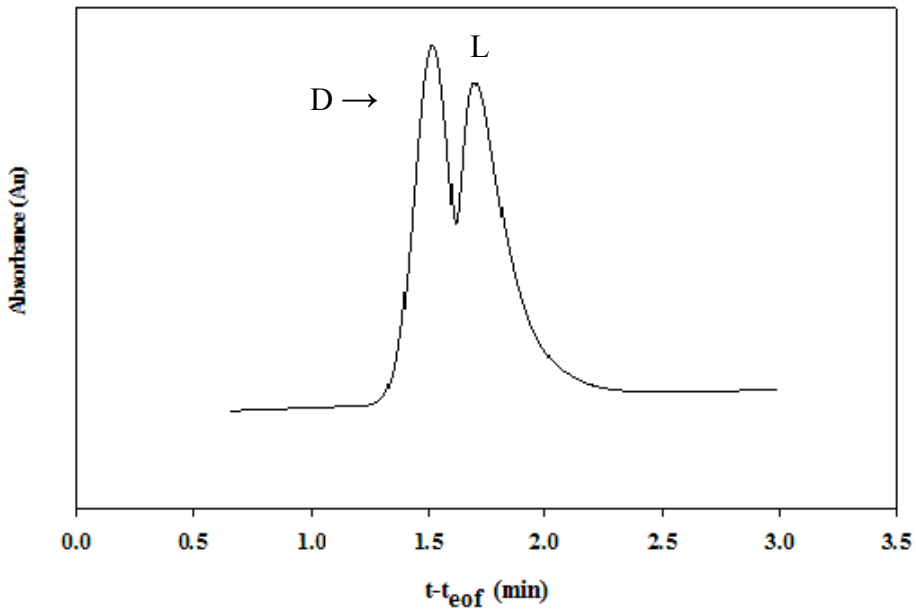

Figure 25: Selectivity versus wait time. ACE conditions: 25 mM sodium phosphate, pH 7.4, 30 μM BSA, 25°C, 20 mbar injection for 5s, 15 kV, detection at 280 nm. The capillary was rinsed for 8 minutes with background electrolyte solution prior to each wait period. The equation of the 4th order polynomial fitting (solid line): $y = 1.3287E\text{-}08x^4 - 1.1936E\text{-}06x^3 + 2.6123E\text{-}05x^2 - 4.7843E\text{-}04x + 3.0905E\text{-}02$, $R^2 = 1$.

Figure 25.

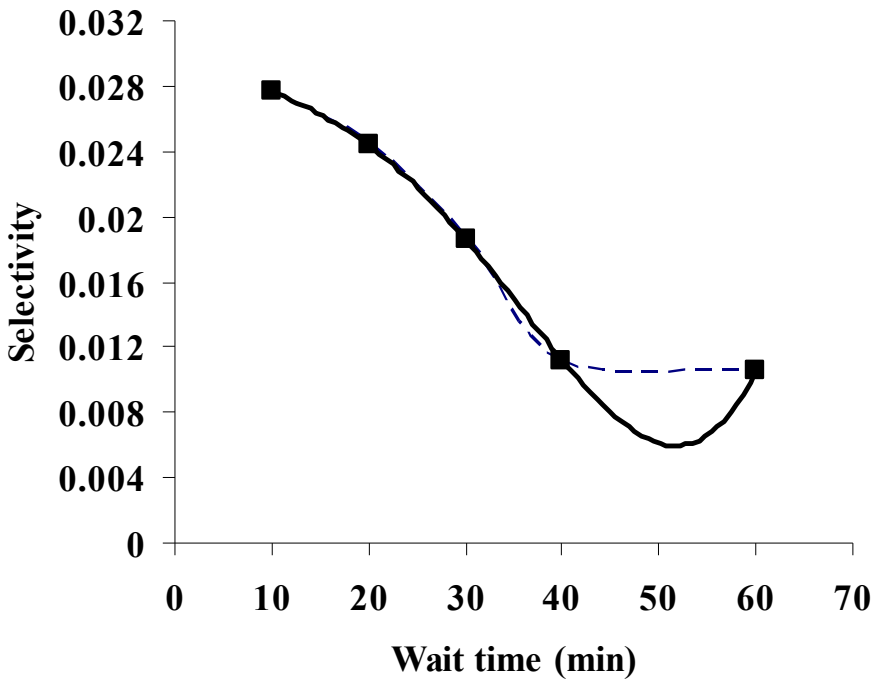
0.032
0.028
0.024
0.02
0.016
0.012
0.008
0.004
0
Selectivity
0
10
20
30
40
50
60
70
Wait time (min)

Figure 26: First derivative of selectivity as a function of wait time.

Figure 26.

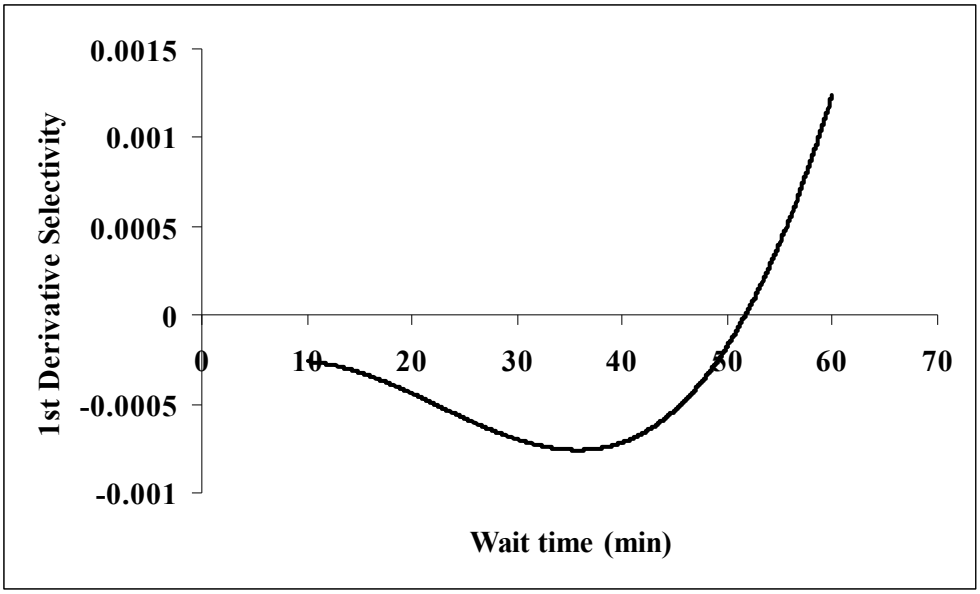
0.0015
0.001
0.0005
0
-0.0005
-0.001
1st Derivative Selectivity
0
10
20
30
40
50
60
70
Wait time (min)

3.1.6. Evaluating selectivity as a function of sample buffer ionic strength

The voltage along the capillary is assumed to be constant, when it is filled only with BGE. When solutes of different mobilities are drawn into the capillary, the solutes will separate into zones, according to their relative mobilities (Equation 5). Each of these solute zones is surrounded by a zone of BGE, and the voltage along the capillary is no longer constant. According to circuit theory, where

$$V = IR \tag{16}$$

and V is the applied voltage, I is the current, and R is the resistance, conductivity differences between zones will determine the magnitude of voltage experienced in that zone. The voltage will be low in zones of high mobility solute and high in zones of low mobility solute. The local field strength described by:

$$V/L \tag{17}$$

where V is the applied voltage and L is the total length of the capillary, will therefore be different in the solute zone based upon the mobility. Changes in the local field strength with respect to that of the surrounding BGE can lead to diffusion through electromigration dispersion (Swedberg, 1990). The effects of electrodispersion can be minimized by decreasing the mobility difference between that of the solute and the BGE ions. This can be carried out by adjusting the concentration of the BGE, of the sample buffer, or both. Increasing the concentration of the BGE can lead to band broadening due to Joule heating if the conductivity of the BGE is high. For this reason, only the effect of the sample buffer concentration was examined in this section.

Tryptophan samples were prepared in sodium phosphate buffer, pH 7.4, at a concentration of 5 – 25 mM. The effects of electrodispersion were assessed by measuring the selectivity as a function of sample buffer ionic strength for four separate injections. Representative electropharograms are shown in Figures 27-30, for the 5 mM, 8 mM, 15 mM, and 25 mM sample buffer concentrations, respectively. Subsequently, a plot of the average selectivity versus sample buffer ionic strength was made (Figure 31) and fitted using a third-order polynomial, which yielded a regression coefficient of 1. The first-derivative curve of the selectivity with respect to sample buffer ionic strength was plotted and appears in Figure 32. The average selectivity (n = 4) for the 5 mM, 8 mM, 15 mM, and 25 mM concentrations were 9.95×10^{-3}, 1.03×10^{-2}, 1.03×10^{-2}, and 8.74×10^{-3}, respectively.

The slope of the first derivative plot indicated that the enantioselection decreased as the sample buffer concentration increased, suggesting the difference in the mobilities of tryptophan and the BGE increased with buffer concentration. The maximum average selectivity was the same for samples prepared in 8 mM and 15 mM sodium phosphate. Although these values were the same, the RSD between consecutive injections was 0.03 for the samples prepared in the 8 mM buffer and 0.24 for the samples prepared in the 15 mM buffer. This indicated the variability in electrophoretic mobility was higher between consecutive injections for samples prepared in the 15 mM buffer. This also suggested higher variability between the sample plug mobility and the BGE mobility when samples were prepared in 15 mM sodium phosphate. Therefore the 15 mM buffer was not employed in subsequent studies.

Figure 27: D,L-tryptophan (0.54mg/ml) prepared in 5 mM sodium phosphate, pH 7.4. ACE conditions: 25 mM sodium phosphate, pH 7.4, 30 μM BSA, 25°C, 20 mbar injection for 5s, 15 kV, detection at 280 nm.

Figure 27.

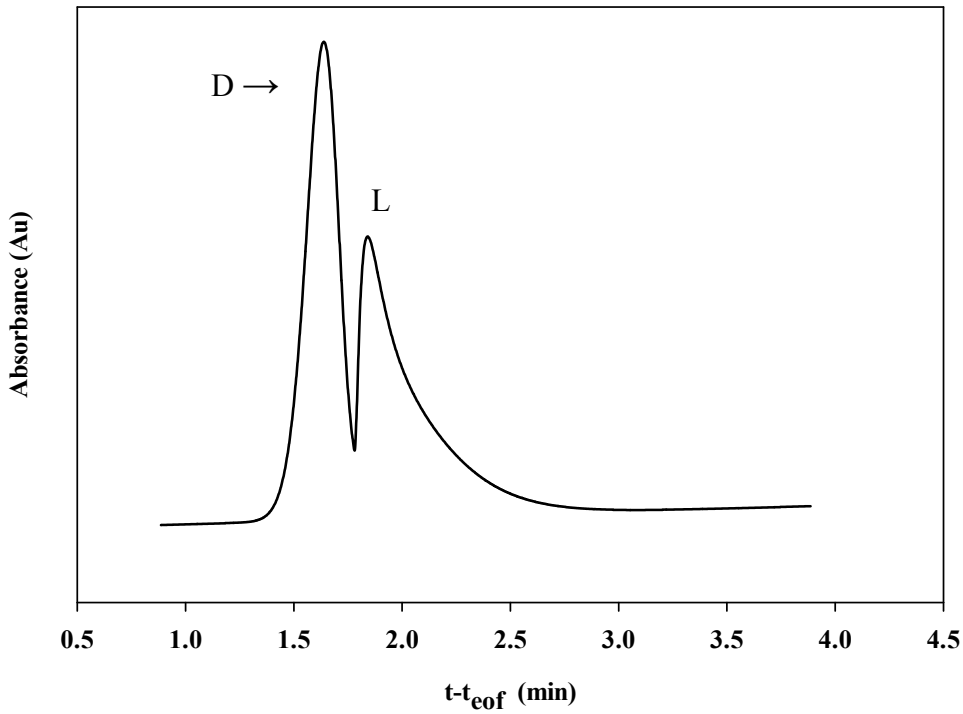

Figure 28: D,L-tryptophan (0.54mg/ml) prepared in 8 mM sodium phosphate, pH 7.4. ACE conditions: 25 mM sodium phosphate, pH 7.4, 30 μM BSA, 25°C, 20 mbar injection for 5s, 15 kV, detection at 280 nm.

Figure 28.

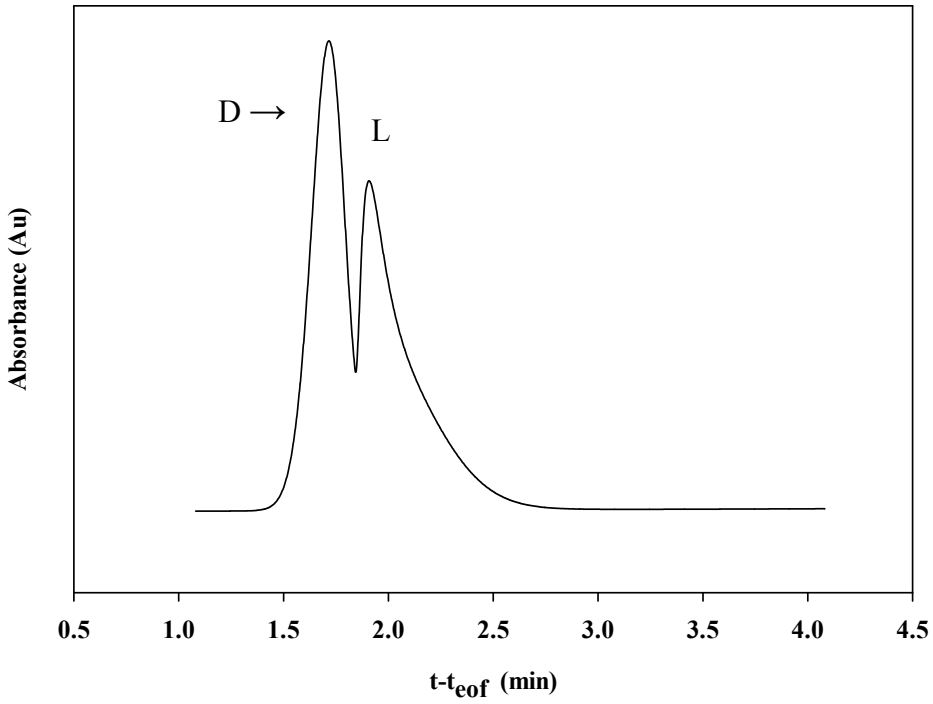

Figure 29: D, L-tryptophan (0.54mg/ml) prepared in 15 mM sodium phosphate, pH 7.4. ACE conditions: 25 mM sodium phosphate, pH 7.4, 30 μM BSA, 25°C, 20 mbar injection for 5s, 15 kV, detection at 280 nm.

Figure 29.

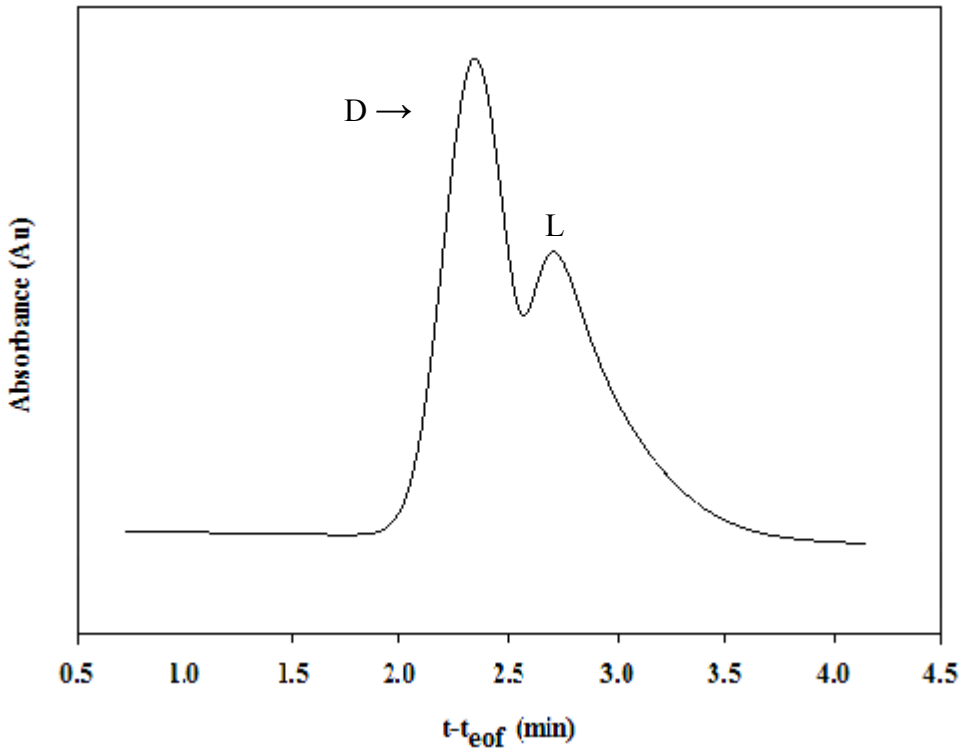

Figure 30: D,L-tryptophan (0.54mg/ml) prepared in 25 mM sodium phosphate, pH 7.4. ACE conditions: 25 mM sodium phosphate, pH 7.4, 30 μM BSA, 25°C, 20 mbar injection for 5s, 15 kV, detection at 280 nm.

Figure 30.

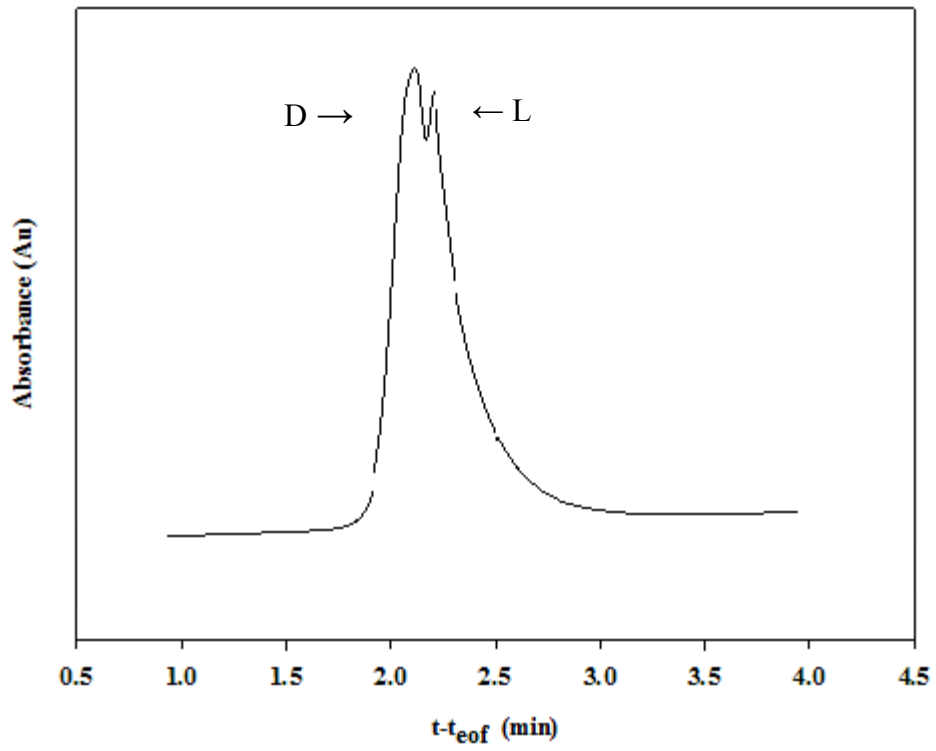

Figure 31: Selectivity versus sample buffer concentration. ACE conditions: 25 mM sodium phosphate, pH 7.4, 30 μM BSA, 25°C, 20 mbar injection for 5s, 15 kV, detection at 280 nm. The equation of the 3rd order polynomial fitting (solid line): $y = 9.7225E\text{-}08x^3 - 1.4028E\text{-}05x^2 + 2.8471E\text{-}04x + 8.8652E\text{-}03$, $R^2 = 1$.

Figure 31.

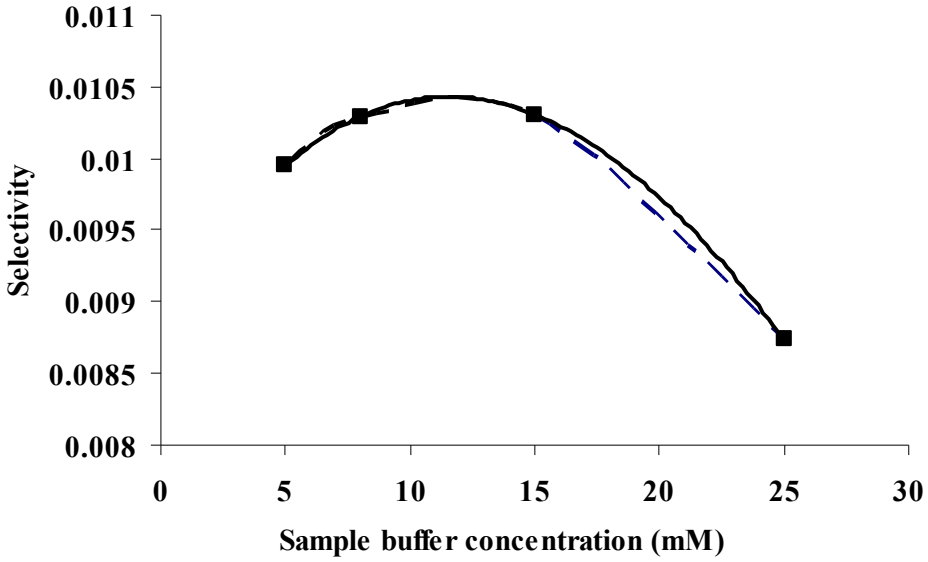
0.011
0.0105
0.01
0.0095
0.009
0.0085
0.008
Selectivity
0
5
10
15
20
25
30
Sample buffer concentration (mM)

Figure 32: First derivative of selectivity as a function of sample buffer concentration (mM).

Figure 32.

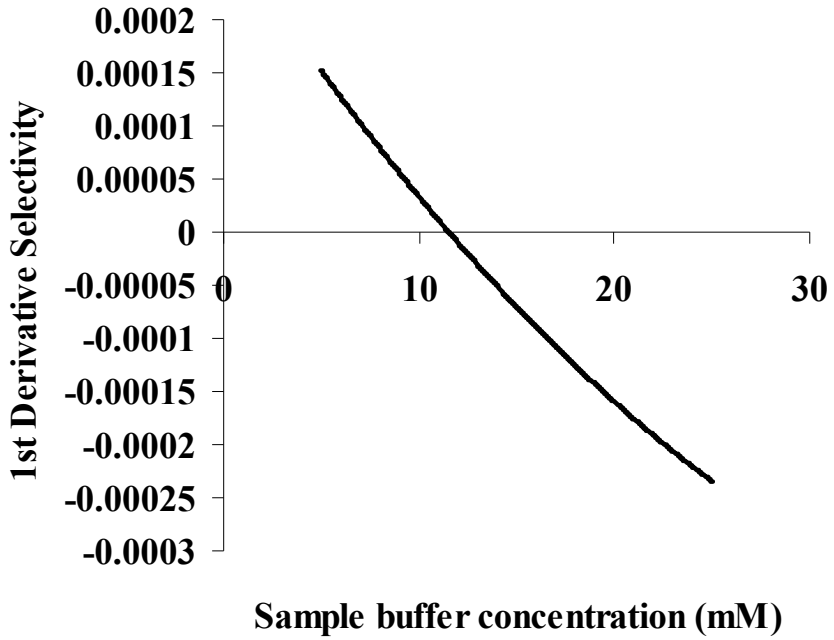
0.0002
0.00015
0.0001
0.00005
0
-0.00005
-0.0001
-0.00015
-0.0002
-0.00025
-0.0003
0
10
20
30
1st Derivative Selectivity
Sample buffer concentration (mM)

Electrodispersion caused by mismatched solute and BGE mobility will lead to detected peak tailing or fronting as a result of the solute moving slower or faster than the bulk liquid, respectively. The shape of the detected peaks at both the 5 mM and 8 mM sample concentrations presented peak tailing, which suggested that the tryptophan zone was moving slower than the BGE; however the extent of tailing at 8 mM was less than that observed at 5 mM. This indicated that the conductivity in the sample zone increased with ionic strength, and caused the tryptophan ions to migrate faster in the capillary.

The effect of electrodispersion on enantioselection was negligible when the concentration of the sample buffer was no more than three orders of magnitude lower than the BGE 25 mM concentration. This was in agreement with previously reported studies (Bruin et al., 1989). As a result, subsequent studies were carried out using samples prepared in 8 mM sodium phosphate, pH 7.4.

3.2. Capillary electrophoresis applications for studying competitive binding

3.2.1. Determining sample concentration

In CE both the protein and the protein-drug complex are under a voltage current that may change their shapes, leading to the generation of new binding sites or modification of existing binding sites. As a result, the optimized conditions from section 3.1 were retested on a new capillary and a BSA concentration of 35 μM in the BGE improved baseline separation. Therefore it was used in subsequent experiments.

In studies using CE it is assumed that the solute's mobility is independent of the solute's initial sample concentration (Bose et al., 1997; Yang et al., 1996; El-Hady, et al., 2010). As shown in Figure 33 for tryptophan (Tryp) and 5- fluoro-tryptophan, the mobility shift of the L-enantiomer initially increases as the concentration of drug is increased. A noticeable change in mobility occurred at concentrations greater than 0.9 mg/ml. This suggests that tryptophan concentrations within the range of 0.1 mg/ml and 0.9 mg/ml can be used for binding studies. As a result of the D-enantiomer not forming a drug-protein complex with BSA, its mobility shift for both drug molecules was essentially unchanged.

Figure 33: Mobility shifts of D,L-tryptophan and 5-fluoro-D,L-tryptophan as a function of tryptophan and 5-fluoro-tryptophan concentrations, respectively. For both (a) D (■), L (◆)-tryptophan and (b) 5-fluoro-D(■), L (◆)-tryptophan the concentration of BSA in the background electrolyte was held constant at 35 μM and the sample concentrations employed were 0.1, 0.2, 0.4, 0.9, 1.3, 2.2, and 2.6 (mg/ml). ACE conditions: 15 kV, 25°C, injection at 20 mbar for 5 s, and detection at 280 nm.

Figure 33.

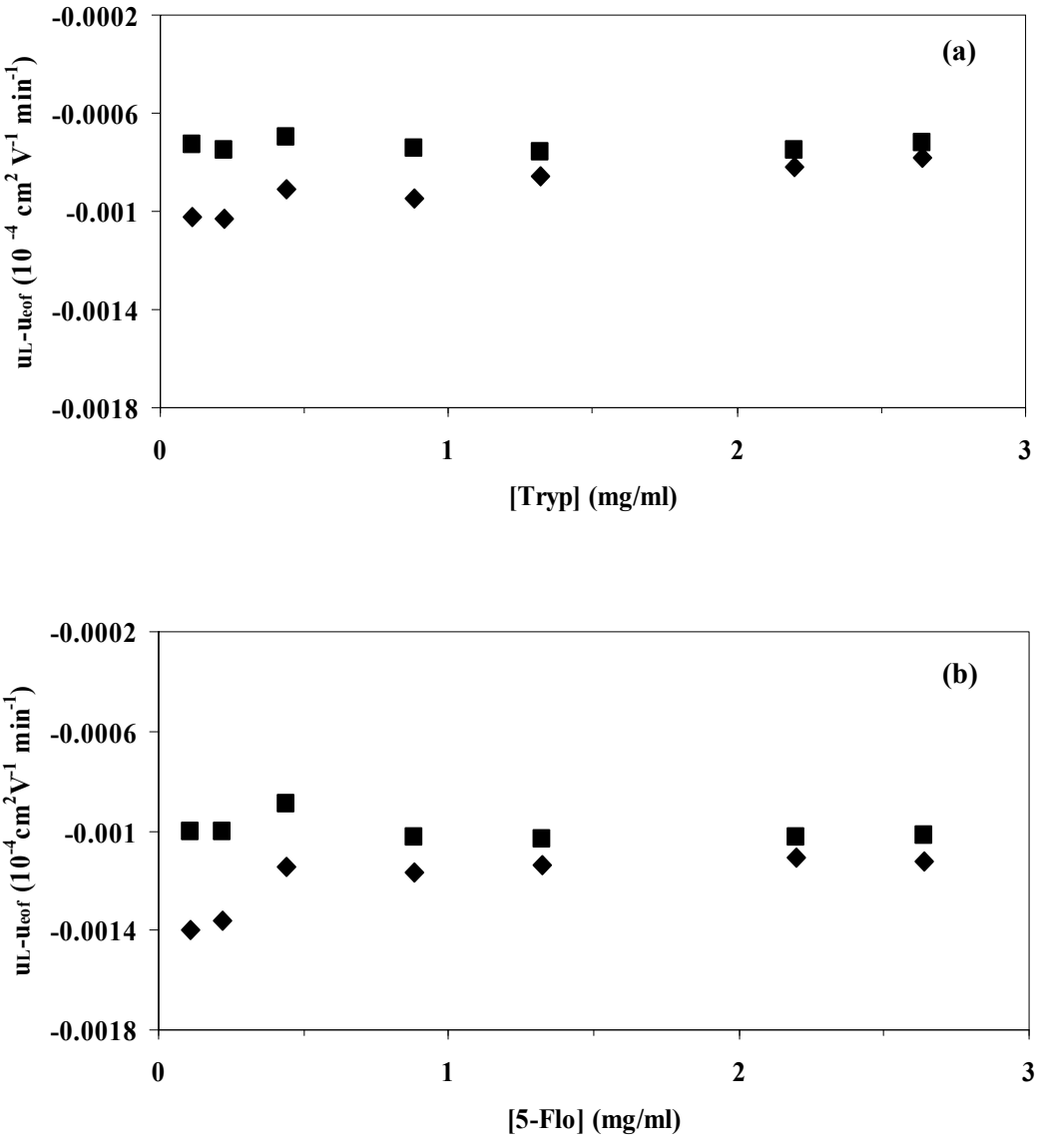
(a)
-0.0002
-0.0006
-0.001
-0.0014
-0.0018
0
1
2
3
[Tryp] (mg/ml)
u_L-u_{eof} (10^{-4} cm^2 V^{-1} min^{-1})
(b)
-0.0002
-0.0006
-0.001
-0.0014
-0.0018
0
1
2
3
[5-Flo] (mg/ml)
u_L-u_{eof} (10^{-4} cm^2 V^{-1} min^{-1})

These observed results can be elucidated by assuming a 1:1 drug-protein complex model. In isotropic conditions enantiomers exhibit the same behavior. The key factor required for enantiomeric separation is the presence of a protein chiral selector in the BGE. Representative electropharograms of D,L-tryptophan and 5-fluoro-D,L-tryptophan in BGE void of BSA are shown in Figures 34 and 35, respectively. Under conditions in which enantiomer-protein interaction is blocked separation will not occur. As the concentration of drug injected into the capillary is increased, the number of drug saturated protein molecules also increases occupying all available binding sites. Concentrations above optimum range result in non-linear isotherm conditions that adversely affect separation efficiency.

Separations under nonlinear isotherm condition will produce changes in the mobility shift, leading to diminished baseline resolution, and distortion of the binding enantiomer peak shape as represented in Figure 36 for D,L-tryptophan. The D-enantiomer peak maintains its Gaussian shape, while the L-enantiomer peak tails. To maintain continuity between drug samples and utilize drug concentrations that would not adversely affect the precision of CE measurements, 0.22 mg/ml (1 mM) was employed for subsequent studies. The final molar ratio of tryptophan:BSA in the capillary for subsequent studies was 1:4.

Figure 34: D,L-tryptophan, 0.22 mg/ml (1mM), run in 25 mM sodium phosphate, pH 7.4, void of BSA. ACE conditions: 15 kV, 25°C, injection at 20 mbar for 5 s, and detection at 280 nm.

Figure 34.

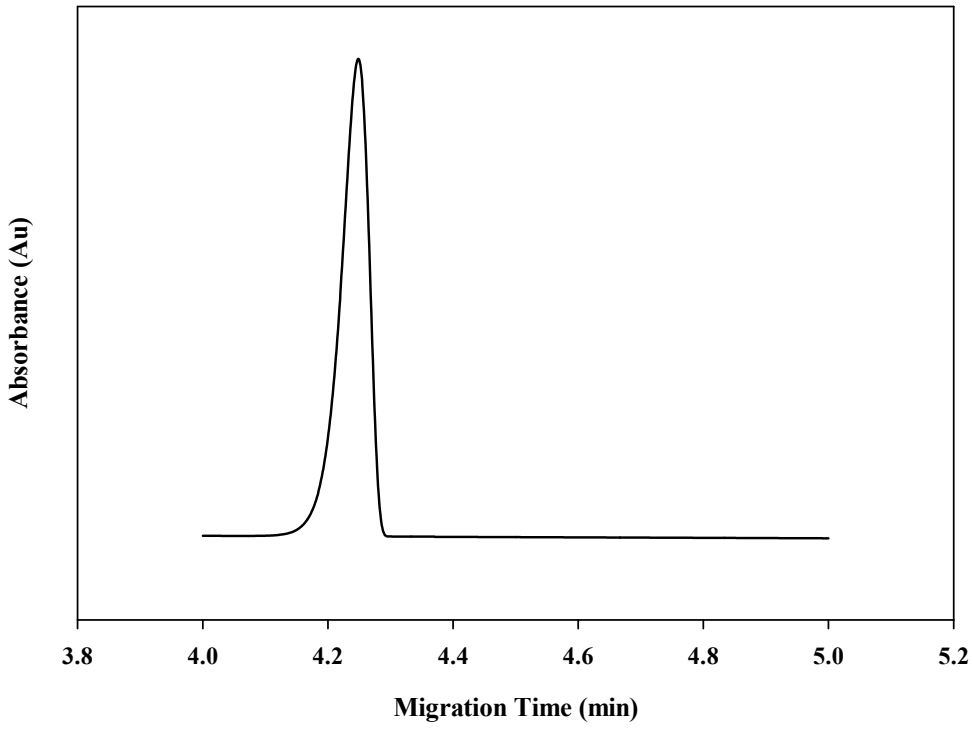

Figure 35: 5-fluoro-D,L-tryptophan, 0.22 mg/ml (1mM), run in 25 mM sodium phosphate, pH 7.4, void of BSA. ACE conditions: 15 kV, 25°C, injection at 20 mbar for 5 s, and detection at 280 nm.

Figure 35.

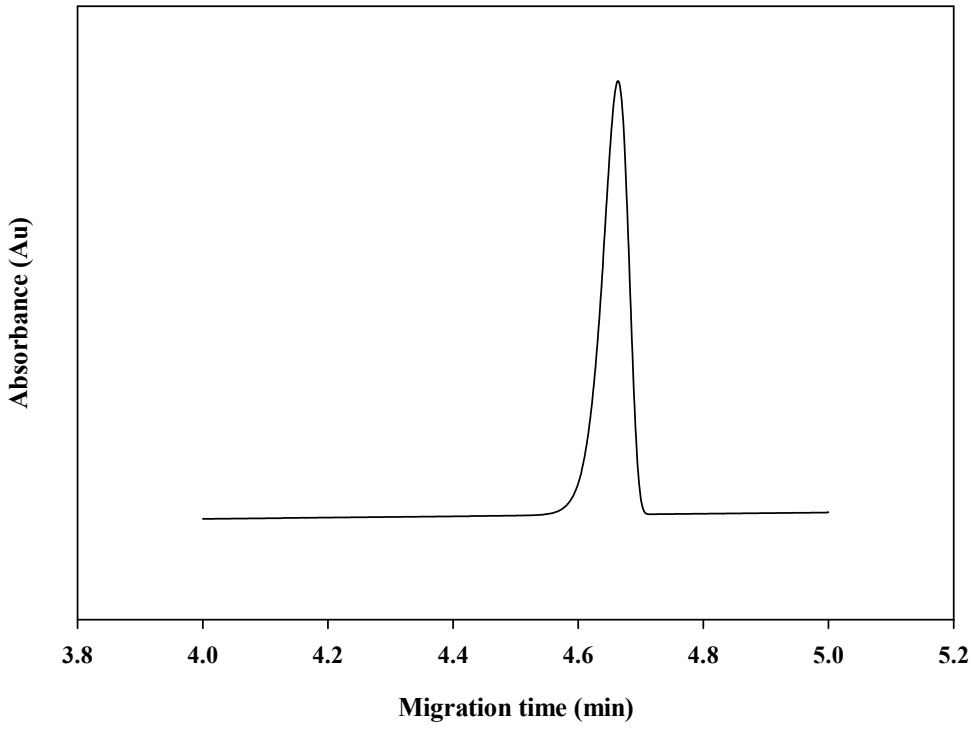

Figure 36: Changes in peak shape due to nonlinear isotherm conditions. BSA concentration was held to 35 μM. D,L-tryptophan sample concentrations used were 0.1 mg/ml, 0.4 mg/ml, and 0.9 mg/ml. ACE conditions: 15 kV, 25°C, injection at 20 mbar for 5 s, and detection at 280 nm.

Figure 36.

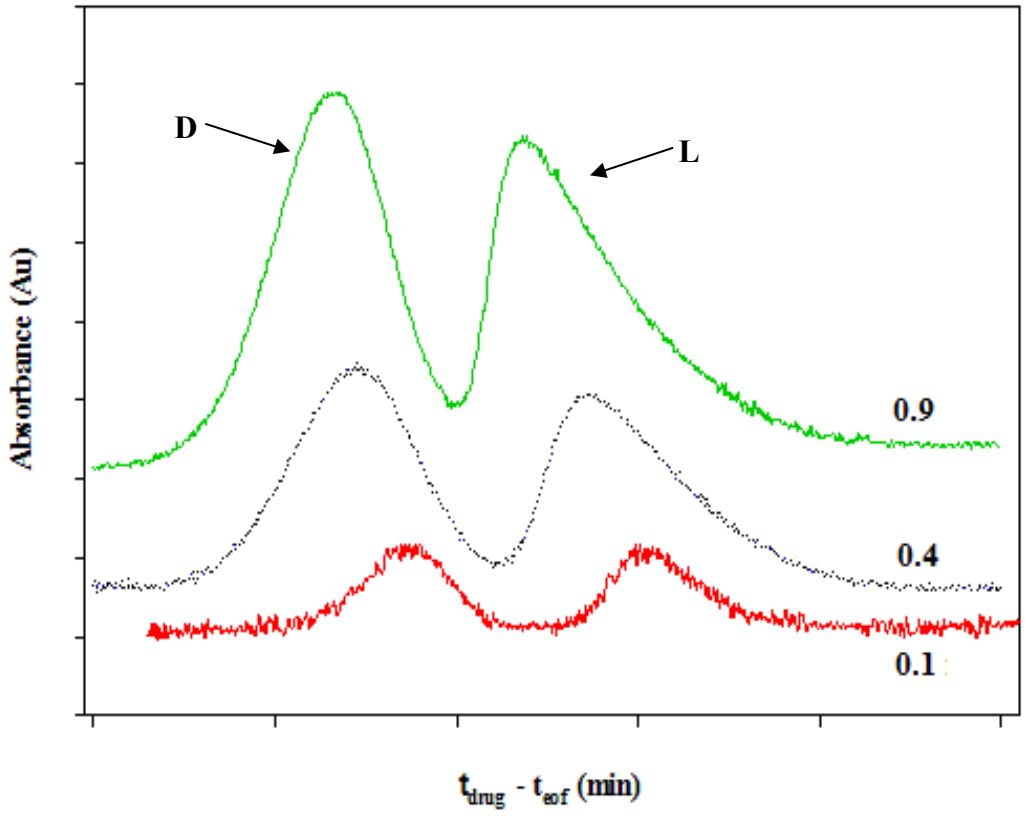

3.2.2. Separation selectivity in the presence of ibuprofen

Differences in enantiomer affinity for a given phase are measured by selectivity $\left(k_2 / k_1 \right)$. The variables k_2 and k_1 are the retention factors for enantiomer 2 and enantiomer 1, respectively. The separation selectivity can be well characterized with the relative mobility difference between enantiomers by Eq.11 (Chankvetadze, 1997; Blaschke & Chankvetadze, 2003).

In initial experiments selectivity was measured in BGE void ibuprofen. As reported in literature, the selectivity of BSA for 5-fluoro-D,L-tryptophan was approximately two times greater than that for D,L-tryptophan, 3.4×10^{-2} (n = 4) and 1.6×10^{-2} (n = 4), respectively (Tittlebach & Gilpin, 1995). The higher selectivity of 5-fluoro-D,L-tryptophan can be ascribed to differences in hydrophobicity between derivatives. It was also reported that 5-fluoro-tryptophan has two chemically distinct binding sites on serum albumin (Gerig & Klinkenborg, 1980). The displacement of tryptophan was studied by determining the selectivity value for tryptophan derivatives in the presence of ibuprofen in the BGE. Ibuprofen was added to the BGE at concentrations of 5.5 μM, 22.1 μM , 33.2 μM, 44.2 μM , and 55.3 μM . These concentrations resulted in displacer:BSA molar ratios of 1:6, 1:1.6, 1:1, 1.3:1, and 1.6:1, respectively. The selectivity decreased initially for both derivatives, until the displacer:BSA molar ratio reached 1:1, Figure 37.

Figure 37: Separation selectivity of BSA for 5-fluoro-D,L-tryptophan (◆) and D,L-tryptophan (▲) as a function of ibuprofen [Ibu] concentration in the background electrolyte. Serum protein concentration was held at 35 μM. The concentration of ibuprofen added to the background electrolyte was 0, 5.5, 22.1, 33.2, 44.2, and 55.3 μM, respectively. ACE conditions: 15 kV, 25°C, injection at 20 mbar for 5 s, and detection at 280 nm. The standard error in the selectivity is shown for each individual concentration of ibuprofen.

Figure 37.

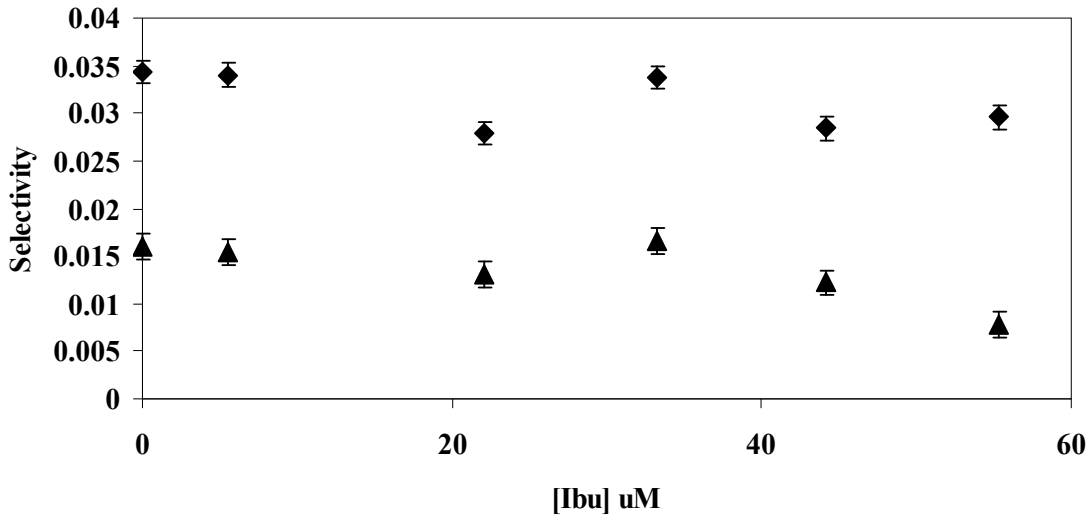
0.04
0.035
0.03
0.025
0.02
0.015
0.01
0.005
0
Selectivity
0
20
40
60
[Ibu] uM

The change in selectivity, defined as the difference between the highest and lowest calculated selectivity value, for D,L-tryptophan was 8.2×10^{-3} and 5-fluoro-D,L-tryptophan 6.4×10^{-3}. At molar ratios in which BSA was in excess, ibuprofen appeared to bind mainly to its primary sites on the protein. Diminished selectivity under these conditions showed that the presence of ibuprofen blocked BSA from binding L-tryptophan. Representative electropharograms are shown in Figures 38 and 39 for D,L-tryptophan and 5-fluoro-D,L-tryptophan both with 22 μM ibuprofen in the BGE. Baseline separation was still observed for 5-fluoro-D,L-tryptophan. This suggested that the affinity of 5-fluoro-D,L-tryptophan binding to BSA was higher than that for D,L-tryptophan. The binding constants were measured for each analog.

Figure 38: Electropharogram of D,L-tryptophan (0.22 mg/ml) at a ibuprofen:BSA molar ratio of 1.6:1 (22 μM ibuprofen). The serum protein concentration was held at 35 μM. ACE conditions: 15 kV, 25°C, injection at 20 mbar for 5 s, and detection at 280 nm.

Figure 38.

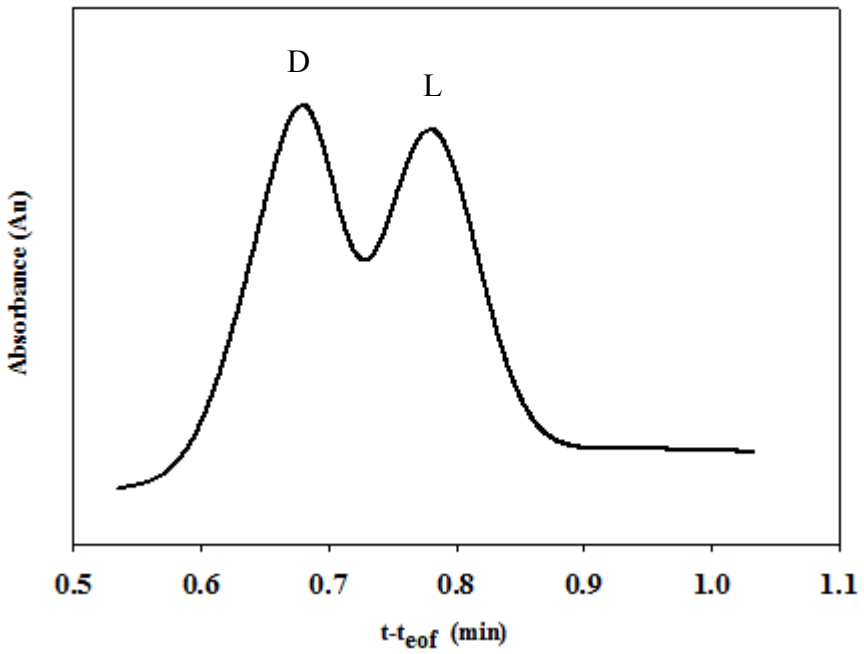

Figure 39: Electropharogram of 5-fluoro-D,L-tryptophan at a ibuprofen:BSA molar ratio of 1.6:1 (22 μM ibuprofen). The serum protein concentration was held at 35 μM. ACE conditions: 15 kV, 25°C, injection at 20 mbar for 5 s, and detection at 280 nm.

Figure 39.

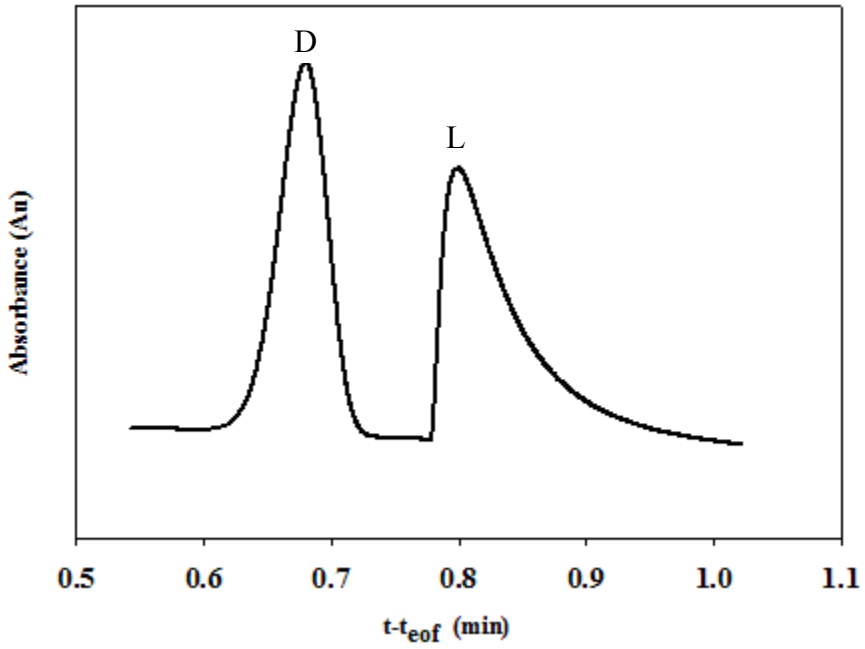

3.2.3. Measuring the binding constant

These observed differences in binding between analogs were elucidated by assuming a 1:1 drug-protein complex model,

$$E + P \overset{K_a}{\leftrightarrow} EP \tag{17}$$

$$K_a = \frac{[EP]}{[E][P]} \tag{18}$$

where K_a, [E], [P], and [EP], denote the association constant, and the molar concentrations of drug, protein, and drug-protein complex, respectively.

In this model, the effective mobility of the drug, μ_{eff}, is described as

$$\mu_{eff} = \chi_E \cdot \mu_E + \chi_{EP} \cdot \mu_{EP} = \left(\left(\frac{[E]}{[E]+[EP]}\right) \times \mu_E\right) + \left(\left(\frac{[EP]}{[E]+[EP]}\right) \times \mu_{EP}\right) \tag{19}$$

The mobility of free (μ_E) and bound (μ_{EP}) drug is weighted by their molar fractions (χ). The capacity factor, referred to as the retention factor in some cases, describes the ratio of bound to free drug. The retention factor, k, is mathematically defined by (Ostergaard, 2007):

$$k = \frac{[EP]}{[E]} = \frac{\mu_{EP} - \mu_E}{\mu_E - \mu_0} = K_a[P] \tag{20}$$

where μ_{EP}, μ_E, and μ_0, are the mobilities of the bound drug, the free drug, and the drug without protein in the BGE. From Equation 20, the binding constant can be experimentally determined. In this study, the mobilities of the L-enantiomer and the D-enantiomer were used to measure μ_{EP} and μ_E, respectively. The retention factors for 5-fluoro-D,L-tryptophan and D,L-tryptophan were measured in a BSA concentration range of 10 – 35 μM.

Figure 40: Binding constant estimates for 5-fluoro-D,L-tryptophan and D,L-tryptophan to BSA (10- 35 μM). (a) Retention factor versus BSA concentration binding plot for 5-fluoro-tryptophan. Equation of the linear fitting: $y = 523.14x + .0013$, $R^2 = 0.95$; (b) Retention factor versus BSA concentration binding plot for tryptophan. Equation of the linear fitting: $y = 198.84x + 0.0019$, $R^2 = 0.93$.

Figure 40.

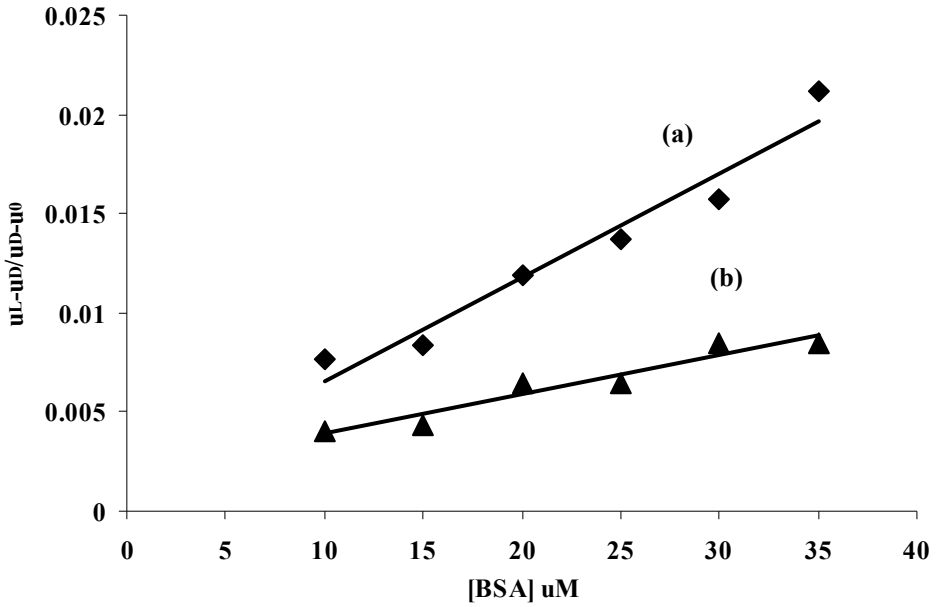
0.025
0.02
0.015
0.01
0.005
0
uL-uD/uD-u0
(a)
(b)
0
5
10
15
20
25
30
35
40
[BSA] uM

The binding constant of 5-fluoro-tryptophan with BSA was 523.14 μM^{-1} with a correlation coefficient of 0.95. The binding constant of tryptophan with BSA was 198.84 μM^{-1} with a correlation coefficient of 0.93. Plots are shown in Figure 40. The results demonstrated that 5-fluoro-tryptophan had a larger affinity to serum albumin than that of tryptophan. Thus the difference in selectivity of BSA for 5-fluoro-D,L-tryptophan and D,L-tryptophan in the presence of ibuprofen was due to the higher binding affinity of the fluoro-analog.

The binding constant determined for L-tryptophan from the CE method agreed with the value of a previous NMR study under similar experimental conditions reported to be 230 ± 90 μM^{-1} (Fielding et al., 2005). Differences in buffer ionic strength and temperature fluctuation, may have contributed to the wide range of values reported across laboratories for tryptophan-BSA binding studies.

3.2.4. Measuring selectivity by preformed displacer-protein binary complexes

With the protein free floating in solution, drug-protein interaction is variable. Such conditions may require higher levels of displacer before effects are observed. Separations with preformed displacer-protein complexes provide a direct approach to characterize drug-drug displacement (Li et al., 2011). In a separate experiment using D,L-tryptophan because of its marked change in selectivity, ibuprofen was equilibrated with BSA at a displacer:BSA molar ratio of 1:7 for two hours and 4 .5 hours before measurements were taken to establish preformed ibuprofen-BSA binary complexes in the BGE.

3. 3. Capillary electrophoresis applications for studying binding of glycated serum proteins.

3.3.1. Characterization of extent of glycation

Capillary Electrophoresis

Capillary electrophoretic analysis of intact BSA in sodium phosphate buffer, pH 7.4 offered an incomplete separation of modified proteins. The incomplete separation could have been caused by proteins sticking to the capillary wall. At physiological pH, protein absorption to the capillary may be pronounced (Graf et al., 2005). Modification of BSA by glucose rearranged the separation profile, such that the number of peaks increased over time (Figure 41). The presence of these peaks in the electropharogram suggested there were a variety of new products forming during the modification process. The number of new products formed increased with incubation time.

Mass Spectrometry

To test the applicability of the capillary electrophoretic data, the mass was evaluated for unmodified and modified BSA. The molecular weight of the unmodified BSA was found to be approximately 66, 438 Da. Consistent with previous reports, the masses of modified BSA derived from incubation with glucose were found to increase with increasing incubation time (Schmitt, et al., 2005).

Figure 41: CE/UV peak profiles of unmodified and modified BSA in 25 mM sodium phosphate at pH 7.4. Unmodified BSA (A), BSA modified by glucose for 1 week (B), BSA modified by glucose for 2 weeks (C), BSA modified by glucose for 3 weeks (D). All incubations were carried out at 25°C. ACE conditions: 25°C, 20 mbar injection for 5s, 15 kV, detection at 280 nm.

Figure 41.

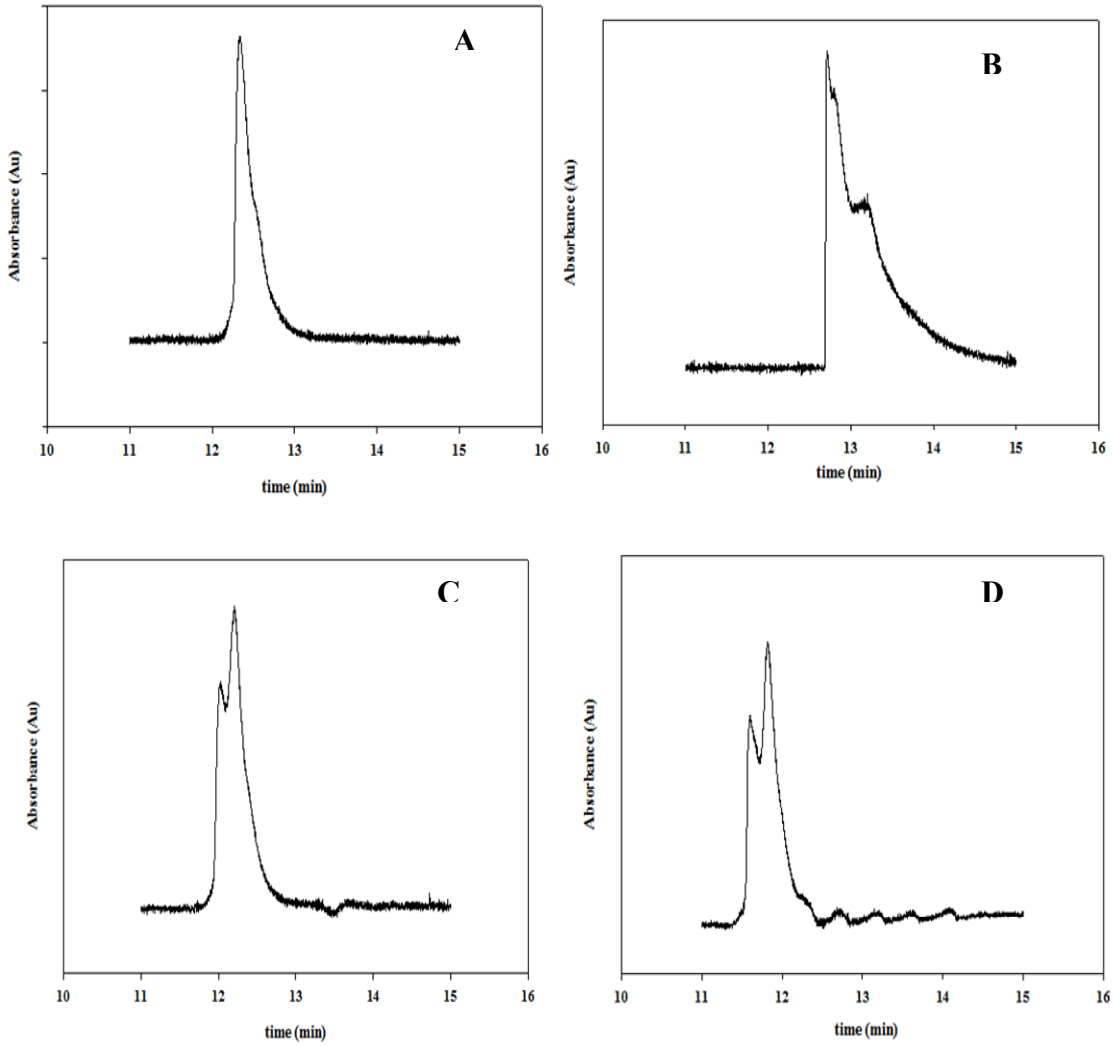

The highest mass of BSA was measured for the 3 week glucose incubation. The data from the electrophoretic characterization earlier were supported by the mass spectrometric results. The increase in molecular weight induced by glycation corresponds to the attachment of glucose units to the amino residues of the protein (Rondeau & Bourdon, 2011). The number of glucose units bound to the protein was deduced from the mass difference between the unmodified and modified protein. The maximum number of glucose units added after one, two and three weeks of incubation were 9, 70, and 76, respectively. The masses of all protein samples for weeks 1 – 3, along with the approximate number of glucose molecules added to each newly glycated BSA are given in Tables I- III.

Nuclear Magnetic Resonance

The ^{1}H-NMR spectrum of unmodified BSA showed no peaks in the spectral region at ~ 5.0 to 5.55 ppm studied. The ^{1}H –NMR of modified BSA incubated for 3 weeks in D-glucose consisted of an envelope of peaks. Notable were the resolved doublets at 5.24 ppm and 5.50 ppm. Based on the available data in the literature (Bubb, 2003; Cui et al., 2007), the resonance at 5.24 ppm was attributed to proton-proton (JHH) coupling in free α-glucose. There was a large amount of free glucose in the sample, which resulted in the signal going off scale in the plot. From this large amount of free glucose two Carbon-13 satellite signals on either side of this main peak were observed, whose combined intensities were 1.1 % of the main peak. The resonance from the ^{1}H-NMR spectrum at 5.50 ppm indicated glucose was linked to BSA through a glycosidic bond (Figure 42) (Bao et al., 2012). This verified protein structural modification.

Table I: Data from mass spectrometric analysis of unmodified and modified BSA after a 1 week incubation in 14 mM D-glucose at 25°C. The modified BSA with the highest number of glucose molecules bound is highlighted. The concentration of BSA was 35 μM.

Table I.

Mass BSA	Mass of Glycated BSA	Mass Difference	Added Glucose Molecules
66438	66755	317	2
	66888	450	2
	67674	1236	7
	67080	642	4
	67703	1265	7
	67871	1433	8
	67399	961	5
	68094	**1656**	**9**
	67387	949	5

Table II: Data from mass spectrometric analysis of unmodified and modified BSA after a 2 week incubation in 14 mM D-glucose at 25°C. The modified BSA with the highest number of glucose molecules bound is highlighted. The concentration of BSA was 35 μM.

Table II.

Mass BSA	Mass of Glycated BSA	Mass Difference	Added Glucose Molecules
66438	66755	317	2
	78808	12370	69
	66888	450	2
	76135	9697	54
	69294	2856	16
	79132	**12694**	**70**
	72732	6294	35
	67674	1236	7
	78212	11774	65
	74747	8309	46

Table III: Data from mass spectrometric analysis of unmodified BSA and modified BSA after a 3 week incubation in 14 mM D-glucose at 25°C. The modified BSA with the highest number of glucose molecules bound is highlighted. The concentration of BSA was 35 μM.

Table III.

Mass BSA	Mass of Glycated BSA	Mass Difference	Added Glucose Molecules
66438	66600	162	1
	80067	**13629**	**76**
	70930	4492	25
	67760	1322	7
	71409	4971	28
	78433	11995	67
	75313	8875	49
	80134	**13696**	**76**
	74435	7997	44
	66755	317	2

Figure 42: This is a plot of the spectral region at ~ 5.0 – 5.55 ppm showing signals from the H1 proton (shown in red) on α-D-glucose. The red spectrum is that of the unmodified BSA (control). The black spectrum is that of modified BSA after a 3 week incubation in 14 mM D-glucose at 25°C.

Figure 42:

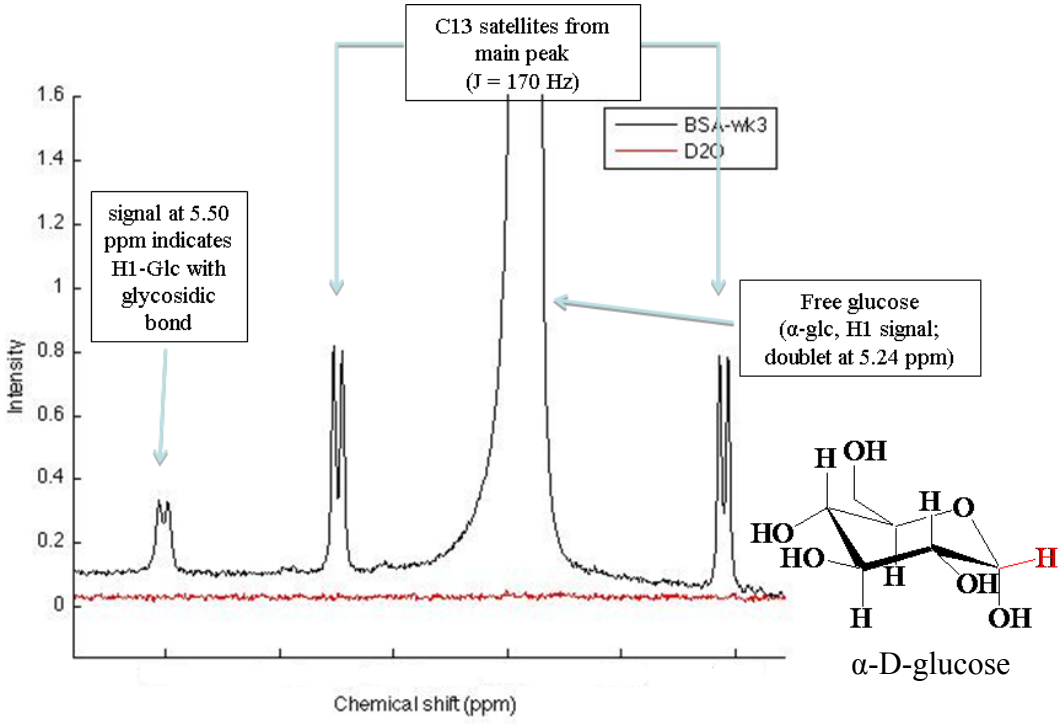
C13 satellites from main peak (J = 170 Hz)
BSA-wk3
D2O
signal at 5.50 ppm indicates H1-Glc with glycosidic bond
Free glucose (α-glc, H1 signal; doublet at 5.24 ppm)
Intensity
Chemical shift (ppm)
α-D-glucose

3.3.2. Chiral recognition of glycated BSA

The chiral recognition of tryptophan analogs by BSA was altered by the extent of glycation. Representative electropharograms for D,L-tryptophan, 5-fluoro-D,L-tryptophan, and 5-hydroxy-D,L-tryptophan are shown in Figures 45- 47, respectively. The selectivity was calculated for four separate injections of D,L- tryptophan and 5-fluoro-D,L-tryptophan. It was not possible to separate 5-hydroxy-D,L-tryptophan by unmodified or modified BSA as previously reported (Hödl et al., 2006). As a result, the changes in the 5-hydroxy-D,L-tryptophan peak area were measured for subsequent weeks and used to approximate changes in its chiral recognition by BSA as follows:

$$\left(\mathrm{Area}_{n+1} \Big/ \mathrm{Area}_{n} \right) \times 100 \qquad (21)$$

where n denotes the week(s) of incubation in D-glucose solution.

Glycation of BSA altered the chiral recognition of D,L-tryptophan, 5-fluoro-D,L-tryptohan, and 5-hydroxy-D,L-tryptophan after one week. The decline in enantioselection was most pronounced for D,L-tryptophan at 0.051 (Figure 45). The selectivity for 5-fluoro-D,L-tryptophan declined by 0.032 and the peak area of 5-hydroxy-D,L-tryptophan decreased by 13.4% (Figure 47, 49). The chiral recognition continued to decline after week 2 for both D,L-tryptophan and 5-hydroxy-D,L-tryptophan, however that of 5-fluoro-D,L-tryptophan increased. Although the trend in decreased enantioselection reversed for all analogs after three weeks, chiral recognition did not return to its starting values, (Figures 46, 48, and 50).

Figure 43: D,L-tryptophan (0.22 mg/ml) binding by unmodified BSA (A) and 1 week modified BSA (B). The serum protein concentration was held at 35 μM. ACE conditions: 15 kV, 25°C, injection at 20 mbar for 5 s, and detection at 280 nm.

Figure 43.

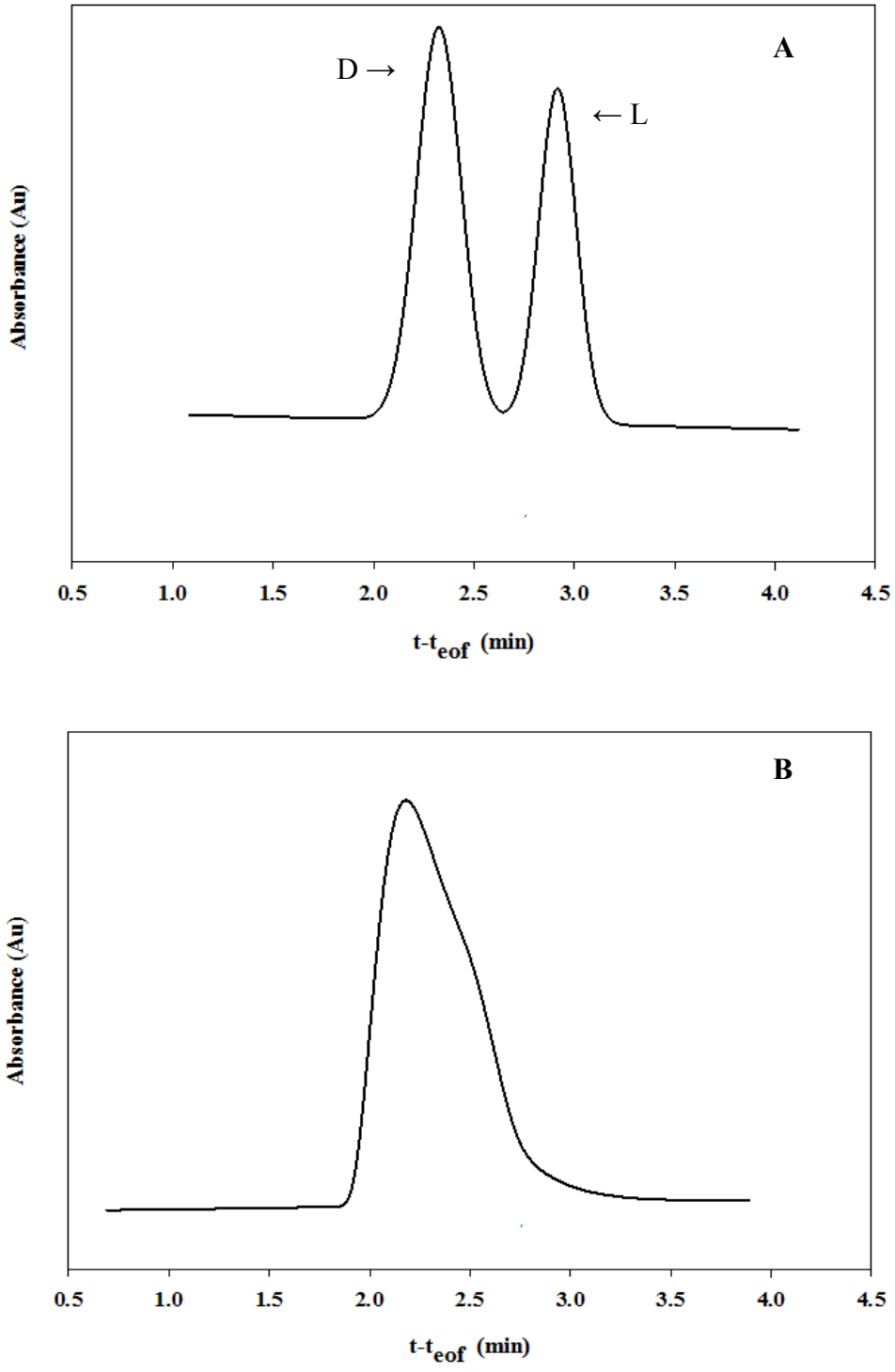
A
D →
← L
Absorbance (Au)
0.5
1.0
1.5
2.0
2.5
3.0
3.5
4.0
4.5
t-t$_{eof}$ (min)
B
Absorbance (Au)
0.5
1.0
1.5
2.0
2.5
3.0
3.5
4.0
4.5
t-t$_{eof}$ (min)

Figure 44: D,L-tryptophan (0.22 mg/ml) binding by 2 week modified BSA (A) and 3 week modified BSA (B). The serum protein concentration was held at 35 μM. ACE conditions: 15 kV, 25°C, injection at 20 mbar for 5 s, and detection at 280 nm.

Figure 44.

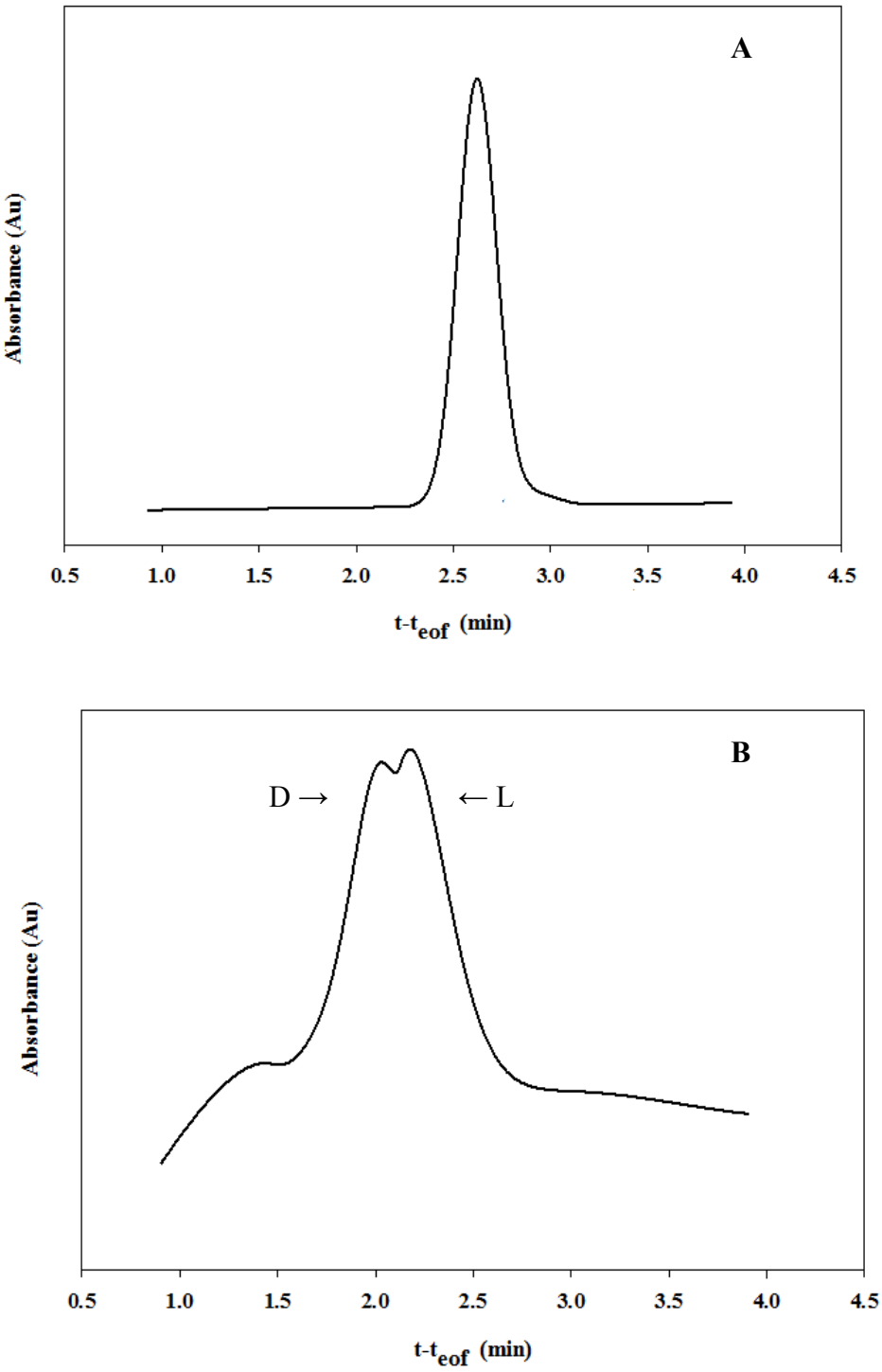
A
Absorbance (Au)
0.5
1.0
1.5
2.0
2.5
3.0
3.5
4.0
4.5
t-t$_{eof}$ (min)
B
D →
← L
Absorbance (Au)
0.5
1.0
1.5
2.0
2.5
3.0
3.5
4.0
4.5
t-t$_{eof}$ (min)

Figure 45: 5-fluoro-D,L-tryptophan (0.22 mg/ml) binding by unmodified BSA (A) and 1 week modified BSA (B). The serum protein concentration was held at 35 μM. ACE conditions: 15 kV, 25°C, injection at 20 mbar for 5 s, and detection at 280 nm.

Figure 45.

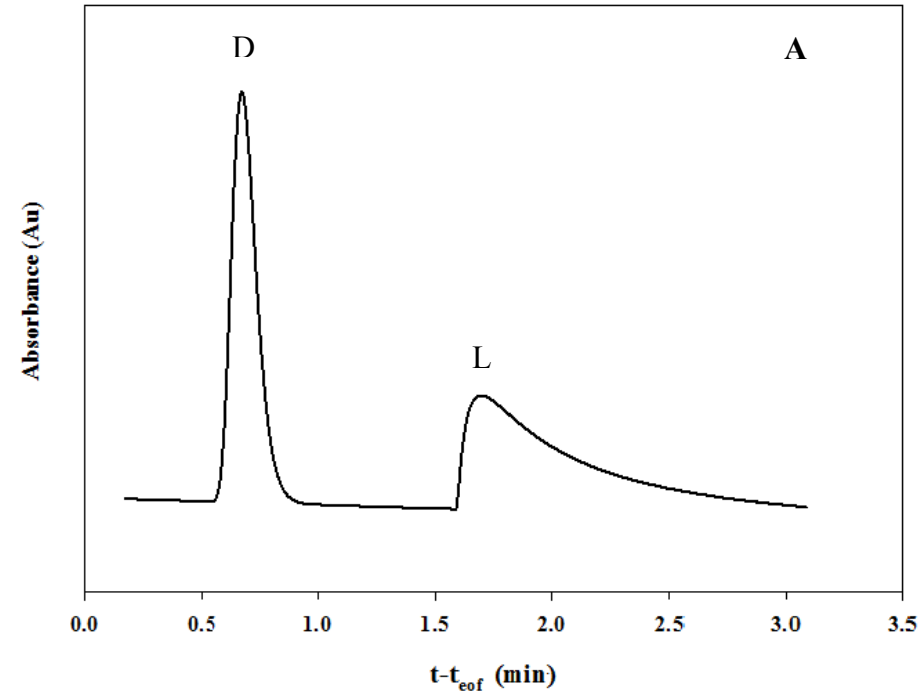
D
A
L
Absorbance (Au)
0.0
0.5
1.0
1.5
2.0
2.5
3.0
3.5
t-t$_{eof}$ (min)

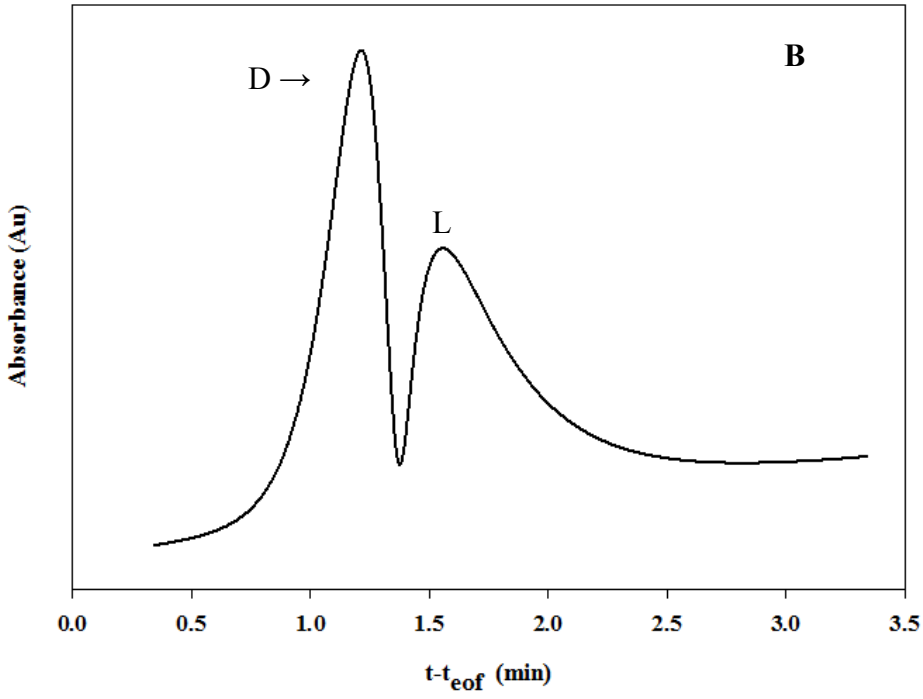
D →
B
L
Absorbance (Au)
0.0
0.5
1.0
1.5
2.0
2.5
3.0
3.5
t-t$_{eof}$ (min)

Figure 46: 5-fluoro-D,L-tryptophan (0.22 mg/ml) binding by 2 week modified BSA (A) and 3 week modified BSA (B). The serum protein concentration was held at 35 μM. ACE conditions: 15 kV, 25°C, injection at 20 mbar for 5 s, and detection at 280 nm.

Figure 46.

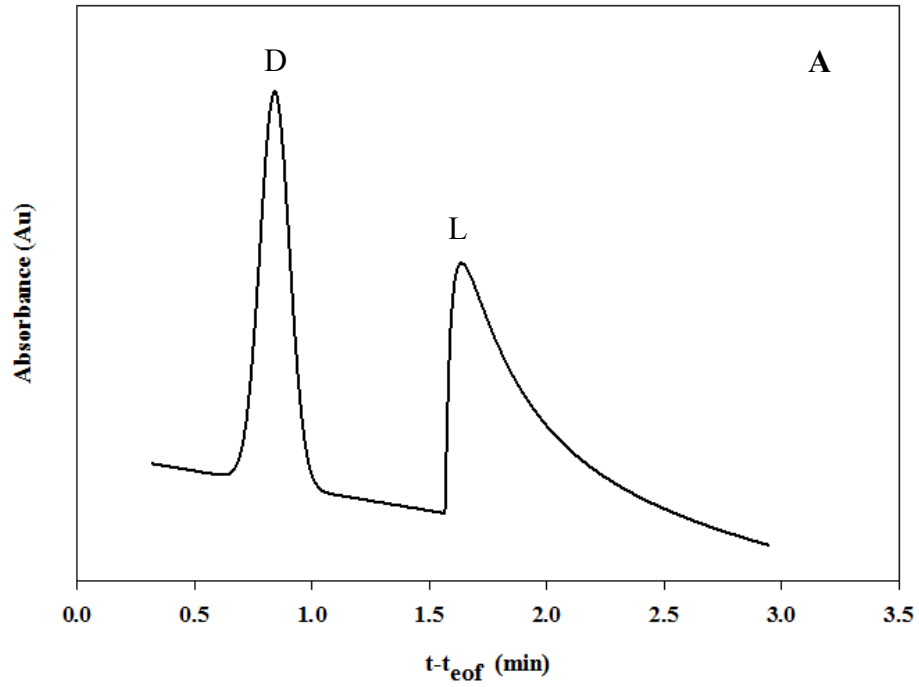
D
A
L
Absorbance (Au)
0.0
0.5
1.0
1.5
2.0
2.5
3.0
3.5
t-t$_{eof}$ (min)

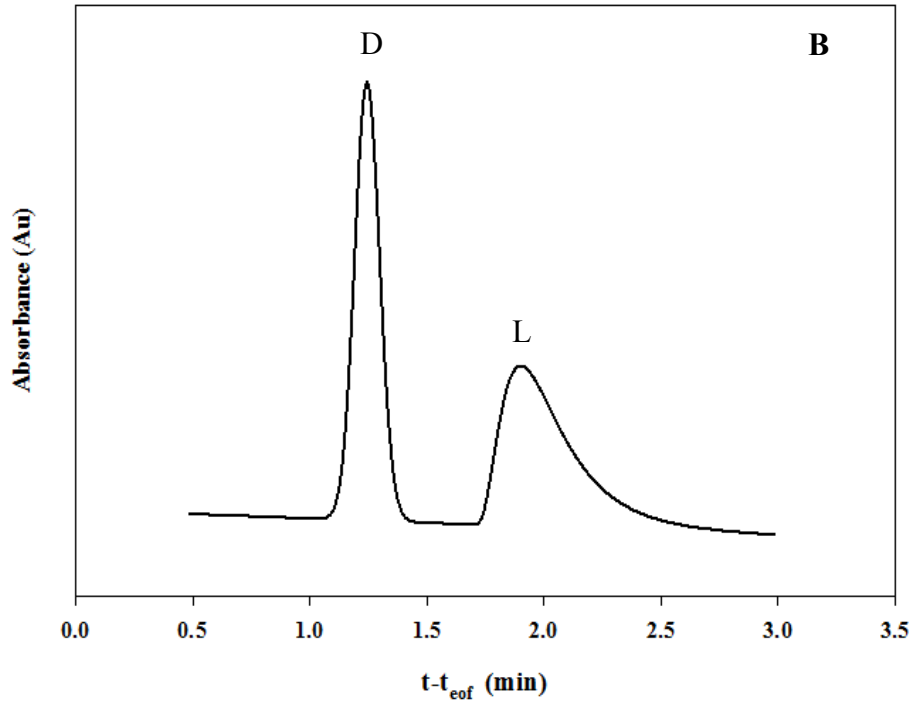
D
B
L
Absorbance (Au)
0.0
0.5
1.0
1.5
2.0
2.5
3.0
3.5
t-t$_{eof}$ (min)

Figure 47: 5-hydroxy-D,L-tryptophan (0.22 mg/ml) binding by unmodified BSA (A) and 1 week modified BSA (B). The serum protein concentration was held at 35 μM. ACE conditions: 15 kV, 25°C, injection at 20 mbar for 5 s, and detection at 280 nm.

Figure 47.

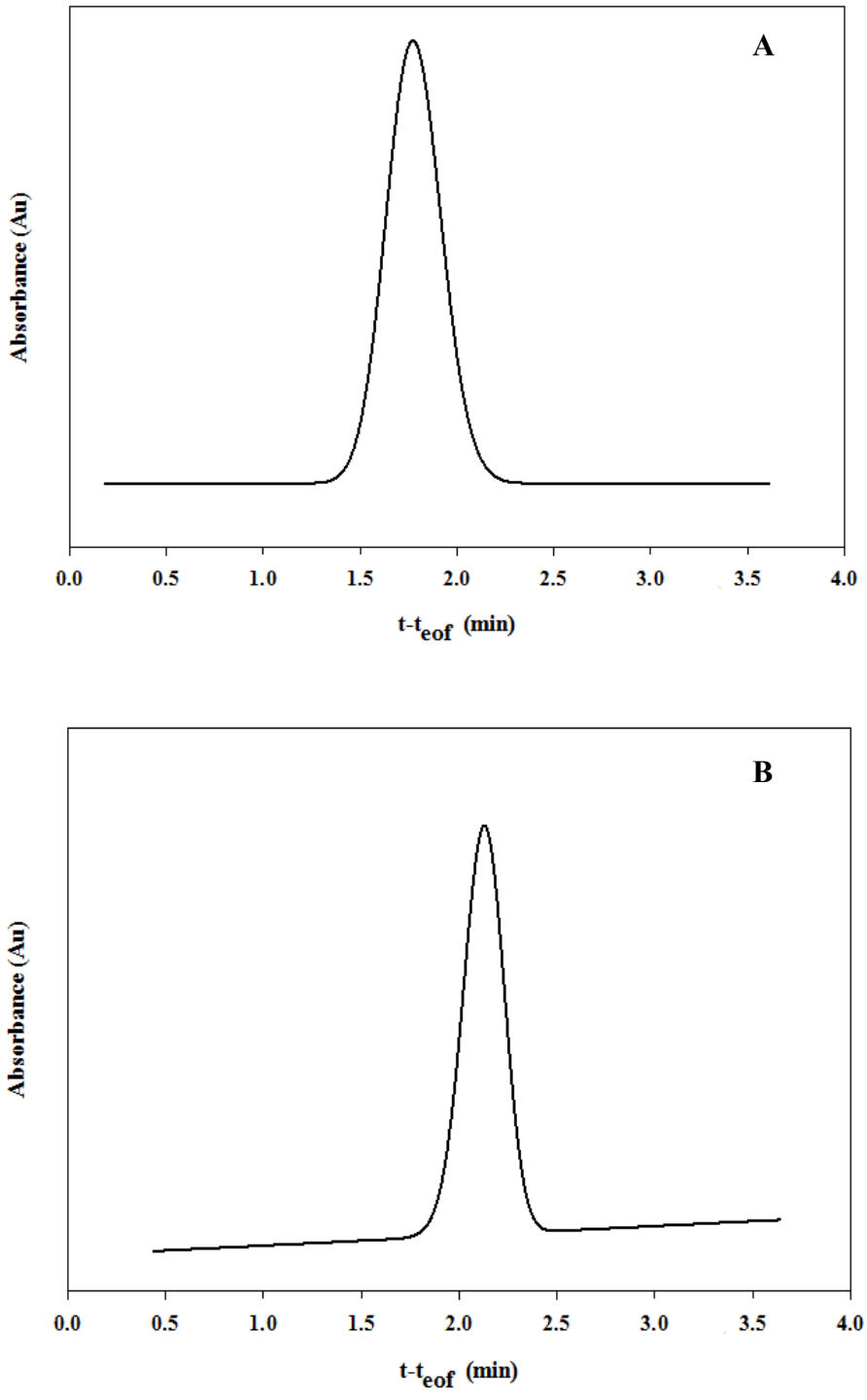
A
Absorbance (Au)
0.0
0.5
1.0
1.5
2.0
2.5
3.0
3.5
4.0
t-t$_{eof}$ (min)
B
Absorbance (Au)
0.0
0.5
1.0
1.5
2.0
2.5
3.0
3.5
4.0
t-t$_{eof}$ (min)

Figure 48: 5-hydroxy-D,L-tryptophan (0.22 mg/ml) binding by 2 week modified BSA (A) and 3 week modified BSA (B). The serum protein concentration was held at 35 μM. ACE conditions: 15 kV, 25°C, injection at 20 mbar for 5 s, and detection at 280 nm.

Figure 48.

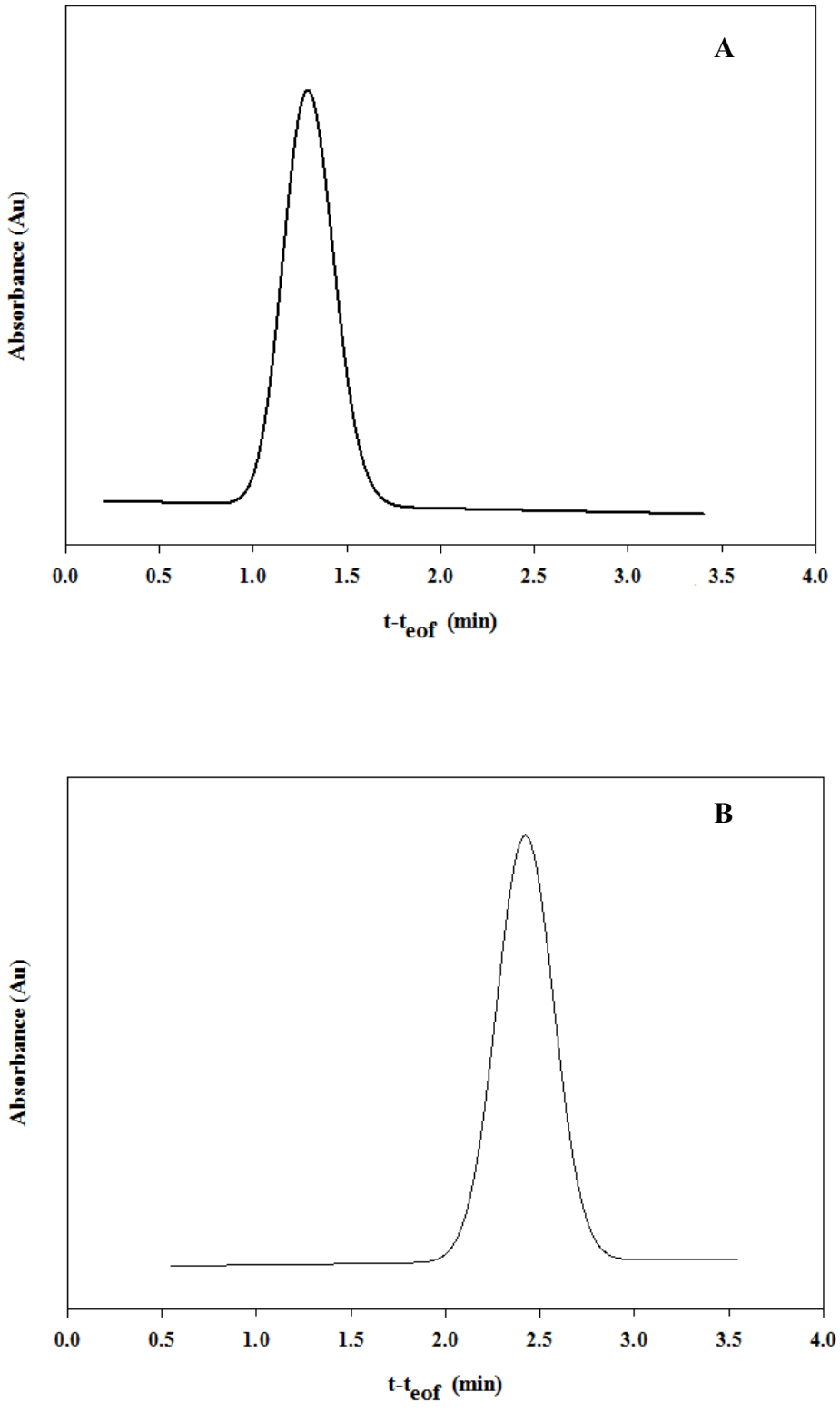
A
Absorbance (Au)
0.0
0.5
1.0
1.5
2.0
2.5
3.0
3.5
4.0
t-t$_{eof}$ (min)
B
Absorbance (Au)
0.0
0.5
1.0
1.5
2.0
2.5
3.0
3.5
4.0
t-t$_{eof}$ (min)

Figure 49: Effect of glycation extent on BSA selectivity of D,L-tryptophan. The serum protein concentration was held at 35 μM. ACE conditions: 15 kV, 25°C, injection at 20 mbar for 5 s, and detection at 280 nm.

Figure 49.

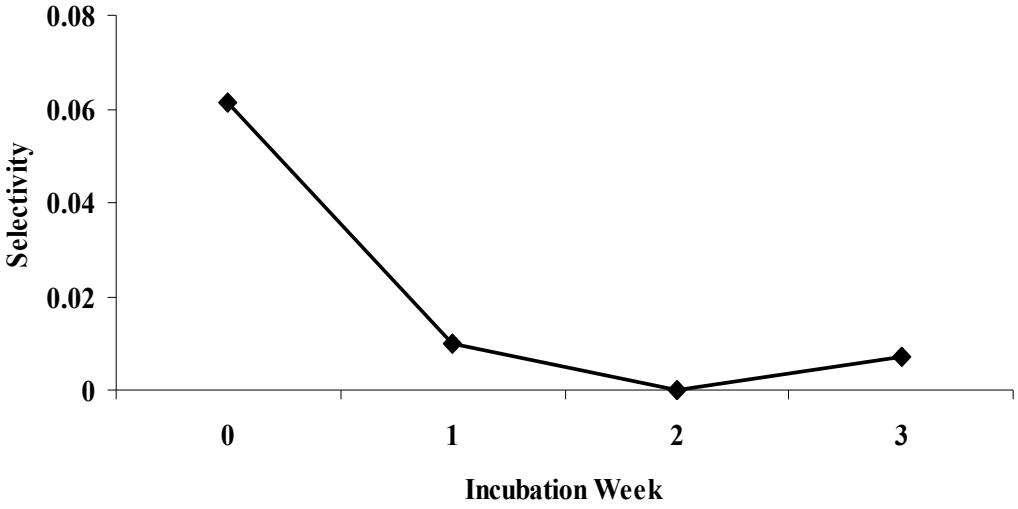

Figure 50: Effect of glycation extent on BSA selectivity of 5-fluoro-D,L-tryptophan. The serum protein concentration was held at 35 μM. ACE conditions: 15 kV, 25°C, injection at 20 mbar for 5 s, and detection at 280 nm.

Figure 50.

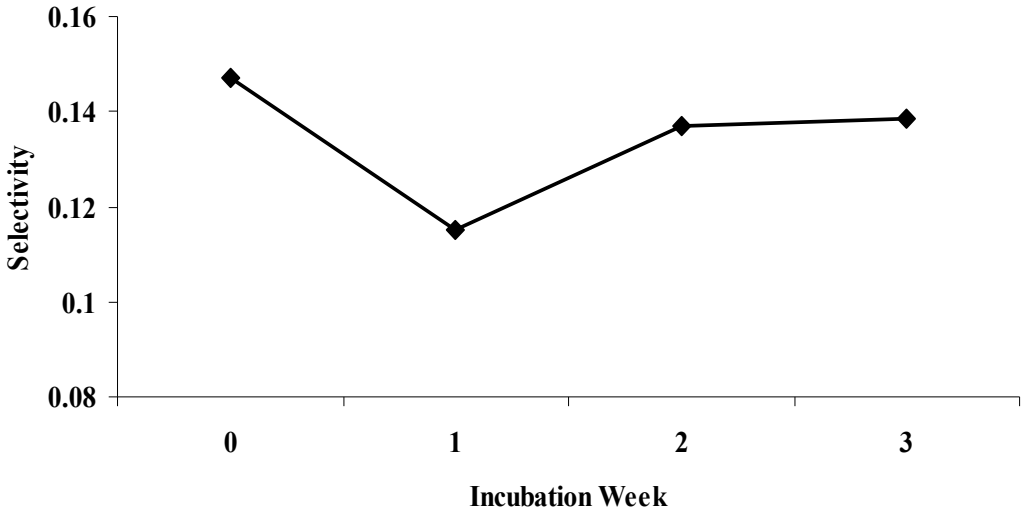

Figure 51: Effect of glycation extent on BSA selectivity of 5-hydroxy-D,L-tryptophan. The serum protein concentration was held at 35 μM. ACE conditions: 15 kV, 25°C, injection at 20 mbar for 5 s, and detection at 280 nm.

Figure 51.

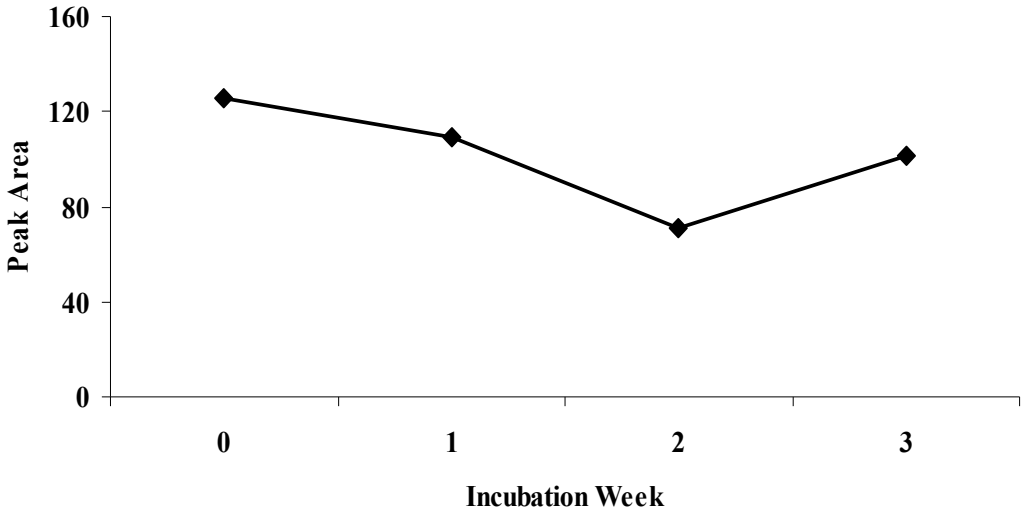

The results indicate that albumin functional properties are impacted by glycation-induced modifications of its structure. Some of the main glycation sites are located in the vicinity of known drug binding sites (Wa et al., 2007). The extent of glycation depends upon the time of incubation and in periods of less than 10 days, early stage glycation products that arise from Schiff base reactions occur in the central body of the protein (Cohen, 2003; Schmitt et al., 2005; Coussons et al., 1997). The latter stages of glycation occur on the C- and N- terminal regions causing the body of the protein to be effected by glycation first. The L-tryptophan binding site (site II) is located in a hydrophobic cleft between two predominant helical structures in the body of the protein (Peyrin et al., 1999; Kragh-Hansen et al., 2001). Any changes in the helical arrangement of BSA induced by the glycation process will alter its binding, which correlates to shifts in enantioselection of tryptophan.

Based upon this, a postulated explanation for the observed fluctuations in enantioselection is that the glycation induced by incubating BSA in D-glucose for two weeks, reduced the helical stability of BSA and led to a decreased binding of L-tryptophan. An earlier study showed that low levels of glucose partially denatured the protein and decreased the degree of L-tryptophan binding (Barzegar et al., 2007) supporting the results. The effects of this structural change on binding, were not observed in the case of 5-fluoro-D,L-tryptophan due to its higher binding affinity for BSA. By allowing the BSA to incubate in D-glucose solution for 3 weeks, binding affinity of tryptophan recovered, suggesting further glycation enhanced the helical stability of BSA. Previous studies by equilibrium dialysis have shown stabilization of the protein's structure occurs when high concentrations of glucose are present on the

protein (Bohney & Feldhoff, 1992). Further support of these results, is BSA incubated in high concentrations of glucose have been reported to exhibit similar binding properties to unmodified BSA (Bohney & Feldhoff, 1992). The recovery of binding by BSA observed after 3 weeks of incubation in D-glucose may be attributed to this stabilization. Further structural studies will need to be carried out to verify these postulated conclusions.

Chapter 4

Conclusion and Future Studies

4.1. Summary

In this dissertation a satisfactory capillary electrophoresis method using protein CSPs for enantiomer separation was developed. In the first section of this dissertation, the influences of separation voltage, surface regeneration protocols using sodium hydroxide/water, background electrolyte rinsing time, sample buffer ionic strength, and protein diffusion were studied. In doing this, the tryptophan-albumin system was used as a model at a pH, temperature, and ionic strength optimal for BSA binding. The results indicate that accurate binding measurements are obtained not only by assuring the conditions of the microenvironment are conducive for protein binding, but also by optimizing relevant experimental conditions of the capillary electrophoresis instrument. Also from this study, it was determined that unlike previously proposed, allowing the liquid to stand still in the capillary prior to separation, does not adversely effect separation, but can enhance separation. Future protein diffusion studies aimed at characterizing this relationship should be carried out to gain a better understanding of the mechanisms involved.

In the last two sections of this work, it was demonstrated that CE can be applied for studying biochemical processes. It presents itself as both a means for developing serum albumin based selective analysis techniques and a convenient approach for

characterizing the molecular interactions of protein with drugs. In its use for studying the displacement of tryptophan by ibuprofen, it was found that possible preformed ibuprofen-BSA complexes may have altered binding and thereby introduce error in binding measurements. Future studies, that incorporate steps for controlling or normalizing for these contributions, would be of value for calculating accurate binding constants.

In the last section, it was indicated by differences in the chiral recognition of non-glycated BSA and BSA glycated at various degrees, that NMR affirmed structural change on BSA led to alterations in its binding of tryptophan. Conformational and functional changes of BSA depend upon the amount of glycation. A better understanding of the differences in binding is possible through more detailed structural studies.

REFERENCES

Akapo, S., McCrea, C., Gupta, J., Roach, M., Skinner, W. (2009) Chiral HPLC analysis of formoterol stereoisomers and thermodynamic study of their interconversion in aqueous pharmaceutical formulations. *J Pharm Biomed Anal* **49,** 632-637.

Altria K., Elder, D. (2004) Overview of the status and applications of capillary electrophoresis to the analysis of small molecules. *J Chromatogr A* **1023,** 1-14.

Amini, A., Pettersson, C., Westerlund, D. (1997) Enantioresolution of disopyramide by capillary affinity electrokinetic chromatography with human alpha(1)-acid glycoprotein (AGP) as chiral selector applying a partial filling technique. *Electrophoresis* **18,** 950-957.

Armstrong, D., Nair, U. (1997) Capillary electrophoresis enantioseparations using macrocyclic antibiotics as chiral selectors. *Electrophoresis* **18,** 2331-2342.

Armstrong, D., Rundlett, K., Reid, G. (1994) Use of a Macrocyclic Antibiotic, Rifamycin –B, and Indirect Detection for the Resolution of Rcemic Amino-Alcohols by CE. *Anal Chem* **66,** 1690-1695.

Ascoli, G.A., Domenici, E., Bertucci, C. (2006) Drug binding to human serum albumin: Abridged review of results obtained with high-performance liquid chromatography and circular dichroism. *Chirality* **18,** 667-679.

Bao, H., Tarbasa, M., Chae, H., You, S. (2012) Molecular Properties of Water-Unextractable Proteglycans from Hypsizygus Marmoreus and Their in Vitro Immunomodulatory Activities. *Molecules* **17,** 207-226.

Barzegar, A., Moosavi-Movahedi, A., Sattarahmady, N., Hosseinpour-Faizi, M., Aminbakhsh, M., Ahmad, F., Saboury, A., Ganjali, M., Norouzi, P. (2007) Spectroscopic studies of the effects of glycation on human serum albumin on L-Trp binding. *Protein Pept Lett* **14,** 13-18.

Basken, N., Mathias, C., Green, M. (2009) Elucidation of the Human Serum Albumin (HSA) Binding Site for the Cu-PTSM and Cu-ATSM Radiopharmaceuticals. *J Pharm Sci* **98,** 2170-2179.

Berezhkovskiy, L. (2006) Determination of drug binding to plasma proteins using competitive equilibrium binding to dextran-coated charcoal. *J Pharmacokinet Pharmacodyn* **33,** 595-608.

Betts, A., Clark, T., Yang, J., Treadway, J., Li, M., Giovanelli, M., Abdiche, Y., Stone, D., Paralkar, V. (2010) The Application of Target Information and Preclinical Pharmacokinetic/Pharmacodynamic Modeling in Predicting Clincal Doses of a Dickkopf-1 Antibody for Osteoporosis. *J Pharmacol Exp Ther* **333,** 2-13.

Bhusman, R., Kumar, R. (2009) Analytical and preparative enantioseparation of DL-penicillamine and DL-cysteine by high-performance liquid chromatography on alpha-acid glycoprotein and beta-cyclodextrin columns using ninhydrin as a reversible tagging reagent. *J Chromatogr A* **1216,** 3413-3417.

Blaschke, G., Chankvetadze, B., in: R. Nuebert, H. Rüttinger (Eds.), Drugs and the Pharmaceutical Sciences, Affinity Capillary Electrophoresis in Pharmaceutics and Biopharmaceutics, Marcel Dekker, New York, 2003, p.177.

Bohney, J., Feldhoff, R. (1991) Effects of Nonenzymatic Glycosylation and Fatty Acids on tryptophan Binding to Human Serum Albumin. *Biochem Pharmacol* **43,** 1829-1834.
Bohney, J., Feldhoff, R. (1992) Effects of nonenzymatic glycosylation and fatty acids on tryptophan binding to human serum albumin. *Biochem Pharmacol* **43,** 1829-1834.

Bose, S., Yang, J., Hage, D., (1997) Guidelines in selecting ligand concentrations for the determination of binding constants by affinity capillary electrophoresis. *J Chromatogr B* **697,** 77-88.

Bruin, G., Chang, J., Kuhlman, R., Zegers, K., Kraak, J., Poppe, H. (1989) Capillary Zone Electroretic Spearations of Proteins in Polyethylene Glycol-Modified Capillaries. *J Chromatogr* **471,** 429-436.

Bubb, W. (2003) NMR Spectroscopy in the Study of Carbohydrates:Characterizing the Structural Complexity. *Concepts Magn Reson Part A* **19A (1),** 1-19.

Bullock, J.A., Yuan, L.C. (1991) Free Solution Capillary Electrophoresis of Basic-Proteins in Uncoated Fused-Silica Capillary Tubing. *J Microcolumn Sep* **3,** 241-248.

Carter, D.C., Ho, J.X. (1994) Structure of serum albumin. *Adv Protein Chem* **45,** 153-203.

Chankvetadze, B., in:Capillary Electrophoresis In Chiral Analysis, John Wiley & Sons, Ltd., West Sussex, England, 1997, p. 26.

Christodoulou, E. (2010) An Overview of HPLC Methods for the Enantiomer Separation of Active Pharmaceutical Ingrediantes in Bulk and Drug Formulations. *Curr Org Synth* **14,** 2337-2347.

Cirilli, R., Ferretti, R., La Regina, G., Morelli, G., Pierini, M., Piscitelli, F., Silvestri, R. (2010) Enantioselective HPLC combined with spectroscopic methods: A valid strategy to determine the absolute configuration of potential beta-secretase inhibitors. *Talanta* **82,** 1306-1312.

Cohen, M.P. (2003) Intervention strategies to prevent pathogenetic effects of glycated albumin. *Arch Biochem Biophys* **419,** 25-30.

Coussons, P., Jacoby, J., McKay, A., Kelly, S., Price, N. (1997) Glucose modification of human serum albumin: A structural study. *Free Radic Biol Med* **22,** 1217-1227.

Cui, F., Tao, W., Xu, Z., Guo, W., Xu, H., Ao, Z., Jin, J., Wei, Y. (2007) Structural analysis of anti-tumor heteropolysaccharide GFPS1b from the cultured mycelia of Grifola frondosa GF9801. *Bioresour Technol* **98,** 395- 401.

Davankov, V. (1998) The nature of chiral recognition: Is it a three-point interaction? *Chirality* **9,** 99-102.

Ding, H-M., Shao, L., Liu, R., Xiao, Q., Chen, J.(2005) Silica nanotibes for lysozyme immobilization. *J Colloid Interface Sci* **290,** 102-106.

Docoslis, A., Rusinski, L., Giese, R., van Oss, C. (2001) Kinetics and interaction constants of protein adsorption onto mineral microparticles-measurement of the constants at the onset of hysteresis. *Colloids Surf B* **22,** 267-283.

Doghramiji, P.P., (2006) Trends in the pharmacologic management of insomnia. *J Clin Psychiatry* **67,** 5-8.

El-Hady, D., Kühne, S., El-Maali, N., Wätzig, H. (2010) Precision in affinity capillary electrophoresis for drug-protein binding studies. *J Pharm Biomed Anal* **52,** 232-241.

Ermakov, S., Zhukov, M., Capelli, L., Righetti, P. (1995) Wall Adsorption in Capillary Electrophoresis-Experimental Study and Computer-Simluation. *J Chromatogr A* **699,** 297-313.

Fanali, G., di Masi, A., Trezza, V., Marino, M., Fasano, M., Ascenzi, P. (2012) Human serum albumin: From bench to bedside. *Mol Aspects Med* **33,** 209-290.

Fielding, L., Rutherford, S., Fletcher, D. (2005) Determination of protein-ligand binding affinity by NMR: observations from serum albumin model systems. *Magn Reson Chem* **43,** 463-470.

Gassman, E., Kuo, J., Zare, R. (1985) Electrokinetic separation of chiral compounds. *Science* **4727,** 813-814.

Gerig, J. Klinkenborg, J. (1980) Binding of 5-Fluoro-L-Tryptohan to Human Serum Albumin. *J Am Chem Soc* **102,** 4267-4268.

Giddings, J.C. (1969) Generation of Variance, Theoretical Plates, Resolution, and Peak Capacity Electrophoresis and Sedimentation. *Sep Sci* **4,** 181.

Gilpin, R., Ehtesham, S., Gregory, R. (1991) Liquid Chromatographic Studies of the Effect of Temperature on the Chiral Recognition of Tryotphan by Silica-Immobilized Bovine Albumin. *Anal Chem* **63,** 2825-2828.

Graf, M, Garcia Galera R., Wätzig, H. (2005) Protein adsorption in fused-silica and polyacrylamide-coated capillaries. *Electrophoresis* **26,** 2409-2417.

Gray, J. (2004) The interactions of proteins with solid surfaces. *Curr Opin Struct Biol* **14,** 114-115.

Guan, J., Yan, F., Shi, S., Wang, S.L. (2012) Optimization and validation of a new CE method for the determination of pantoprazole enantiomers. *Electrophoresis* **33,** 1631-1636.

Guiochon, G., Tarafder, A. (2011) Fundamental challenges and opportunities for preparative supercritical fluid chromatography. *J Chromatogr A* **1218,** 1037-1114.
Hage, D.S., Jackson, A., Sobansky, M.R., Schiel, J.E., Yoo, M.J., Joseph, K.S. (2009) Characterization of drug-protein interactions in blood using high-performance affinity chromatography. *J Sep Sci* **32,** 835-853.

Herr, A., Molho, J., Santiago, J. Mungal, M., et al. (2000) Electroosmotic capillary flow with nonuniform zeta potential. *Anal Chem* **72,** 1053-1057.

Hödl, H., Koidl, J., Schmid, M., Gübitz, G. (2006) Chiral resolution of tryptophan derivatives by CE using canine serum albumin and bovine serum albumin as chiral selectors. *Electrophoresis* **27,** 4755-4762.

Hsu, L.C., Kim, H., Yang, X.Q., Ross, D. (2011) Large Scale Chiral Chromatography for the Separation of an Enantiomer to Accelerate Drug Development. *Chirality* **23,** 361-366.

Ilisz, I., Fodor, G., Berkecz, R., Ivanyi, R., Szente, L., Peter, A. (2009) Enantioseparation of beta-substituted tryptophan analogues with modified cyclodextrins by capillary zone electrophoresis. *J Chromatogr A* **1216,** 3360-3365.

Johansson, J., Landgren, M., Fernell, E., Vumma, R., Ahlin, A., Bjerkenstedt, L., Venizelos, N. (2011) Altered tryptophan and alanine transport in fibroblasts from boys with attention-deficit/hyperactivity disorder (ADHD): an in vitro study. *Behav Brain Funct* **7,** 40.

Jones, H.K., Nguyen, N.T., Smith, R.D. (1990) Variance Contributions to Band Spread in Capillary Zone Electrophoresis. *J Chromatogr* **504,** 1-19.

Kitagawa, F., Otsuka, K. (2011) Recent progress in capillary electrophorestic analysis of amino acid enantiomers. *J Chromatogr B Analyt Technol Biomed Life Sci* **879,** 3078-3095.

Koizumi, K., Ikeda, C., Ito, M., Suzuki, J., Kinoshita, T., Yasukawa, K. (1998) Influence of Glycosylation on the Drug Binding of Human Serum Albumin. *Biomed Chromatogr* **12,** 203-210.

Kraak, J., Busch, S., Poppe, H. (1992) Study of Protein Drug-Binding using Capillary Zone Electrophoresis. *J Chromatogr* **608,** 257-264.

Kragh-Hansen, U., Hellec, F., Foresta, B., Maire, M., Moller, J. (2001) Detergents as probes of hydrophobic binding cavities in serum albumin and other water-soluble proteins. *Biophys J* **80,** 2898-2911.

Kurrat, R., Prenosil, J., Ramsden, J. (1997) Kinetics of human and bovine serum albumin adsorption at silica-titania surfaces. *J Colloid Interface Sci* **185,** 1-8.

Lammerhoffer, M. (2010) Chiral recognition by enantioselective liquid chromatography: Mechanisms and modern chiral stationary phases. *J Chromatogr A* **1217,** 814- 856.

Langlois, X., Megens, A., Lavreysen, H., Atack, J., Cik, M., te Riele, P., Peeters, L., Wouters, R., Vermeire, J., Hendrickx, H., Macdonald, G., De Bruyn, M. (2012) Pharmacology of JNJ-37822681, a Specific and Fast-Dissociating D-2 Antagonist for the Treatment of Schizephrenia. *J Pharmacol Exp Ther* **342,** 91-105.

Li, H., Zeng, H.L., Chen, Z.F., Lin, J.M. (2009) Chip-based enantioselective open-tubular capillary electrochromatography using bovine serum albumin-gold nanoparticle conjugates as the stationary phase. *Electrophoresis* **30,** 1022-1029.

Li, S., Lloyd, D. (1993) Direct Chiral Separations by Capillary Electrophoresis Using Capillaries packed with an alpha(1)-Acid Glycoprotein Chiral Stationary-Phase. *Anal Chem* **65,** 3684-3690.

Li, Z., Wei, C., Zhang, Y., Wang, D., Liu, Y. (2011) Investigation of competitive binding of ibuprofen and salicyclic acid with serum albumin by affinity capillary electrophoresis. *J Chromatogr B* **879,** 1934-1938.

Lin, C., Fang, I., Deng, Y., Liao, W., Cheng, H., Huang, W. (2004) Capillary electrophorestic studies on the migration behavior of cationic solutes and the influence of interactions of cationic solutes with sodium dodecyl sulfate on the formation of micelles and critical micelles concentration. *J Chromatogr A* **1051,** 85-94.

Liu, X., Dahdouh, F., Salgado, M., Gomez, F. (2008) Recent Advances in Affinity Capillary Electrophoresis (2007). *J Pharm Sci* **98,** 394-410.

Liu, Y.C., Yang, Z.Y., Du., J., Yao, X., Lei, R., Zheng, X.D., Liu, J.N., Hu, H., Li, H. (2008) Study on the interactions of kaempferol and quercetin with intravenous immunoglobulin by fluorescence quenching, Fourier transformation infrared spectroscopy and circular dichroism spectroscopy. *Chem Pharm Bull* **56,** 443-451.

Lu, H, Guonan, C. (2010) Recent advances of enantioselections in capillary electrophoresis and capillary electrochromatography. *Anal Methods* **3,** 488-508.

Malmsten, M. (1998) Formation of adsorbed protein layers. *J Colloid Interface Sci* **207,** 186-199.

Marle, I., Jonsson, S., Isaksson, R., Pettersson, C., Pettersson, G. (1993) Chiral Stationary Phases Based On Intact and Fragmented Cellobiohydrolase-I Immobilized on Silica. *J Chromatogr* **648,** 333-347.

Masci, G., Ladogana, R.D., Cametti, C. (2012) Assemblies of Thermoresponsive Diblock Copolymers: Micelle and Vesicle Formation Investigated by Means of Dielectric Relaxation Spectroscopy. *J Phys Chem B* **116,** 2121-2130.

Mathur, S., Badertscher, Scott, M., Zenobi, R. (2007) Critical evaluation of mass spectrometric measurement of dissociation constants: accuracy and cross-validation against surface plasmon resonance and circular dichroism for the calmodulin-melittin system. *Phys Chem Chem Phys* **9,** 6187-6198.

McConnell, O., Bach, A., Balibar, C. (2007) Enantiomeric separation and determination of absolute stereochemistry of asymmetric molecules in drug discovery- Building chiral technology toolboxes. *Chirality* **19,** 658-682.

McMenamy, R., Oncley, J. (1958) Specific Binding of L-tryptophan to Serum Albumin. *J Biol Chem* **233,** 1436-1447.

Mikulikova, K, Miksik, I., Deyl, Z. (2005) Non-enzymatic postranslational modification of bovine serum albumin by oxo-compounds investigated by chromatographic and electrophoretic methods. *J Chromatogr B Analyt Technol Biomed Life Sci* **815,** 315-331.

Muck-Seler, D., Pivac, N. (2011) Serotonin. *Period. Biol.* **113,** 29- 41.

Munch, G., Schicktanz, D., Behme, A., Gerlach, M., Riederer, P., Palm, D., et al. (1999) Amino acid specificity of glycation and protein-AGE crosslinking reactivities determined with a dipeptide SPOT library. *Nat Biotechnol* **17,** 1006-1110.

Nakanishi, K., Sakiyama, T., Imamura, K. (2001) On the adosrption of proteins on solid surfaces, a common but very complicated phenonmenon. *J Biosci Bioeng* **91,** 233-244.

Natishan, K (2005) Recent progress in the analysis of pharmaceuticals by capillary electrophoresis. *J Liq Chromatogr Relat Technol* **28,** 1115-1160.

Niederhofer, H. (2011) Develoing biochemical profiles for various psychiatric diseases. *Med. Hypotheses* **77,** 532-533.

Nikolaou, A., Thomas, D., Kampanellou, C., Alexandraki, K., Andersson, L.G., Sundin, A., Kaltsas, G. (2010) The value of C-11-5-hydroxy-tryptophan positron emission tomography in neuroendocrine tumor diagnosis and management: experience from one center. *J. Endocrinol Invest.* **33,** 794-799.

Núñez, M.C., García-Rubiño, M. E., Conejo-García, A., Cruz-López, O., Kimatrai, M., Gallo, M.A., Espinosa, A., and Campos, J.M. (2009). Homochiral Drugs: A Demanding Tendency of the Pharmacaeutical Industry. *Curr. Med. Chemistry* **16,** 2064- 2074.

Ostergaard, J. (2007) Application of Retention Factor in Affinity Electrokinetic Chromatography and Capillary Electrophoresis. *Anal Sci* **23,** 489-492.

Oettl, K., Stauber, R. (2007) Physiological and pathological changes in the redox state of human serum albumin critically influence its binding properties. *Br J Pharmacol* **151,** 580-590.

Oravcova, J., Bohs, B., Linder, W. (1996) Drug-protein binding studies: new trends in analytical and experimental methodology. *J Chromatogr B* **677,** 1-28.

Peters, T.J. (1996) All about Albumin-Biochemistry, Genetics, and Medical Applications. Academic Press, San Diego.

Peyrin, E., Guillaume, Y., Guinchard, C. (1999) Characterization of solute binding at human serum albumin site II and its geometry using a biochromatographic approach. *Biophys J* **77,** 1206-1212.

Ren, L., Li., D. (2001) Electroosmotic flow in heterogenous microchannels. *J Colloid Interface Sci* **243,** 255-261.

Ribeiro, A.E., Gomes, P.S., Pais, L.S., Rodrigues, A.E. (2011) Chiral Separation of Ketoprofen Enantiomers by Preparative and Simulated Moving Bed Chromatography. *Sep Sci Technol* **46,** 1726-1739.

Robinson, O., Overstreet, C., Allen, P., Pine, D., Grillon, C.(2012) Acute Tryptophan Depletion Increases Translational Indices of Anxiety but not Fear: Serotonergic Modulation of the Bed Nucleus of the Stria Terminalis. **37,** 1963 -1971.

Rondeau, P, Bourdon, E. (2011) The glycation of albumin: Structural and functional impacts. *Biochimie* **93,** 645-658.

Rudnev, A., Foteeva, L., Kowol, C., Berger, R., Jakupec, M., Arion, V., Timerbaev, A., Keppler, B. (2006) Preclinical characterization of anticancer gallium(II) complexes: Solubility, stability, lipophilicity and binding to serum proteins. *J Inorg Biochem* **100,** 1819-1826.

Schmitt, A., Gasic-Milenkovic, J., Schmitt, J. (2005) Characterization of advanced glycation end products: Mass changes in correlation to side chain modifications. *Analyt Biochem* **346,** 101-106.

Schmitt, A., Schmitt, J., Munch, G., Gasic-Milencovic, J. (2005) Chracterization of advanced glycation end products for biochemical studies: side chain modifications and fluorescence chracteristics. *Anal Biochem* **338,** 201-215.

Schmitt, U., Branch, S.K., Holzgrabe, U. (2002) Chiral separations by cyclodextrin-modified capillary electrophoresis- Determination of the enantiomeric excess. *J Sep Sci* **25,** 959-974.

Smith, N., Evans, M. (1994) Capillary Zone Electrophoresis in Pharmaceutical and Biomedical Analysis. *J Pharm Biomed Anal* **12,** 579-611.

Sokoliess, T., Koller, G. (2005) Approach to method development and validation in capillary electrophoresis for enantiomeric purity of active basic pharmaceutical ingredients. *Electrophoresis* **26,** 2330-2341.

Speybrouck, D., Corens, D., Argoullon, J.M. (2012) Screening Strategy for Chiral and Achiral Separations in Supercritical Fluid Chromatography Mode. *Curr Top Med Chem* **12,** 1250-1263.

Sudlow, G., Birkett, D., Wade, D. (1975) Characterization of 2 Specific Drug Binding-Sites on Human-Serum Albumin. *Mol Pharmacol* **12,** 824-832.

Sudlow, G., Birkett, D., Wade, D. (1976) Further Chracterization of Specific Drug Binding-Sites on Human-Serum Albumin. *Mol Pharmacol* **12,** 1052-1061.

Sun, Y., Wang, B. (2012) Molecular Recognition Mechanism of Chiral (S)-Ibuprofen's Hydrogen Bonds Self-assembly Imprinted Polymer. *Chem Res Chin Univ* **33,** 838-842.

Swedberg, S. (1990) Characterization of Protein Behavior in High-Performance Capillary Elelctrophoresis Using a Novel Capillary System. *Anal Biochem* **185,** 51-56.

Tanaka, Y., Terabe, S. (2001) Recent advances in enantiomer separations by affinity capillary electrophoresis using proteins and peptides. *J Biochem Biophys Methods* **48,** 103-116.

Tanaka, Y., Terabe, S. (1997) Separation of the enantiomers of basic drugs by affinity capillary electrophoresis using a partial filling technique and alpha(1)-acid glycoprotein as a chiral selector. *Chromatographia* **44,** 119-128.

Thompson, M.R., McKenzie, D.R., Likos, J.J., Gard, J.K. (2009) Protein-free ligand screening: simplification of chiral chromatographic development via novel adaptation of NMR screening methodologies. *Magn Reson Chem* **47,** 541-550.

Thornalley, P. (1999) The clinical significance of glycation. *Clin Lab* **5-6,** 263-273.

Towns, J., Regnier, F. (1992) Impact of Polycation Adsorption on Efficiency and Electroosmotically Driven Transport in Capillary Electrophoresis. *Anal Chem* **64,** 2473-2478.

Tittelbach, V., Gilpin, R. (1995) Species Dependency of the Liquid Chromatographic Properties of Silica-Immobilized Serum Albumins. *Anal. Chem.* **67,** 44-47.

Tran, N., Taverna, M., Miccoli, L., Angulo, J. (2005) Poly(ethylene oxide) facilitates the characterization of an affinity between strongly basic proteins with DNA by affinity capillary electrophoresis. *Electrophoresis* **26,** 3105-3112.

Uccello-Barretta, G., Vanni, L., Balzano, F. (2010) Nuclear magnetic resonance approaches to the rationallization of chromatographic enantiorecognition processes. *J Chromatogr A* **1217,** 928-940.

van der Veen, M., Norde, W. Stuart, M.(2004) Electrostatic interactions in protein adsorption probed by comparing lysozyme and succinylated lysozyme. *Colloids Surf B* **35,** 33-40.

Ventura, M., Murphy, B., Goetzinger, W. (2012) Ammonia as a preferred additive in chiral and achiral applications of supercritical fluid chromatography for small, drug-like molecules. *J Chromatogr A* **1220,** 147-155.

Ward, T., Oswald, T. (1997) Enantioselectivity in capillary electrophoresis using the macrocyclic antibiotics. *J Chromatogr A* **792,** 309-325.

Winn, M., Roy, A.D., Gruschow, S., Parameswaran, R.S., Goss, R.J.M. (2008) A convenient one-step synthesis of L-aminotryptophans and improved synthesis of 5-fluorotryptopphan. *Bioorg Med Chem Lett* **18,** 4508-4510.

Wong, M.M., Holzheuer, Webster, G.K. (2008) A comparison of HPLC and SFC chiral method development screening approaches for compounds of pharmaceutical interest. *Curr Pharm Anal* **4,** 101-105.

Wu, R., Zou, H., Ye, M., Lei, Z., Ni, J. (2001) Separation of basic, acidic and neutral compounds by capillary electrochromatography using uncharged monolithic capillary columns modified with anionic and cationic surfactants. *Electrophoresis* **22,** 544-551.

Yang J., Hage, D. (1993) Chracterization of the Binding and Chiral Separation of D- and L-Tryptophan on a High-Performance Immobilized Human Serum Albumin Column. *J Chromatogr* **645,** 241-250.

Yang, J., Hage, D. (1994) Chiral Separations in Capillary Electrophoresis Using Human Serum Albumin as a Buffer Additive. *Anal Chem* **66,** 2719-2725.

Ye, Q., Ouyang, P.K., Ying, H. (2011) A review-biosynthesis of optically pure ethyl (S)-4-chloro-3-hydroxybutanoate ester: recent advances and future perspectives. *Appl Microbiol Biotechnol* **89,** 513-522.

Zhang, A., Gao, W., Ma Binbin, Jin, L., Lin, C. (2012) Enantiomeric separations of chiral polychlorinated biphenyls on three polysaccharide-type chiral stationary phases by supercritical fluid chromatography. *Anal Bioanal Chem* **403,** 2665-2672.

Zhang, X.P., Zhang, C.Y., Sun, G.L., Xu, X.D., Tan, Y.F., Wu, H.F., Cao, R.N., Liu, J., Wu, J.W. (2012) Cyclodextrins and Their Derivatives in The Resolution of Chiral Natural Products: A Review. *Instrum Sci Technol* **40,** 194-215.

APPENDIX

List of Abbreviations

API	Active Pharmaceutical Ingredients
ACE	Affinity Capillary Electrophoresis
CE	Capillary Electrophoresis
NMR	Nuclear Magnetic Resonance
EOF	Electroosmotic Flow
CSPs	Chiral Stationary Phases
HSA	Human Serum Albumin
BSA	Bovine Serum Albumin
AGP	α_1-acid glycoprotein
OVM	Ovumocoid
HPLC	High Pressure Liquid Chromatography
BGE	Background Electrolyte
SDS	Sodium dodecyl sulfate
UV	Ultra Violet
NaOH	Sodium hydroxide
pH	$- \log[H]^+$
Trp	D,L-Tryptophan

List of Abbreviations (Continued)

5-Flo	5-fluoro-D,L-tryptophan
Ibu	Ibuprofen
Au	Absorbance Units
DAD	Diode Array Detector
R^2	Square of the correlation coefficient
μ_{an}	electrophoretic mobility of solute